

**BRACING REQUIREMENTS FOR ELASTIC STEEL BEAMS**

**APPROVED:**

\_\_\_\_\_  
**Joseph A. Yura**

\_\_\_\_\_  
**Michael Engelhardt**

**To my parents**

**BRACING REQUIREMENTS FOR ELASTIC STEEL BEAMS**

by

**Brett Alan Phillips, B.S.C.E.**

**THESIS**

**Presented to the Faculty of the Graduate School of**

**The University of Texas at Austin**

**in Partial Fulfillment**

**of the Requirements**

**for the Degree of**

**MASTER OF SCIENCE IN ENGINEERING**

**THE UNIVERSITY OF TEXAS AT AUSTIN**

**December 1990**

## **Acknowledgements**

The author would like to express his most sincere gratitude to Dr. Joseph Yura for his exceptional guidance and patience during the course of this research. The author would also like to thank Swarnalatha Vegesna and Robert Marceau for their invaluable assistance and encouragement.

The support of the Texas State Department of Highways and Public Transportation, the Center for Transportation Research, Phil M. Ferguson Structural Engineering Laboratory, and the Graduate School of the University of Texas at Austin were all essential to the successful completion of this investigation and thesis.

**Brett Alan Phillips**

## Table of Contents

Chapter 1 Introduction .....	1
1.1 Beam Buckling Strength .....	1
1.2 Beam Bracing .....	3
1.3 Previous Approaches to Beam Bracing .....	11
1.4 Limitations of Current Approaches .....	14
1.5 Objectives of Research Program .....	14
Chapter 2 Analytical Program .....	16
2.1 General .....	16
2.2 Description of BASP Computer Program .....	16
2.3 Design Equations for Intermediate Lateral Bracing .....	20
2.4 Design Equations for Intermediate Torsional Bracing .....	22
2.5 Modifications for Moment Diagram Effects and Load Height .....	25
Chapter 3 Experimental Program .....	32
3.1 General .....	32
3.2 Loading and Support System .....	34
3.3 Instrumentation .....	37
3.4 Lateral Bracing System .....	39
3.5 Torsional Bracing .....	41
Chapter 4 Test Results .....	46
4.1 Test Procedure .....	46
4.2 Determination of Critical Load .....	47
4.3 Determination of Initial Imperfections .....	51
4.4 Test Series A - No bracing .....	52
4.5 Test Series B Lateral Bracing .....	53
4.6 Test Series C, Compression Flange Torsional Bracing .....	54
4.7 Test Series D, E, and F .....	56

Chapter 5 Comparison and Discussion of Test Results .....	59
5.1 General .....	59
5.2 Effect of Imperfections on Lateral Bracing Requirements .....	59
5.3 Comparison of Test Results and Design Equations for Lateral Bracing .....	62
5.4 Effect of Imperfections on Torsional Bracing .....	64
5.5 Comparison of Test Results and Design Equations for Torsional Bracing .....	66
5.6 Effect of Torsional Brace Location .....	72
5.7 Forced Imperfections .....	74
Chapter 6 Summary and Conclusions .....	75
6.1 Summary of the Investigation .....	75
6.2 Conclusions .....	75
6.3 Recommendations .....	76
Appendix A .....	77
Appendix B .....	98
Bibliography .....	100

## List of Tables

1.1 Lateral Bracing Stiffness Requirements .....	6
3.1 Measured Lateral Brace Stiffness .....	40
4.1 Measured Initial Deflection and Twist .....	51
4.2 Test Series A - No Bracing .....	53
4.3 Test Series B - Lateral Bracing .....	54
4.4 Test Series C - Compression Flange Torsional Bracing .....	56
4.5 Test Series D, E, and F .....	58

## List of Figures

1.1 Geometry of Buckled Beam .....	2
1.2 Lateral Brace Location .....	5
1.3 Cross-Section Distortion .....	5
1.4 Buckled Shape of Bridge Girders .....	9
1.5 Effects of Cross-Section Distortion .....	9
1.6 Cross-Section Distortion .....	10
1.7 Continuous vs. Discrete Bracing .....	10
2.1 Boundary Conditions used in BASP Program .....	18
2.2 Finite Element Mesh used in BASP .....	18
2.3 First Mode Buckled Shape .....	19
2.4 Second Mode Buckled Shape .....	19
2.5 Limiting Values of Critical Moment .....	21
2.6 Comparison of Lateral Bracing under Uniform Moment .....	22
2.7 Comparison of Torsional Bracing under Uniform Moment .....	24
2.8 Interaction of Lateral and Torsional Bracing .....	25
2.9 Comparison of Lateral Bracing under Centroid Point Loading .....	28
2.10 Comparison of Torsional Bracing under Centroid Point Loading .....	28
2.11 Comparison of Lateral Bracing under Top Flange Point Loading .....	29
2.12 Comparison of Torsional Bracing under Top Flange Point Loading .....	29
2.13 Comparison of Lateral Bracing under Top Flange Point Loading .....	31
2.14 Comparison of Torsional Bracing under Top Flange Point Loading .....	31
3.1 Schematic of Test Setup .....	33
3.2 Overall Test Setup .....	33
3.3 Average Cross-Section Properties of Test Beam .....	34
3.4 Gravity Load Simulator .....	36
3.5 Lateral Stiffness of Gravity Load Simulator Due to Friction .....	36
3.6 End Roller Bearings .....	37
3.7 Knife Edges .....	38
3.8 Schematic of Lateral Brace .....	40
3.9 Lateral Bracing System .....	41
3.10 Torsional Bracing .....	42
3.11 Torsional Brace Fixtures .....	42
3.12 Brace Fixture Components .....	43
3.13 Adjusted Torsional Brace Stiffness .....	45



### List of Figures (Cont.)

4.1 Typical Load-Deflection Curve for First Mode Test .....	49
4.2 Typical Load-Deflection Curve for Second Mode Test .....	49
4.3 Typical Load-Twist Curve for First Mode .....	50
4.4 Meck Plotting Technique .....	50
5.1 Test Results for Beams with Lateral Bracing .....	61
5.2 Effects of Initial Imperfections on Lateral Bracing .....	61
5.3 Lateral Bracing, 0.16" Imperfection .....	63
5.4 Lateral Bracing, 0.22" Imperfection .....	63
5.5 Test Results For Beams with Torsional Bracing .....	65
5.6 Effect of Imperfections on Torsional Bracing .....	65
5.7 Test Results, Torsional Bracing with 0.04" Imperfection .....	67
5.8 Test Results, Torsional Bracing with 0.22" Imperfection .....	68
5.9 Torsional Bracing, 0.04" Imperfection, No Stiffener .....	69
5.10 Torsional Bracing, 0.04" Imperfection, 2"x1/4" Stiffener .....	69
5.11 Torsional Bracing, 0.04" Imperfection, 4"x1/4" Stiffener .....	70
5.12 Torsional Bracing, 0.16" Imperfection, 4"x1/4" Stiffener .....	70
5.13 Torsional Bracing, 0.22" Imperfection, No Stiffener .....	71
5.14 Torsional Bracing, 0.22" Imperfection, 2"x1/4" Stiffener .....	71
5.15 Torsional Bracing, 0.22" Imperfection, 4"x1/4" Stiffener .....	72
5.16 Torsional Brace Location - 0.16" Initial Imperfection .....	73
5.17 Torsional Brace Location - 0.22" Initial Imperfection .....	73
5.18 Forced Initial Imperfections .....	74

## Chapter 1 Introduction

### 1.1 Beam Buckling Strength

The flexural capacity of beams with large unbraced lengths is often limited by a mode of failure known as lateral torsional buckling. Lateral torsional buckling generally involves both an out-of-plane displacement and a twist of the beam cross-section as shown in Figure 1.1. Timoshenko (1960) presented the following equation for the elastic critical buckling moment of a doubly-symmetric beam failing by lateral torsional buckling.

$$M_{cr} = \frac{\pi}{L} \sqrt{EI_y GJ + \frac{\pi^2 E^2 I_y^2 h^2}{4L^2}} \quad (1.1)$$

where  $L$  = unbraced length,  $E$  = modulus of elasticity,  $I_y$  = weak axis moment of inertia,  $G$  = shear modulus,  $J$  = St. Venant's torsional constant, and  $h$  = distance between flange centroids. Equation 1.1 is applicable to beams where the twist and lateral displacement at the beam ends are prevented.

The first term under the radical denotes St. Venant torsional resistance of the cross-section while the second term is related to the warping torsional resistance. The unbraced length used in this equation should be the distance between points of full lateral support. When a beam is subject to a loading other than uniform moment, the maximum moment capacity may be significantly greater than that given by Equation 1.1. For this reason, a modifying factor can be applied to adjust for portions of the beam that are

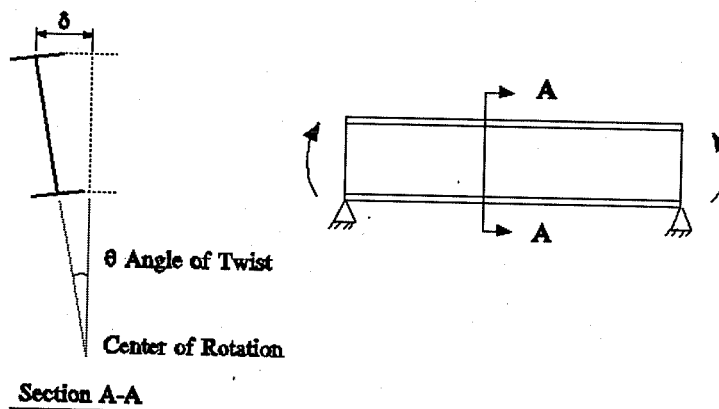


Figure 1.1 - Geometry of Buckled Beam

subject to a lower moment. While many methods have been presented for the determination of the moment gradient modifier, the *AISC-LRFD* (second edition), recommends that this factor, known as the  $C_b$  factor, be calculated using the following equation:

$$C_b = \frac{12.5M_{\max}}{2.5M_{\max} + 3M_2 + 4M_{c1} + 3M_4} \quad (1.2)$$

where  $M_{\max}$  = maximum moment on span,  $M_2$  = moment at 1/4 span,  $M_4$  = moment at 3/4 span,  $M_{c1}$  = moment at mid-span (all moments are taken as positive). This equation appears in a modified form in Kirby and Nethercot (1979) and will also appear in the second edition of the *AISC-LRFD* specification.

Kitipornchai and Richter (1978) examined the influence of load height

and concluded that in general the buckling strength of a beam is significantly increased when loads act below the shear center and significantly reduced when loads act above the shear center. Adjustments to account for the effects of load height can be found in Bleich (1978) and the SSRC Guide (1988).

## 1.2 Beam Bracing

In practice, beams are braced in a variety of ways in order to increase their buckling strength. Braces can be placed continuously along the length of a beam, as in the case of a floor system, or they can be placed at discrete intervals. In some cases, bracing of beams may be provided by another part of the load-carrying system such as a slab, secondary stringer, or purlin.

The effectiveness of a brace is determined by its ability to prevent twist of the cross-section. For this reason a brace should be placed at the point where it will best counteract the twisting of the cross-section. For the brace to be effective in preventing twist, it must possess not only the required strength but also a definite minimum stiffness. Historically, the determination of these requirements has been left to engineering judgement. Common practice to determine the required brace strength is to design the brace for two percent of the axial force in the compression zone of the beam. While the two percent rule usually provides sufficient strength in the brace, it does not guarantee that the brace will provide sufficient stiffness to raise the buckling load of the critical member to the desired level.

Bracing can be categorized into two main types, lateral bracing and torsional bracing. Lateral bracing increases the buckling strength of a member by restraining the lateral movement of the beam. Since most buckling problems involve twisting about a point near or below the tension

flange as shown in Figure 1.1, lateral bracing is most efficient when placed at the compression flange of the member. Figure 1.2 shows the relationship between  $M_{cr}$  and brace stiffness for a lateral brace at mid-span placed at either the centroid or the top flange. For full or complete bracing, a top flange brace stiffness of 10 k/in is required to reach the maximum moment associated with buckling between the braces,  $M_{cr}/M_o = 3.6$ , where  $M_o$  is the buckling capacity with no brace. If the lateral brace is at the centroid instead of the top flange, an eighteen fold increase in brace stiffness is required to reach the same moment. Figure 1.2 also shows the effect of cross-section distortion on the stiffness requirements for braces placed at the centroid. While distortion does not significantly effect the stiffness requirements of braces placed at the compression flange, it will significantly increase the required stiffness for braces placed at the centroid. When the brace is placed at a distance below the top flange, the compression flange can move laterally by distorting the web as shown in Figure 1.3.

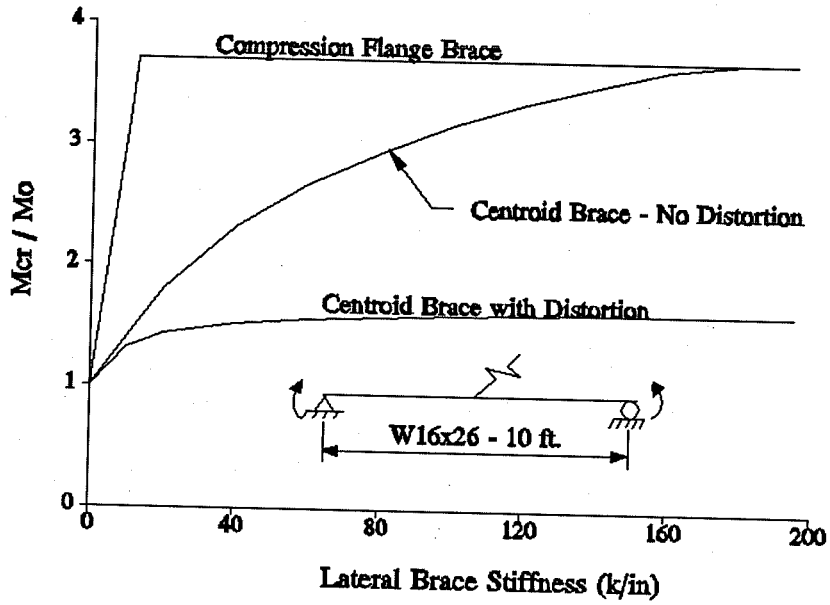


Figure 1.2 - Lateral Brace Location

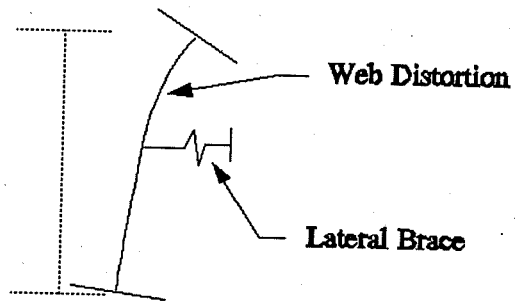


Figure 1.3 - Cross-Section Distortion

Historically, requirements for full lateral bracing have been determined using a simple model presented by Winter (1960). His model was developed for elastic column buckling and therefore can only be used to determine the required strength and stiffness of an ideal lateral brace attached at the compression flange. The ideal stiffness is defined as the stiffness required to force the member to buckle between the brace points. Table 1.1 shows a summary of Winter's ideal stiffness requirements where  $P_e$  is the Euler buckling load of the compression flange between brace points and  $\ell$  is the distance between brace points.

Number of Evenly Spaced Braces	Required Stiffness for Ideal Bracing
1	$2 P_e/\ell$
2	$3 P_e/\ell$
3	$3.41 P_e/\ell$
4	$3.63 P_e/\ell$
Continuous Bracing	$4.0 P_e/\ell$

Table 1.1 - Lateral Bracing Stiffness Requirements

Winter has shown that initial imperfections increase the ideal brace stiffness of a column by a factor of  $(1 + \Delta_o/\Delta)$  where  $\Delta_o$  is the magnitude of the initial imperfection and  $\Delta$  is the additional deflection permitted before the column fails. He also suggested that the required strength of the brace can be computed by multiplying the brace stiffness by  $(\Delta_o + \Delta)$ . Typical values for the deflections are  $\Delta = \Delta_o = L/500$  which gives a brace strength requirement of 0.8 percent of  $P_e$  when one brace is used.

When two or more adjacent beams are loaded simultaneously, they

may buckle in such a way that the lateral restraint provided by the connection member is nearly zero (Figure 1.4). The presence of a connection member such as a diaphragm or bridge deck may, however, provide adequate torsional bracing to stabilize the beams. Bridge decking in the form of a concrete slab or wood planks can provide torsional bracing with a stiffness of  $6EI/S$  where  $E$  and  $I$  are deck properties and  $S$  is the spacing of the girders.

Figure 1.5 shows the behavior of a beam braced torsionally at mid-span. For a beam with no web distortion, the buckling strength increases with brace stiffness until it reaches the load associated with the second mode full bracing. The value of ideal stiffness required to produce this load is not as sharply defined for torsional bracing as it was with lateral bracing. The lower curve in this figure shows typical behavior for a torsionally braced beam with a slender web and no stiffeners. Note that the beam is limited to a much smaller load even at high values of brace stiffness. Figure 1.6 shows schematically the web distortion of a typical slender web beam with a torsional brace placed at the compression flange. Since many beams do not possess the required web stiffness, it is often necessary to either attach a stiffener at locations of torsional bracing or reduce the allowable load of the member to account for web distortion.

Figure 1.7 shows the relationship between brace stiffness and critical load for discrete torsional bracing and continuous torsional bracing. With continuous bracing, the critical moment of the member will increase without limit, until yielding occurs, as the brace stiffness is increased whereas a beam that is braced at discrete intervals will be limited to the critical moment corresponding to buckling between the brace points. For a single brace at mid-span, the maximum moment is reached when the beam reaches the load



corresponding to the second mode of buckling. The second mode can be identified by the "S" shaped curve of the compression flange. The relationship in Figure 1.7 indicates that a design formula for continuous bracing can be used for discrete bracing if the maximum moment is limited to the buckling load between braces.

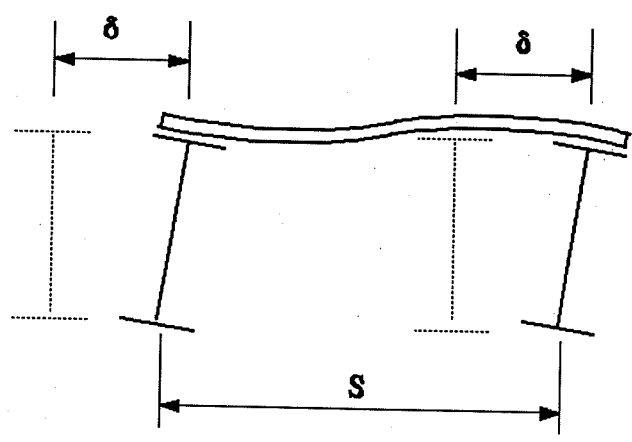


Figure 1.4 - Buckled Shape of Bridge Girders

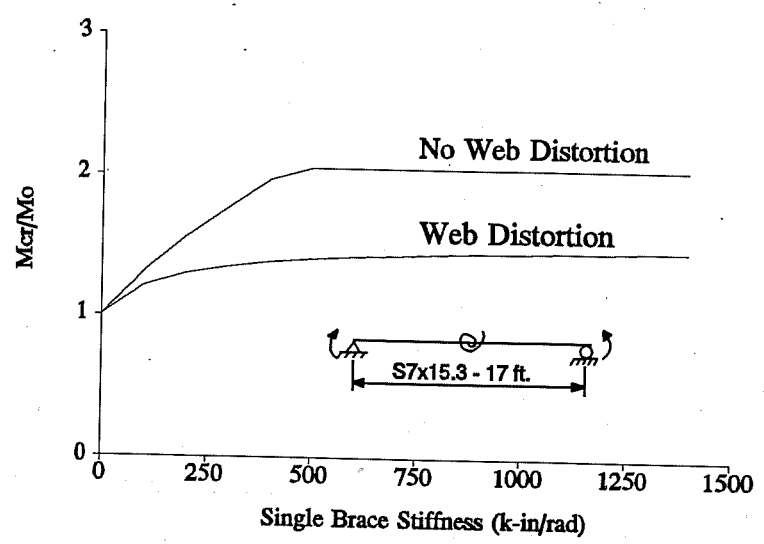


Figure 1.5 - Effects of Cross-Section Distortion

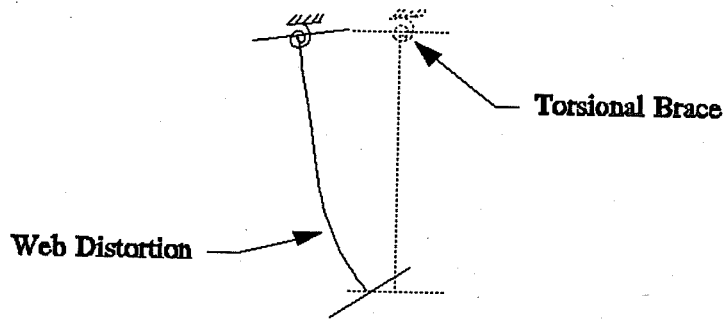


Figure 1.6 - Cross-Section Distortion

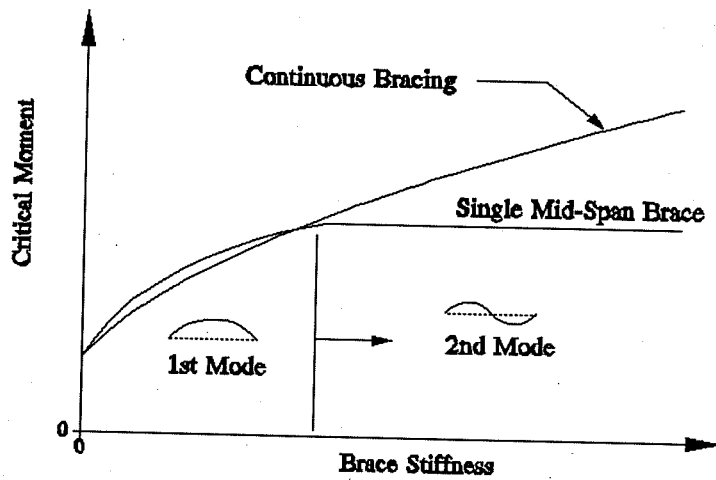


Figure 1.7 - Continuous vs. Discrete Bracing

### 1.3 Previous Approaches to Beam Bracing

Many authors have studied beam bracing requirements and some texts have given a brief review of bracing requirements. A partial list of these texts include Salmon and Johnson (1990), Rhodes and Walker (1982), Kirby and Nethercot (1979), and the SSRC Guide. To provide a brief historical review of the developments in beam bracing, only a few selected papers are presented.

Flint (1951a) presented experimental data for the buckling of a beam with a lateral brace located at mid-span on the top flange, bottom flange, or at the shear center. He also presented graphical solutions for a torsional brace at mid-span. In his graphs, the critical moment increased to a maximum moment of twice the unbraced beam moment at a brace stiffness of infinity. The inaccuracy of this solution can be seen by observing that the critical moment will increase nearly linearly with brace stiffness until the second mode "S" shape is reached at a finite brace stiffness. Flint also indicated that a brace can be effective by only preventing twist of the cross-section while allowing lateral movement to occur.

Flint, (1951b), studied the stability of beams loaded through secondary members. He examined the restoring effect of a load that is applied through a relatively stiff secondary member resting on the top flange of the critical beam. Ignoring the effects of cross-section distortion, Flint found that no lateral buckling can occur in the first mode unless the beam has an initial bow greater than half the flange width.

Winter (1960) has shown that an effective column brace must possess not only the required strength but also a minimum stiffness (Table 1.1). He

examined discrete column bracing both experimentally and analytically and concluded that an initial imperfection has the effect of increasing the required brace stiffness by a factor of  $(1 + \Delta_0/\Delta)$ .

Taylor and Ojalvo (1966) presented solutions for the buckling capacity of a beam with continuous torsional bracing or a discrete torsional brace at mid-span. The beam can be loaded with uniform moment, point loading at mid-span, or uniform load. The analysis used to determine the critical load was an improvement over previous approaches since it included both St. Venant and warping resistance. The buckling load is obtained by using a graphical constant  $m$  in the following equation:

$$M_{cr} = \frac{m}{L} \sqrt{EI_y GJ} \quad (1.3)$$

The main drawback to this equation is that the constant  $m$  must be obtained from a set of graphs corresponding to unique bracing cases. In addition to graphical solutions, Taylor and Ojalvo indicated that the critical moment of a beam with continuous torsional bracing under uniform moment can be determined from the following equation:

$$M_{cr} = \frac{\pi}{L} \sqrt{EI_y GJ + \frac{\pi^2 E^2 I_y^2 h^2}{4L^2} + \frac{\beta_T L^2 EI_y}{\pi^2}} \quad (1.4)$$

where  $\beta_T$  = continuous torsional brace stiffness (k-in/rad per in. length).

Mutton and Trahair (1973) presented equations for the interaction of lateral and torsional bracing for beams subject to equal end moments or central concentrated loads. Their paper gave closed-form equations to find

the amount of additional torsional bracing needed when a lateral brace is placed at the centroid of the beam cross-section. The effects of cross-section distortion were not considered.

Rhodes and Walker (1982) presented an overview of bracing requirements for beams. Graphical solutions were given for beams loaded with uniform moment, point loads, or uniform load braced by continuous or discrete braces. Their evaluation of lateral brace attachment heights indicated that a lateral brace is most effective when placed at the compression flange. The influence of load height on brace stiffness was examined and presented in graphical form. A method for estimating the torsional restraint with flexible brace connections was given as follows,

$$\frac{1}{\alpha_{kr}} = \frac{1}{\alpha_p} + \frac{1}{\alpha_{web}} + \frac{1}{\alpha_j} \quad (1.5)$$

where  $\alpha_{web} = 0.5Et^3$ ,  $t$  = web thickness,  $\alpha_{kr}$  = reduced torsional brace stiffness,  $\alpha_p$  = brace stiffness, and  $\alpha_j$  = stiffness of connection.

Tong and Chen (1988) have studied the buckling behavior of a simply supported beam under uniform moment. To apply their equations, the beam can be braced laterally or torsionally at the mid-span and can be doubly-symmetric or mono-symmetric. Closed-form solutions for the required stiffness of ideal bracing for these cases were obtained. For torsional bracing, the ideal brace stiffness is given by the following equations:

$$K_{ideal} = \frac{2\pi(8 + \alpha_c^2)\sqrt{(4 + \alpha_c^2)}}{\alpha_c^2} \quad (1.6)$$

$$\text{where} \quad \alpha_c^2 = \frac{GJL^2}{\pi^2 EC_w} \quad (1.7)$$

The Tong and Chen solutions do not consider web distortion which often has a significant effect on the bracing requirements as shown in Figure 1.5.

#### 1.4 Limitations of Current Approaches

While the approaches mentioned above provide useful information on the behavior of bracing, they do not provide practical design guidelines for the determination of brace requirements under normal design situations. Few authors have considered the effects of cross-section distortion, initial imperfections, or inelastic behavior. Little work has been done to verify the behavior of partially effective braces or to determine the effects of cross-section distortion, initial imperfections and moment gradients experimentally.

#### 1.5 Objectives of Research Program

A testing program was undertaken to study experimentally the lateral torsional buckling of beams with lateral and torsional bracing. The objective of the program was to develop general design equations and to provide experimental evidence of their validity. The program involved the testing of two 24 foot long W12x14 steel beams with point loads at mid-span. Both lateral braces and torsional braces were applied at the mid-span of the beams. Varying levels of initial imperfection and stiffener sizes were studied. Design

recommendations were developed based on previous literature, finite element computer studies, and the current experimental work.



## **Chapter 2 Analytical Program**

### **2.1 General**

The analytical portion of the research program consisted of two key components; finite element modeling of the test beam and development of design equations for beam bracing. The finite element analysis was conducted to estimate the buckling strength of the test beam and to investigate the behavior of bracing for cases that were not investigated experimentally.

Bracing design equations for initially straight beams are presented and compared to results from finite element studies. These equations are extended in Chapter 5 to cover beams with initial imperfections.

### **2.2 Description of BASP Computer Program**

The finite element program, BASP, an acronym for buckling analysis of stiffened plates, was developed for use on a personal computer at The University of Texas at Austin by Choo (1987). The BASP program will handle many types of restraints including lateral and torsional braces at any node point along the span. It is limited, however, to elastic modeling of initially straight beams with loads acting only in the plane of the web. Due to these limitations, the effects of initial imperfections were not studied using the program. However, BASP does account for web distortion and was used extensively in the development of basic design equations for straight beams.

The W12x14 test beam was modeled on the BASP program using the boundary conditions shown in Figure 2.1. The in-plane supports were modeled as rollers and out-of-plane displacements, at the ends, were prevented. In order to more accurately analyze web distortion that may occur near the brace point, the finite element mesh was broken into finer elements

near the brace locations (Figure 2.2). This change also provided the proper node location for attachment of the torsional bracing.

Figure 2.3 shows the buckled shape of a W12x14 beam with no bracing and Figure 2.4 shows the buckled shape of the same beam with a relatively stiff brace at mid-span. The curves in these plots show the displacement of each line of nodes on the beam mesh. The outer curve corresponds to the nodal line on the top flange while the inner-most curve corresponds to the bottom flange of the beam. Both the center of twist and the amount of cross-section distortion can be estimated and compared by careful observation of these plots.

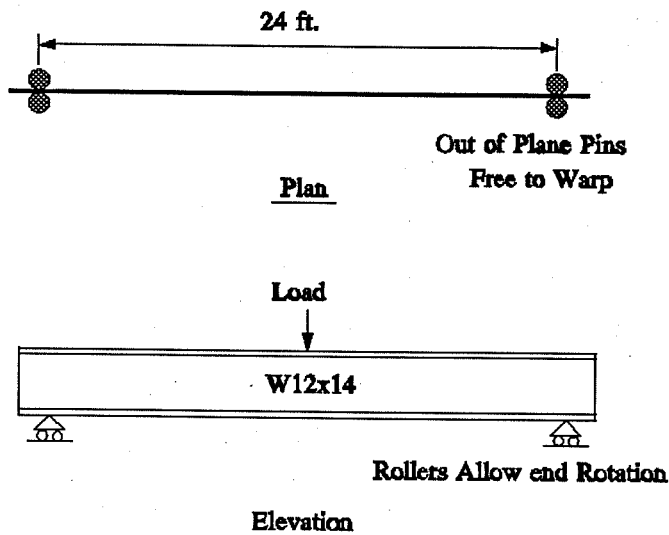


Figure 2.1 - Boundary Conditions used in BASP Program

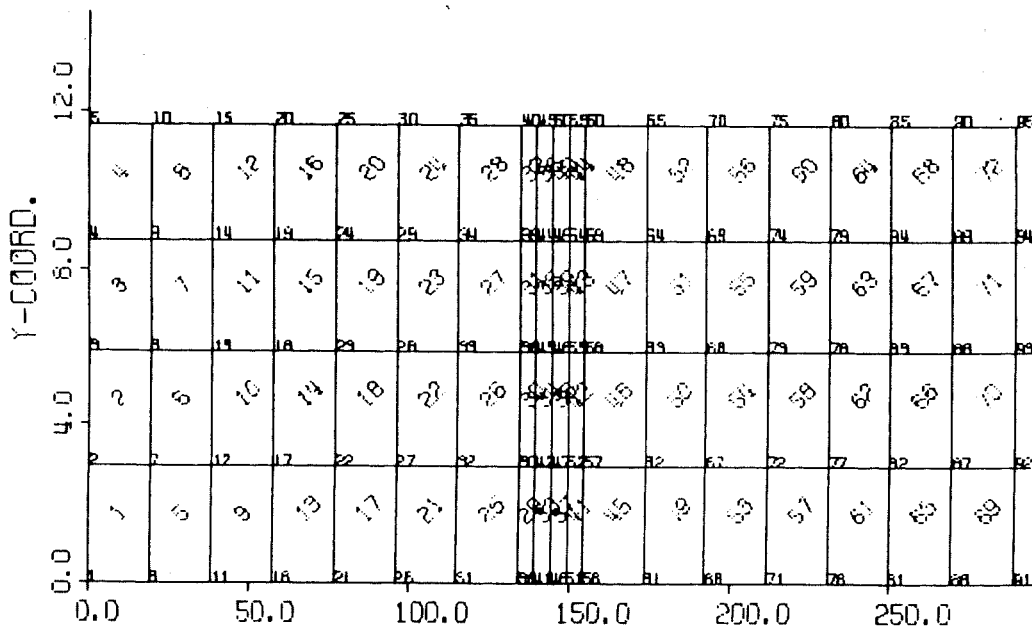


Figure 2.2 - Finite Element Mesh used in BASP

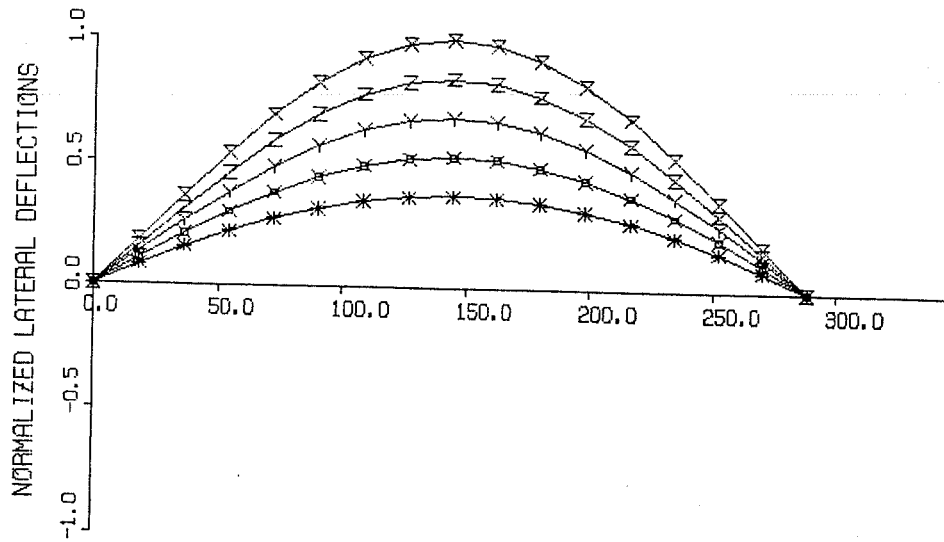


Figure 2.3 - First Mode Buckled Shape

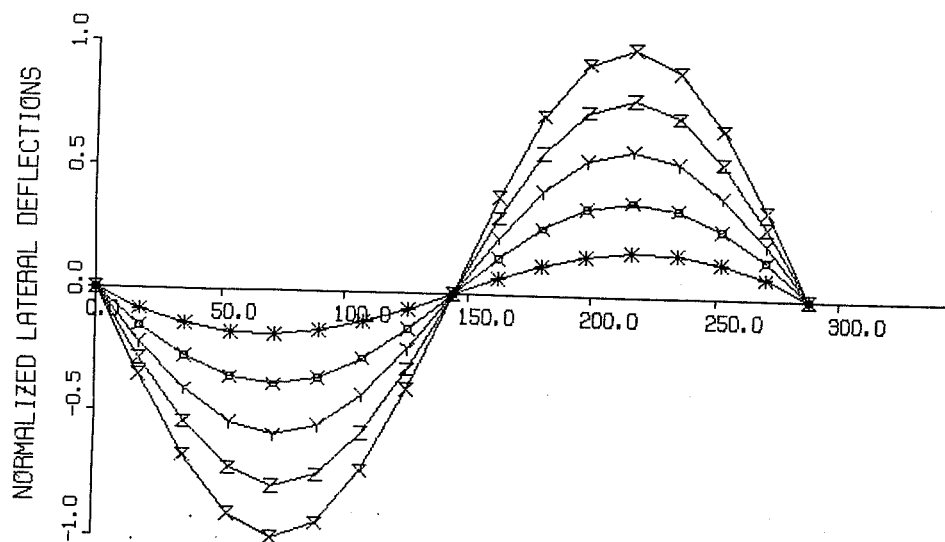


Figure 2.4 - Second Mode Buckled Shape

### 2.3 Design Equations for Intermediate Lateral Bracing

A general design equation has been developed by Yura (1990), for discrete or continuous lateral bracing of beams as follows,

$$M_{CR} = \sqrt{\left(M_o^2 + \frac{P_y^2 h^2 A}{4}\right) (1 + A)} \quad (2.1)$$

$$\text{where } A = \frac{L^2}{\pi} \sqrt{\frac{.67 \beta_L}{EI_y}} \quad (2.2)$$

$$P_y = \frac{\pi^2 EI_y}{L^2} \quad (2.3)$$

where  $M_o$  is given by Equation 1.1, and  $\beta_L$  = equivalent continuous lateral brace stiffness in k/in/in. Since lateral bracing becomes ineffective when placed at a distance below the compression flange, Equation 2.1 applies only to compression flange bracing. Analytical studies using BASP have shown that the effects of cross-section distortion on the effective stiffness of lateral bracing placed at the compression flange are minimal and can be neglected.

When using Equation 2.1, a finite number of discrete lateral braces along a beam should be converted to an effective continuous lateral brace. In general, multiple braces can be represented by summing the stiffness of each brace and dividing by the beam length. By comparison to finite element solutions, a single discrete brace at mid-span can be represented as a continuous brace by dividing the brace stiffness by 75 percent of the beam

length.

When using the continuous bracing analogy, the critical moment must be limited to the moment corresponding to the deflected shape of the fully-braced case. In other words, the critical moment cannot exceed the moment given by Equation 1.1 where  $l$  is taken as the longest distance between braces. Figure 2.5 shows the maximum moment level that can be reached for various numbers of equally spaced braces. Figure 2.6 shows a comparison of Equation 2.1 and solutions given by the BASP program for a beam under uniform moment with three equally spaced braces.

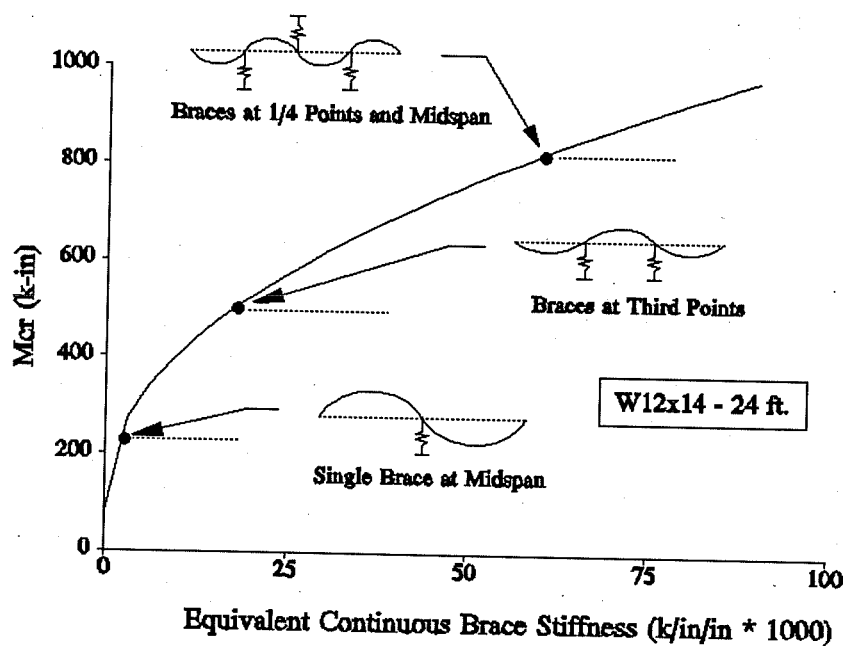


Figure 2.5 - Limiting Values of Critical Moment

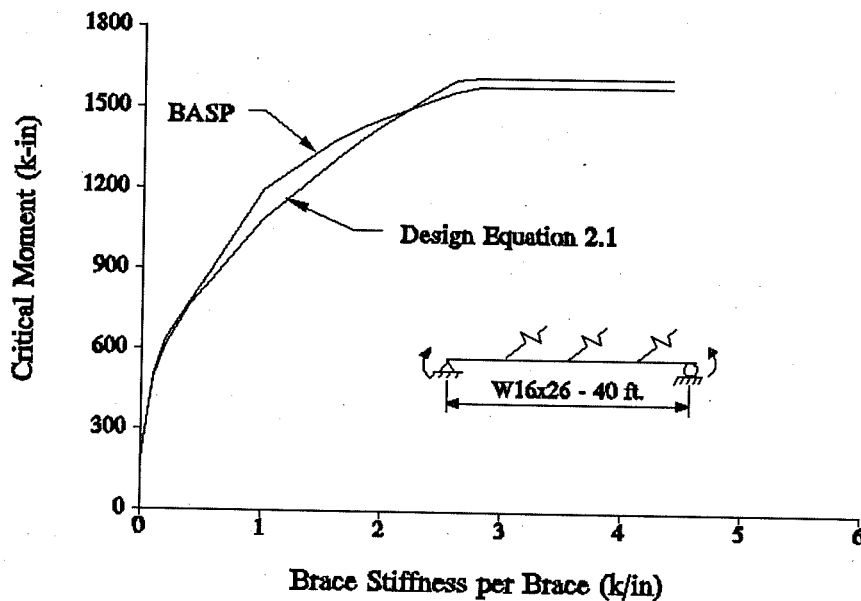


Figure 2.6 - Comparison of Lateral Bracing under Uniform Moment

#### 2.4 Design Equations for Intermediate Torsional Bracing

Taylor and Ojalvo (1973) derived an equation for the critical moment of a beam under uniform moment with continuous torsional bracing along the compression flange as follows,

$$M_{cr} = \sqrt{M_o^2 + \beta_T EI_y} \quad (2.4)$$

where  $M_o$  is given by Equation 1.1, and  $\beta_T$  = equivalent continuous torsional brace (k-in/rad per in. length).

This equation can be used to represent multiple discrete torsional braces by summing the stiffness of each brace and dividing by the beam

length. For a single brace at mid-span the equivalent continuous brace stiffness can be found by dividing the brace stiffness of the single brace by 75 percent of the beam length; this is the same procedure that was suggested for a single lateral brace at mid-span. Figure 2.7 shows a comparison of Equation 2.4 and solutions predicted by the BASP program for a beam under uniform moment with three equally spaced braces. Based on the comparisons shown in Figure 2.6 and 2.7, the design equations for both lateral and torsional bracing provide an accurate determination of the critical moment of a beam with multiple discrete braces.

The analytical studies have shown that the effective stiffness provided by a torsional brace is greatly reduced by web distortion that may occur at the brace location. Since many beams do not possess the required web stiffness, a stiffener must often be attached at locations of torsional bracing. Equation 2.5 can be used to account for the effect of web distortion on the effective brace stiffness or to determine the required stiffener size to develop the desired effective torsional stiffness of the beam cross-section.

$$\frac{1}{\beta_T} = \frac{1}{\beta_b} + \frac{1}{\beta_{sec}} \quad (2.5)$$

$$\text{where } \beta_{sec} = 3.3 \frac{E}{h} \left( \frac{1.5ht_w^3}{12} + \frac{t_s b_s^3}{12} \right) \quad (2.6)$$

where  $\beta_b$  = attached brace stiffness,  $\beta_{sec}$  = total section stiffness,  $t_w$  = thickness of web,  $h$  = depth of web,  $t_s$  = thickness of stiffener,  $b_s$  = width of stiffener. For continuous bracing use  $l$  in place of  $1.5h$  in Equation 2.6.

When a beam is braced with both lateral and torsional bracing,



Equations 2.1 and 2.4 can be combined as follows,

$$M_{CR} = \sqrt{\left(M_o^2 + \frac{P_y^2 h^2 A}{4}\right) (1 + A) + \beta_T EI_y} \quad (2.7)$$

Equation 2.7 is an approximation of the interaction between lateral and torsional bracing. Figure 2.8 compares the interaction given by Equation 2.7 to the interaction predicted by the BASP program. The line labeled "Linear Interaction" corresponds to the levels of bracing that would be required if Equation 2.1 and Equation 2.4 were applied independently.

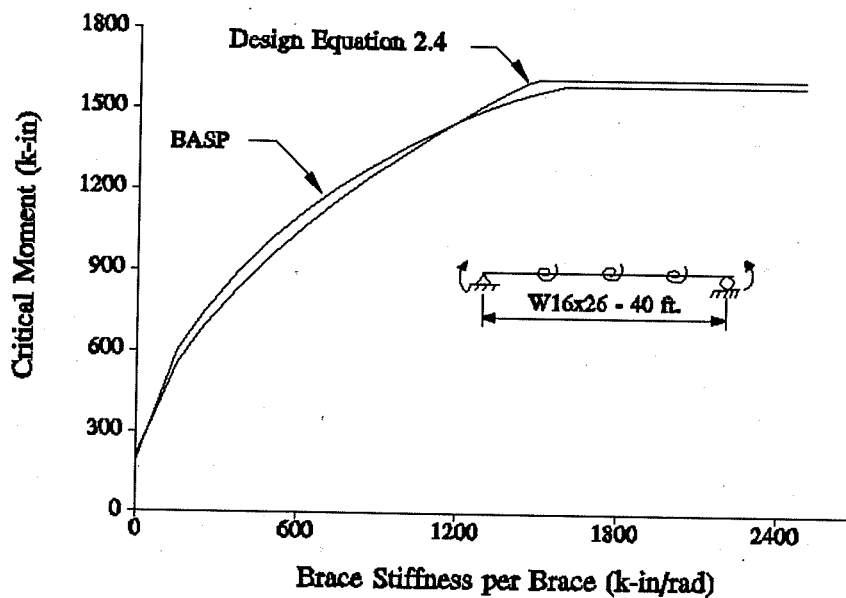


Figure 2.7 - Comparison of Torsional Bracing under Uniform Moment

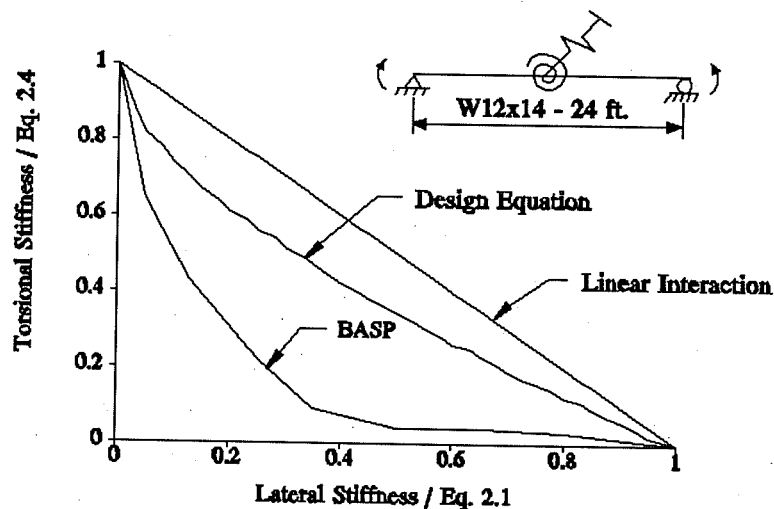


Figure 2.8 - Interaction of Lateral and Torsional Bracing

## 2.5 Modifications for Moment Diagram Effects and Load Height

When a beam is subject to a loading other than uniform moment, the maximum moment capacity may be significantly greater than that found by Equation 2.7. For this reason, an amplification factor can be applied to adjust for portions of the beam that are not subject to the level of moment determined in the solution for critical uniform moment. For beams with bracing, the  $C_b$  factor should be calculated for the unbraced beam and multiplied by the critical moment determined from Equation 2.7 as follows,

$$M_{\max} = C_b M_{cr} \quad (2.8)$$

where  $M_{\max}$  = maximum moment at any location,  $M_{\text{cr}}$  = moment determined from Equation 2.7.

For a beam with multiple braces, the critical moment should be limited to the moment corresponding to buckling of the critical span. This can be determined by calculating the critical moment for each unbraced length (Equation 1.1), and applying the  $C_b$  factor associated with that unbraced length. Figure 2.9 and 2.10 show comparisons of the design equations to solutions predicted by the BASP program for a beam with three lateral or torsional braces and loaded by mid-span point loading at the centroid of the beam cross-section. A  $C_b$  factor of 1.30 was used in the calculation of the design curves for both figures with the maximum load determined from the moment corresponding to buckling between the braces.

The conservativeness of the design equations at high values of brace stiffness is due to the method used to determine the moment corresponding to buckling between brace points. This moment was found from the smallest of the two capacities associated with buckling between different braces. Since the moment levels are much higher between the mid-span brace and the 1/4 span brace, the middle sections will give the lowest  $C_b$  factor and thus the lowest capacity. It is possible to adjust these curves to a higher value of peak load by accounting for the extra out-of-plane restraint provided to the most critical portions of the beam from portions of the beam under less load through the use of effective unbraced length,  $k\ell$ . The design equations shown in both figures give a conservative estimate of the buckling strength

Comparisons to finite element solutions have shown that the effects of top-flange loading can be estimated by removing the warping term in the determination of  $M_o$ . Figure 2.11 and 2.12 show comparisons of design

equations to solutions from the BASP program. The curves labeled "Design Equation" in these figures were calculated using a  $C_b$  factor of 1.30 and ignoring the warping term in the determination of  $M_o$ . The design equation curve for lateral bracing shown in Figure 2.11 is unconservative for small values of bracing. This indicates that additional studies need to be performed to determine a more accurate determination of the effects of load height. The design curves for torsional bracing, however, give an accurate estimate of the buckling strength as shown in Figure 2.12.

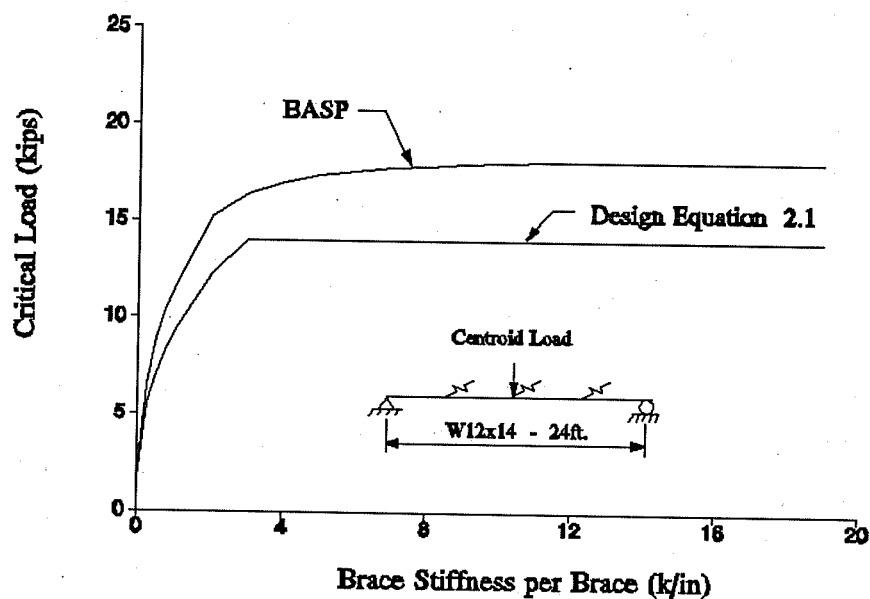


Figure 2.9 - Comparison of Lateral Bracing under Centroid Point Loading

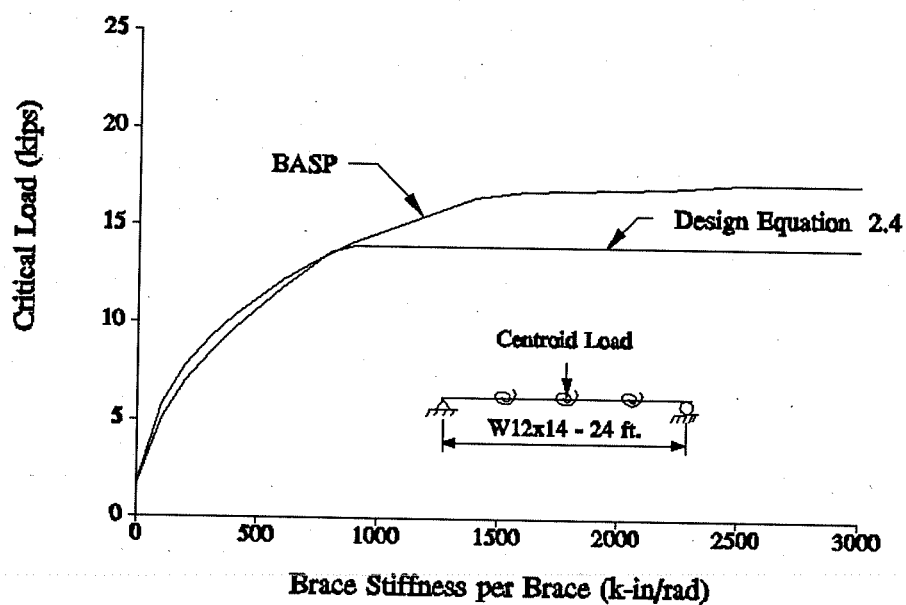


Figure 2.10 - Comparison of Torsional Bracing under Centroid Point Loading

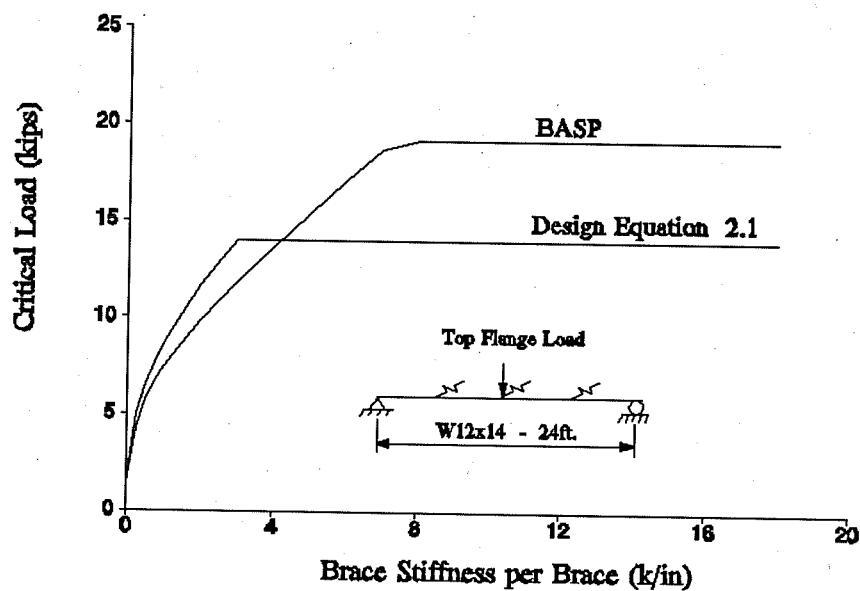


Figure 2.11 - Comparison of Lateral Bracing under Top Flange Point Loading

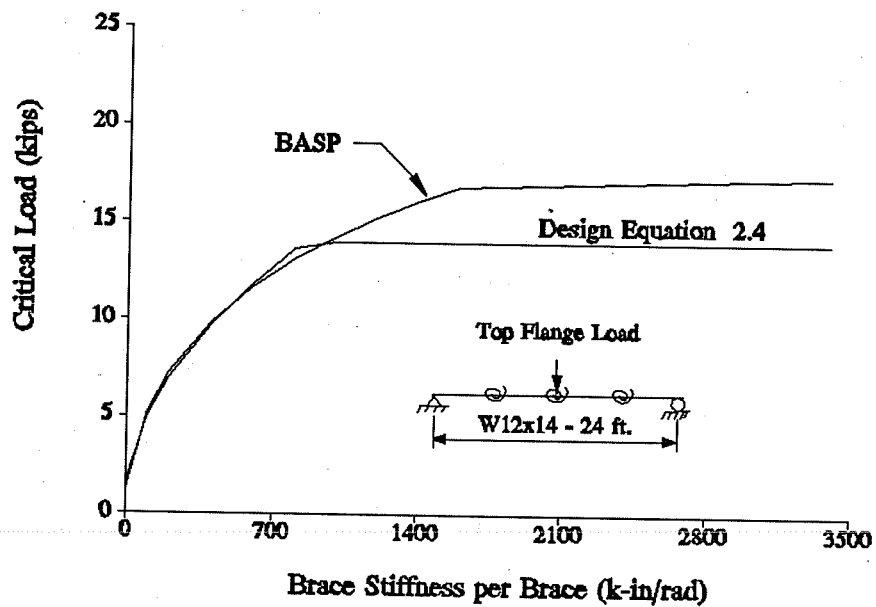


Figure 2.12 - Comparison of Torsional Bracing under Top Flange Point Loading

Figure 2.13 and 2.14 compare the design equations to BASP solutions for beams with a single brace at mid-span. The equivalent continuous brace stiffness used in the calculation of the curves labeled "Design Equation" was found by dividing the brace stiffness by 75 percent of the beam length instead of the total beam length as was done in the preceding figures. A  $C_b$  factor of 1.30 was used and the warping term was ignored in the determination of  $M_o$ .

Based on these figures, the design equations provide an accurate determination of the critical load for a beam with multiple braces or a single brace. Note that in all cases with point loading, the load was applied at a brace point. During this study, all braces had equal stiffness and equal spacing. The accuracy of the design equations has not been verified for other cases.

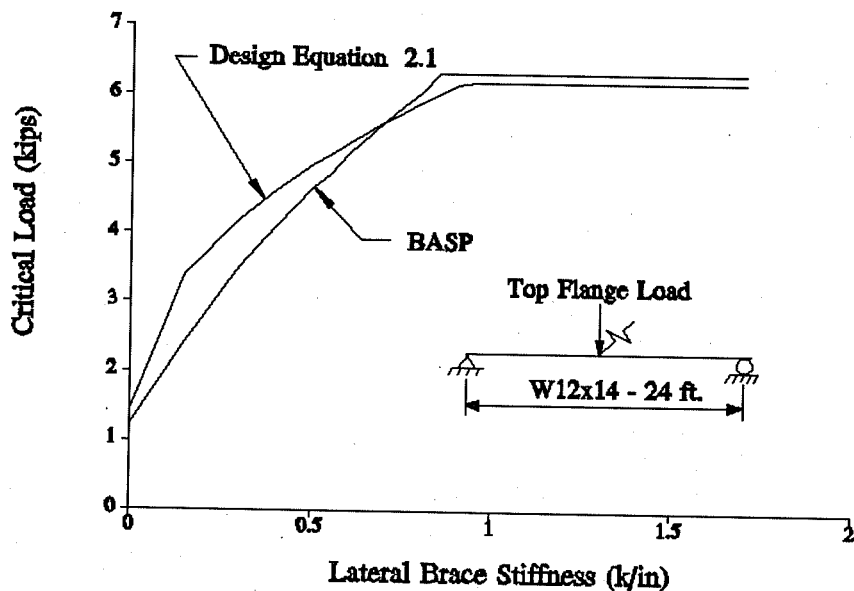


Figure 2.13 - Comparison of Lateral Bracing under Top Flange Point Loading

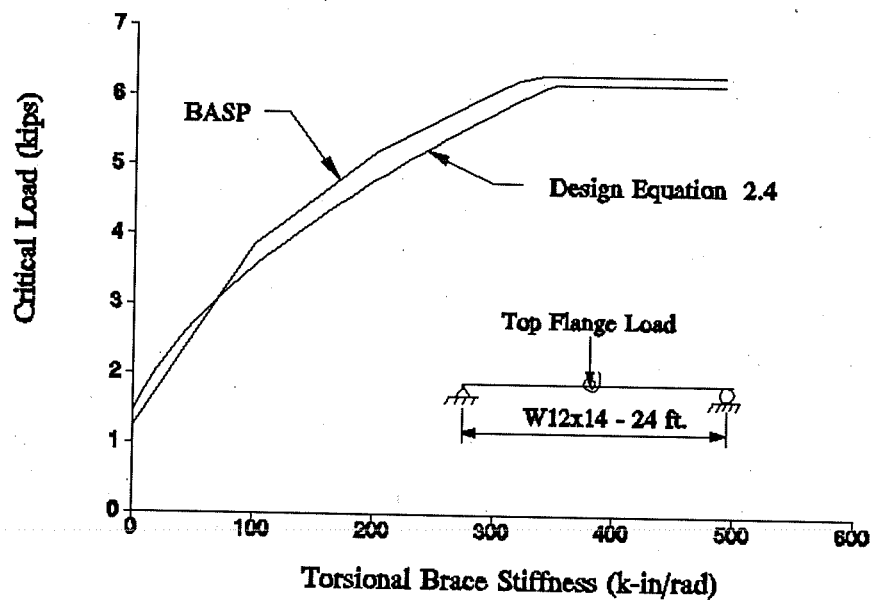


Figure 2.14 - Comparison of Torsional Bracing under Top Flange Point Loading



## Chapter 3 Experimental Program

### 3.1 General

The experimental program consisted of 76 tests designed to evaluate the effects of lateral and torsional brace stiffness, brace location, stiffener size, and initial imperfections on the lateral torsional buckling of steel beams. Two identical simply supported beams were loaded at mid-span as shown in Figure 3.1 until buckling occurred. The buckling load determined from this beam arrangement was an average buckling load for the two beams. Figure 3.2 shows the overall test setup.

Both test beams were taken from the same mill batch of high-strength steel so that all buckling would occur in the elastic range. The measured yield strengths of the flange and web were 65 ksi and 69 ksi, respectively. Figure 3.3 shows the average measured cross-section properties of the two beams.

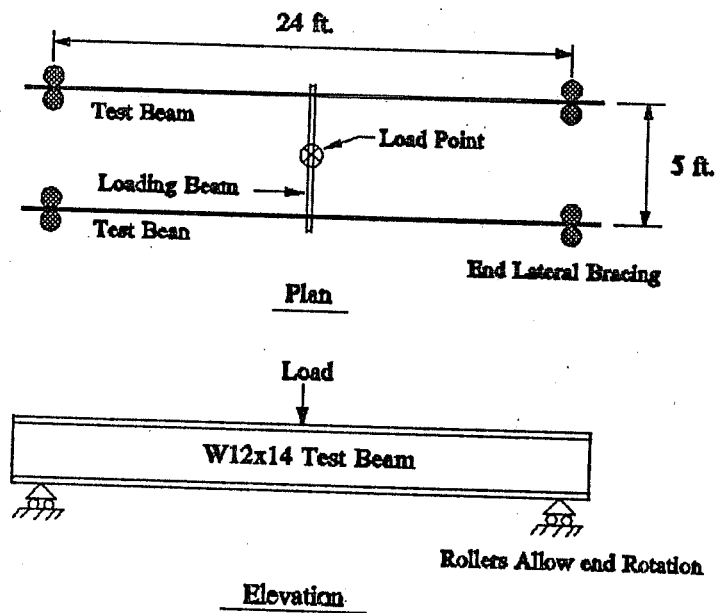


Figure 3.1 - Schematic of Test Setup

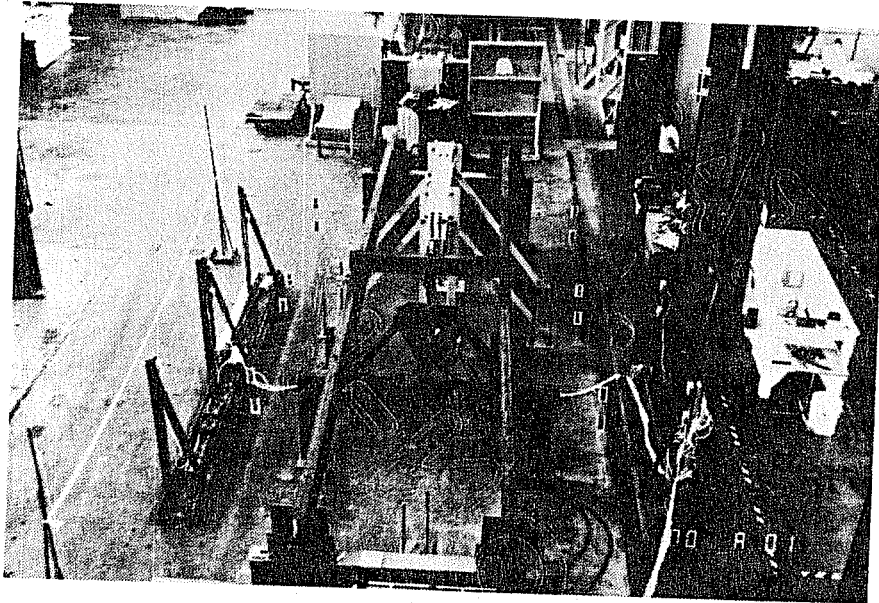
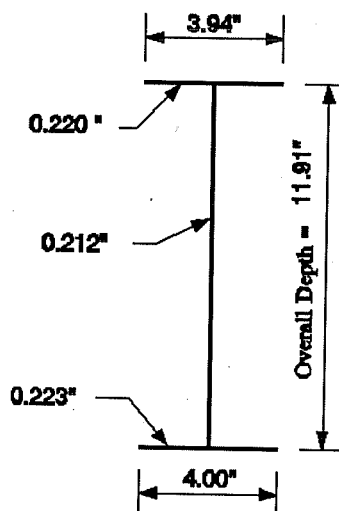


Figure 3.2 - Overall Test Setup

### Calculated Properties

<b>A</b>	<b>4.19 In<sup>2</sup></b>
<b>I<sub>x</sub></b>	<b>86.7 In<sup>4</sup></b>
<b>S<sub>x</sub></b>	<b>14.6 In<sup>3</sup></b>
<b>I<sub>y</sub></b>	<b>2.32 In<sup>4</sup></b>
<b>S<sub>y</sub></b>	<b>1.16 In<sup>3</sup></b>
<b>J</b>	<b>0.065 In<sup>4</sup></b>
<b>h</b>	<b>11.71 In</b>



**Figure 3.3 - Average Cross-Section Properties of Test Beam**

### **3.2 Loading and Support System**

In the laboratory, gravity type loads are usually applied by using a testing machine or a firmly supported jack. This technique works well for structures that displace following the line of action for the loading device. For structures that are allowed to sway or buckle, the line of action of the load will no longer be vertical and care must be taken so that the loading device will not restrain the lateral movement of the test specimen. When a structure sways, the vertical nature of true gravity load must be approximated.

In the twin beam setup, the mid-span load was maintained vertical by the use of a gravity load simulator mechanism shown in Figure 3.4. This mechanism has been used extensively in the testing of structures permitted to sway. The design concept of the simulator is given by Yarimci, Yura, and Lu

(1966) and will not be discussed here. The simulator used in the test setup could safely maintain a load of 44 kips with a sway of six inches.

While the mechanism does a very good job of simulating gravity load it is, however, not perfect. The friction in the bearings produce a slight "lag" in the realignment of the ram to the vertical position during sway. This effect was determined experimentally by applying a lateral load to the base of the loading ram at point o in Figure 3.5 and measuring the corresponding lateral movement. The value of this restraint was determined at six different load levels. During the first test, it was found that the friction in the gravity load simulator produced a sawtooth type load-deflection curve. In order to minimize this effect, a small vibration motor was attached to the frame of the load simulator that served to increase the rate at which the ram was realigned to the vertical position. It was not possible to perform a calibration of the gravity load simulator with the vibration motors running due to the sensitivity of the instrumentation.

The effects of non-ideal behavior, such as restraints at the ends of the beam, were studied using BASP and found to have a significant effect on the buckling load. In light of this, the friction at the end supports was minimized by using ball bearing fixtures that would allow axial lengthening of the beam as well as out of plane rotation at the supports (Figure 3.6). Load was transferred to the test beams through knife-edges placed between the loading beam and the test beam (Figure 3.7). The knife edges were placed at the center of the flange, parallel to the beam span, so that they would not effect the twist of the test beam. The knife edges were connected to the loading tube with roller bearings to prevent the addition of significant warping restraint to the test beams from the applied loading.

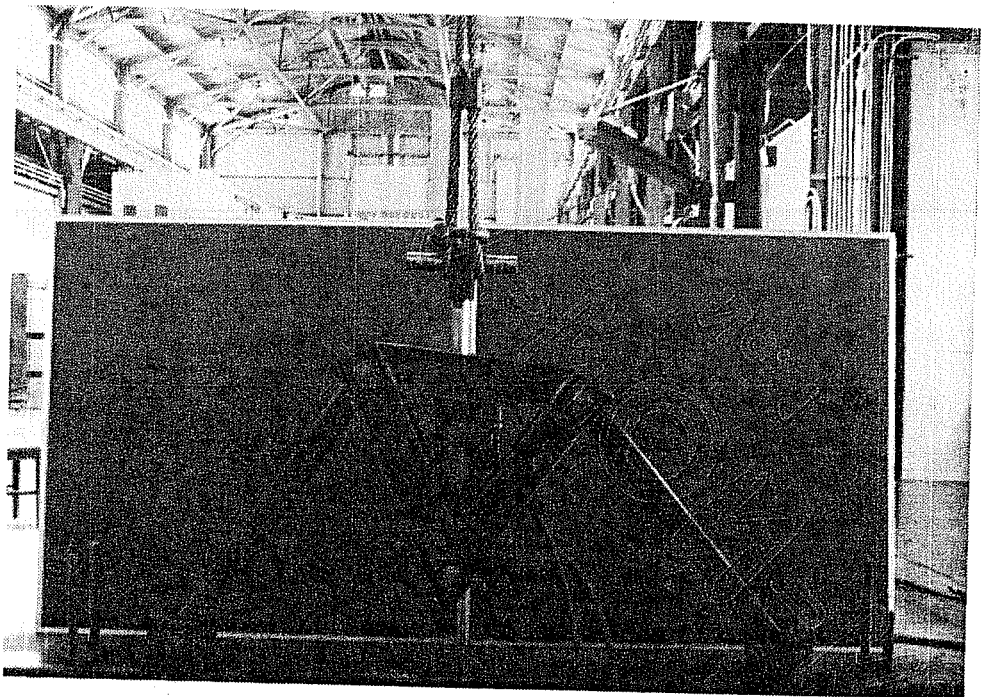


Figure 3.4 - Gravity Load Simulator

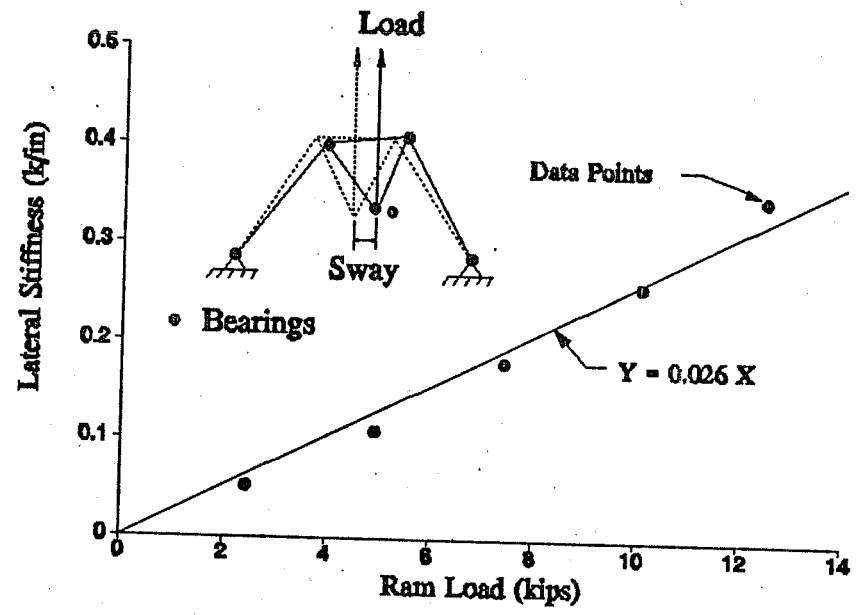
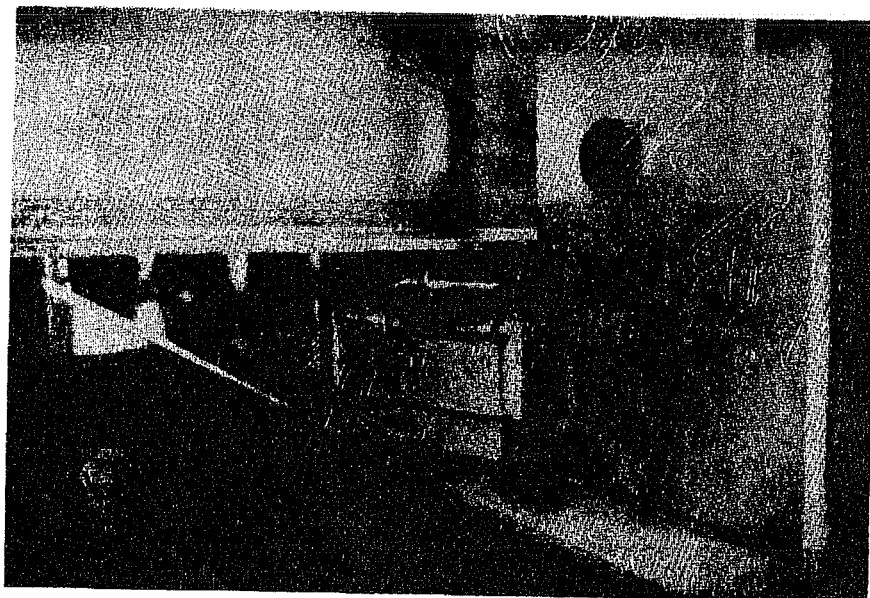


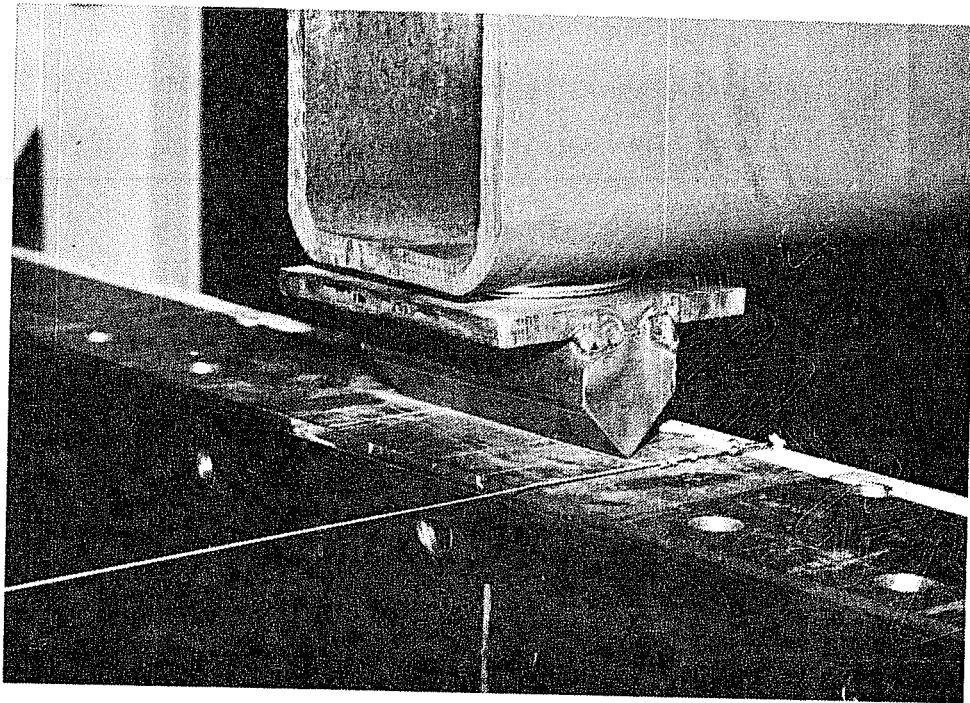
Figure 3.5 - Lateral Stiffness of Gravity Load Simulator Due to Friction



**Figure 3.6 - End Roller Bearings**

### **3.3 Instrumentation**

During testing, lateral deflections, vertical deflections, flange rotation, and load were recorded. Lateral deflection measurements were recorded on both the top and bottom flange at the mid-span and quarter points of each beam. Vertical deflections were recorded at the mid-span of each beam. Load was recorded using a load cell located between the ram and loading tube. The load cell had a capacity of 50 kips and a precision of 50 pounds. A pressure transducer measured the hydraulic pressure in the ram to provide another measure of load. There was no significant difference between load levels reported by the load cell and those calculated from the pressure readings.



**Figure 3.7 - Knife Edges**

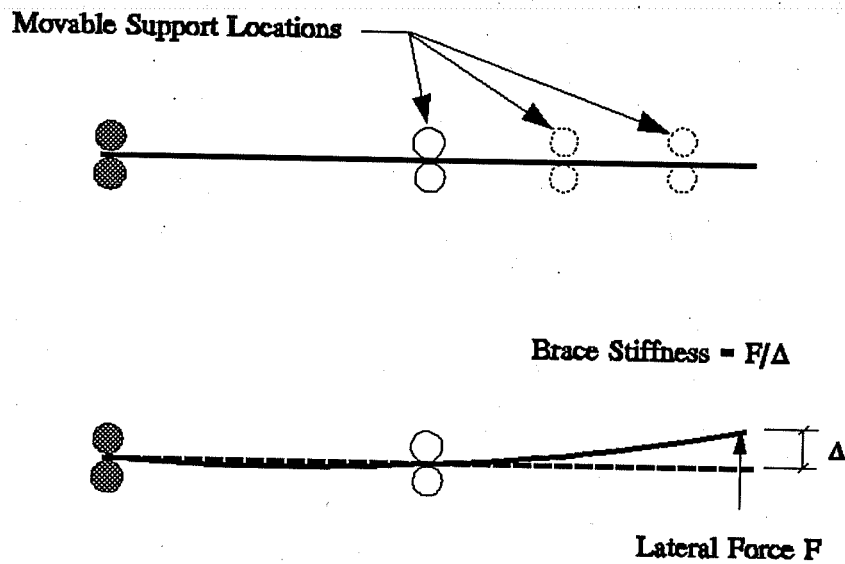
All deflections were recorded using electronic linear displacement gauges. To obtain an accurate measure of lateral deflection directly from the gage readings, the lateral displacement gauges were placed four feet from the test beam in order to minimize the error due to the vertical component of the gauge displacement. This resulted in an accuracy of 0.05 inches at the maximum vertical deflection experienced during testing. Displacement gauges were connected to the top and bottom flanges of each beam at the quarter-span, mid-span, and three-quarter span giving a total of 12 lateral displacement readings at each load level. By placing gauges at both the top and bottom flanges, the average twist of the cross-section could be calculated at each gauge location.

Additional measurements of twist were recorded using two electronic tilt meters. These meters were located at the mid-span of one beam, one on the top flange and one on the bottom flange. Since these meters recorded the tilt of each flange near the brace point, an estimate of the cross-section distortion was obtained for each test. All displacement and load readings were recorded using a computer controlled data acquisition unit in which all data during a load cycle could be recorded within a few seconds.

### **3.4 Lateral Bracing System**

The lateral bracing was provided by a simply supported aluminum bar with an adjustable overhang (Figure 3.8). Six different levels of stiffness were provided in this fashion by simply changing the size of the aluminum bar or the location of the adjustable support. Figure 3.9 shows the lateral bracing system used in the test setup. The stiffness of the lateral bracing system was significantly affected by the stiffness of the accompanying supports, so it was necessary to obtain the effective stiffness of the bar-support system experimentally. The measured value of stiffness for each lateral brace configuration is shown in Table 3.1.

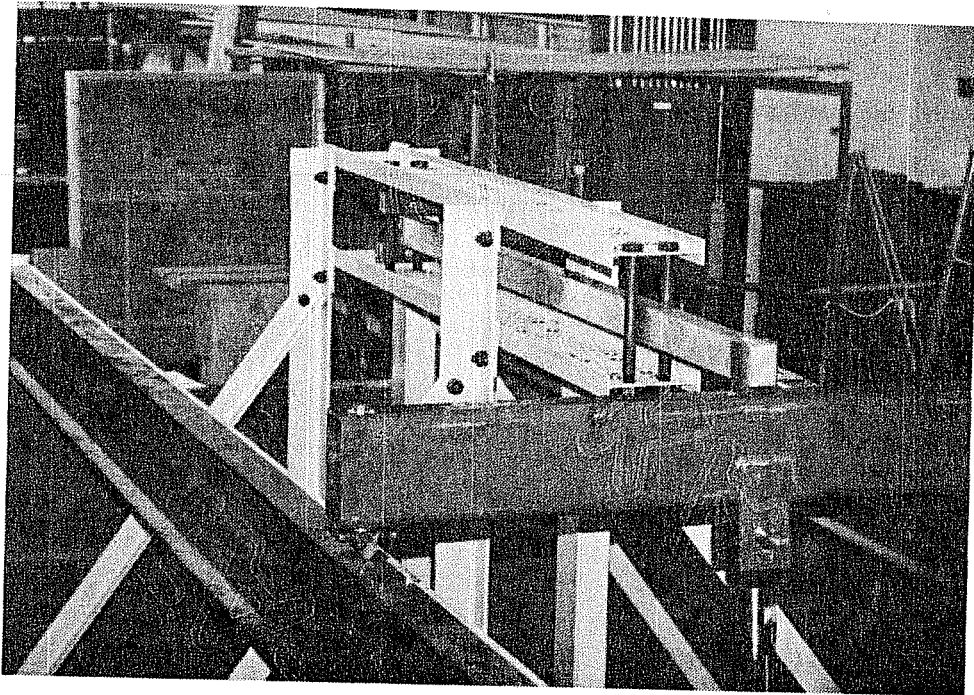




**Figure 3.8 - Schematic of Lateral Brace**

Lateral Brace Configuration	Stiffness Kips/In
1	0.22
2	0.36
3	0.65
4	0.75
5	1.20
6	1.90

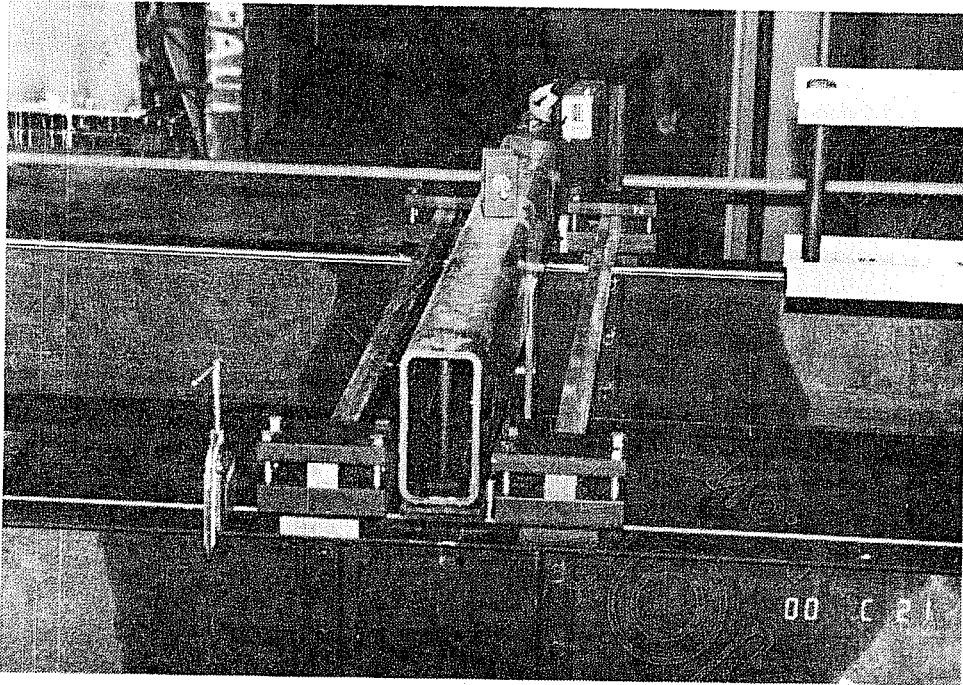
**Table 3.1 - Measured Lateral Brace Stiffness**



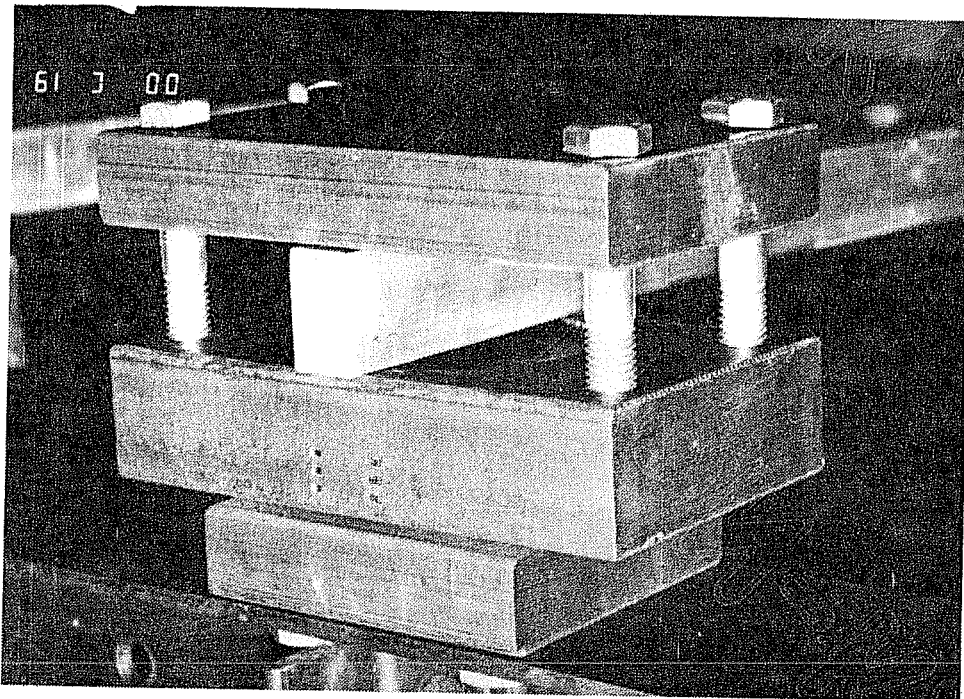
**Figure 3.9 - Lateral Bracing System**

### **3.5 Torsional Bracing**

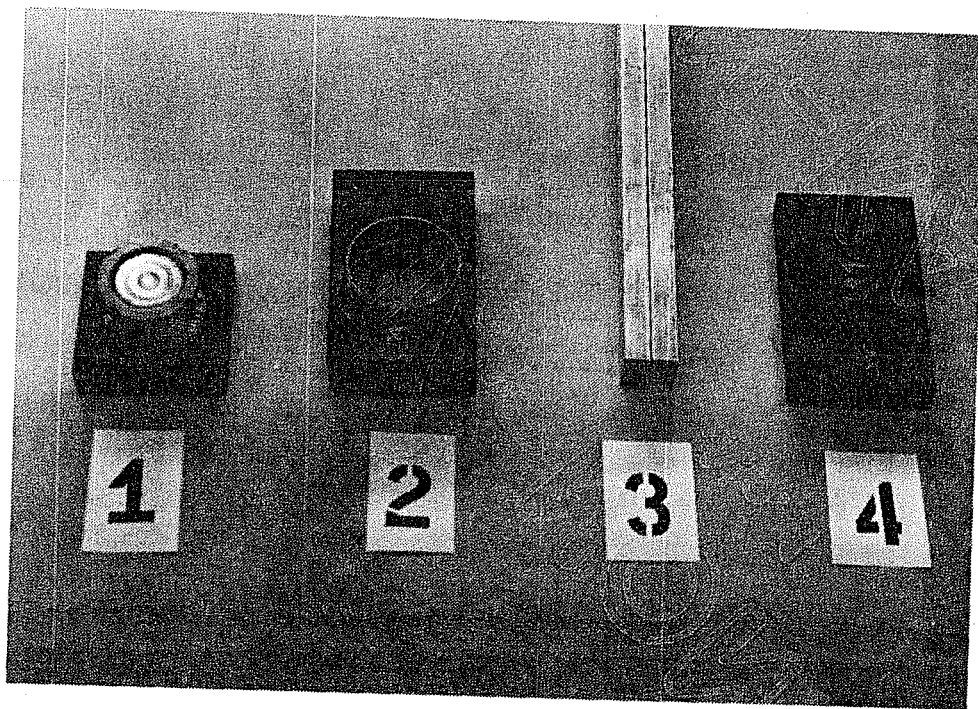
Torsional bracing was provided by connecting a flexible aluminum bar to each test beam spanning between the two beams. During testing, the lateral deflection of the test beams forced the aluminum brace into double curvature as shown in Figure 1.6. Since the brace is bent in double curvature, the brace stiffness is equal to  $6EI/L$  of the aluminum brace. The torsional braces were attached six inches on each side of the mid-span of the test beam to avoid interfering with the loading beam and to provide symmetry. Figure 3.10 shows a typical torsional brace used in the test.



**Figure 3.10 - Torsional Bracing**



**Figure 3.11 - Torsional Brace Fixtures**



**Figure 3.12 - Brace Fixture Components**




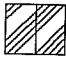


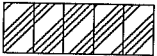
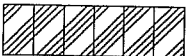
The torsional brace attachment fixtures were designed to prevent the addition of any significant warping restraint to the test beams especially as they buckled into the second mode shape. This required the brace and fixtures to provide a high stiffness in the vertical plane while simultaneously providing little or no restraint in the horizontal plane. Figure 3.11 shows a photo of the overall fixture assembly and Figure 3.12 shows the individual fixture components. Item 1 in Figure 3.12 is the base of the fixture. This was rigidly attached to the test beam and contained a two inch fixed dowel at the center. Item 2 was placed over the dowel on Item 1 and was secured with the use of a bearing nut. Roller thrust bearings were placed between both contact surfaces formed by the attachment of 1 and 2. The aluminum bracing, Item 3, was rigidly connected to the fixture by the use of a cover plate (Item

4). All rotation in the horizontal plane occurred between Item 1 and 2. Each of the eight brace end fixtures were calibrated and found to vary from 1600 to 3700 k-in/rad with an average stiffness of 2900 kip-in/rad. By repeated trials, it was found that a large variation in stiffness would occur depending on the tension that was applied to the bearings in the fixture assembly. Since measuring the brace fixture stiffness between each test would have been prohibitive, the average stiffness of 2900 Kip-In/Rad was used for all fixtures. The total stiffness of the brace-fixture combination was determined from the sum of the fixture flexibility and the brace flexibility as shown in Equation 3.1. Based on the original stiffness measurements, the use of the average fixture stiffness could result in an error of 3% for the lowest level of brace stiffness and an error of 17% for the highest level of brace stiffness. Thus, the total stiffness of each brace-fixture combination was calculated using an average value of 2900 k-in/rad for the fixture stiffness. The total brace stiffness given in Figure 3.13 was calculated for the bar configuration shown and then doubled to account for the bracing on each side of the loading tube.

$$\frac{1}{\beta_T} = \frac{1}{\beta_{brace}} + \frac{1}{\beta_{fixture}} \quad (3.1)$$

where  $\beta_T$  = Torsional Brace Stiffness,  $\beta_{brace}$  = Stiffness of Brace Alone,  $\beta_{fixture}$  = Stiffness of Brace Fixture Alone.

Many tests were performed with stiffeners placed directly beneath the brace attachment points. They were made of 11 inch long steel angles bolted to the web of the test beam. This permitted both the stiffener size and vertical location of the stiffener to be easily adjusted.

No.	Description	Inertia	Bar Stiffness	Fixture Stiffness	Total Brace Stiffness
1	3/4" x 3/4" Bar 	0.027	27.7	2900	55.0
2	1-1/4" x 3/4" Bar 	0.044	45.0	2900	88.6
3		0.088	90.3	2900	175
4	3/4" x 1-1/4" Bars 	0.244	250	2900	462
5		0.366	375	2900	666
6		0.488	501	2900	855
7		0.610	626	2900	1030
8		0.732	752	2900	1190

**Figure 3.13 - Adjusted Torsional Brace Stiffness**

## Chapter 4 Test Results

### 4.1 Test Procedure

The experimental program of 76 tests was divided into six groups. Group A is composed of tests that contained no bracing. Group B is composed of tests with lateral bracing located at mid-span attached to the compression flange. Group C contains tests with compression flange torsional bracing located at mid-span as discussed in Chapter 3. Group D contains results from tests with forced imperfections. Group E contains tension flange torsional bracing and Group F contains a combination of tension flange and compression flange torsional bracing.

The test procedure for each test started with an initial reading of all gauges. A load of approximately one kip was applied to the beams before the vibration equipment was activated so that the knife edges would seat in the grooves on the top flanges of the test beams. Readings were then taken at a constant increment of about 500 pounds until the load on the beams was near the buckling load; the frequency of the readings were then increased. The number of readings taken at or near the buckling load varied greatly between tests and can be seen in the load-deflection curves located in Appendix A. During each test, the inclinations' of the compression and tension flanges were measured near the brace point. These readings were not taken as frequently since the data were recorded manually.

## 4.2 Determination of Critical Load

The lateral torsional buckling load of a beam can be defined as the load at which the member has zero lateral stiffness. Figure 4.1 shows a typical load-deflection curve from a test where the beam buckled in the first mode and Figure 4.2 shows a typical load-deflection curve from a test where the beam buckled in the second mode. The critical load for these tests is characterized by a horizontal or near horizontal line on the load-deflection curve. Since the beams buckled in an "S" shape for all second mode tests, the mid-span deflection was small or zero for all values of load. The critical load can also be found from the horizontal line on the load-twist curve as shown in Figure 4.3. Due to the high yield strength of the W12x14 beam material (approximately 65 ksi), the large deflections needed to reach the critical load of the test beam were achieved without yielding.

Alternative methods have been developed to determine the experimental buckling strength of beams that cannot be loaded to the actual buckling load. Some of the better known procedures for this type of analysis include techniques presented by Southwell (1932) and Meck (1977). The Meck Plotting Technique is applied specifically to beams by using two equations which involve linear relations between functions of the measured lateral deflection and measured twist. The applied moment is plotted against the experimental twist and lateral deflection as shown in Figure 4.4. The inverse slopes of the lines of best fit through the data points for these plots are defined as  $\alpha$  and  $\beta$  where the critical moment is given by

$$M_{cr} = \sqrt{\alpha\beta}$$

The initial lateral twist,  $\theta_0$ , and deflection,  $U_0$ , are found from the negative



horizontal intercepts of the plots shown in Figure 4.4.

Use of the Meck plotting technique for the determination of  $M_{cr}$  gives results practically identical to the load level corresponding to a horizontal line on the load-deflection curve for all tests without bracing. However, the Meck plotting technique did not work for tests that contained bracing or where the load was applied through a flexible loading member. For this reason, the critical load for all tests was obtained from the horizontal portion of the load-deflection curve. The Meck Technique was used, however, to verify the critical load of tests with no bracing as well as to establish the initial imperfection of each beam.

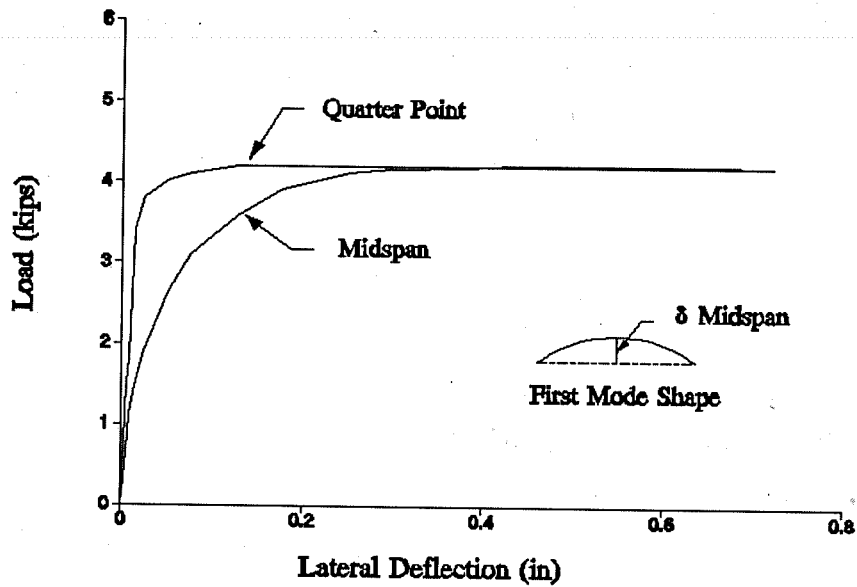


Figure 4.1 - Typical Load-Deflection Curve for First Mode Test

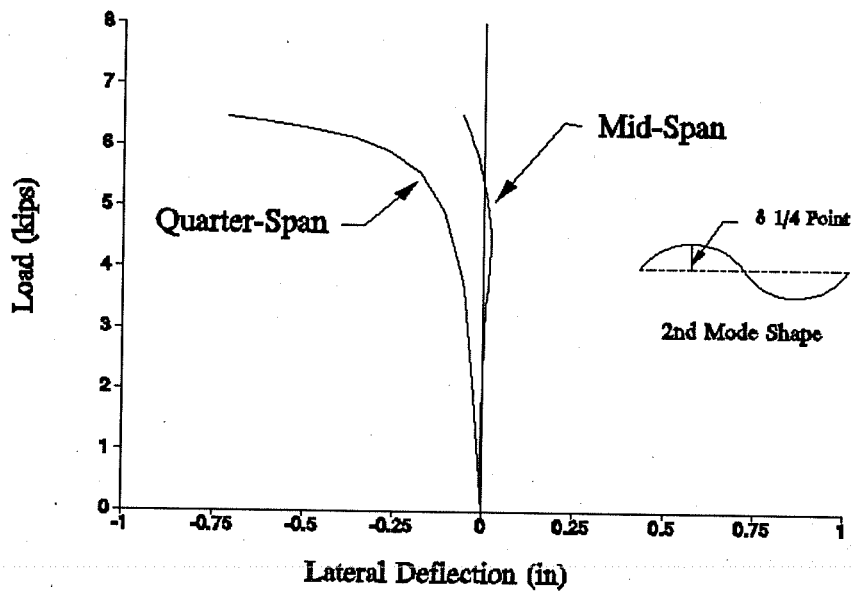


Figure 4.2 - Typical Load-Deflection Curve For Second Mode Test

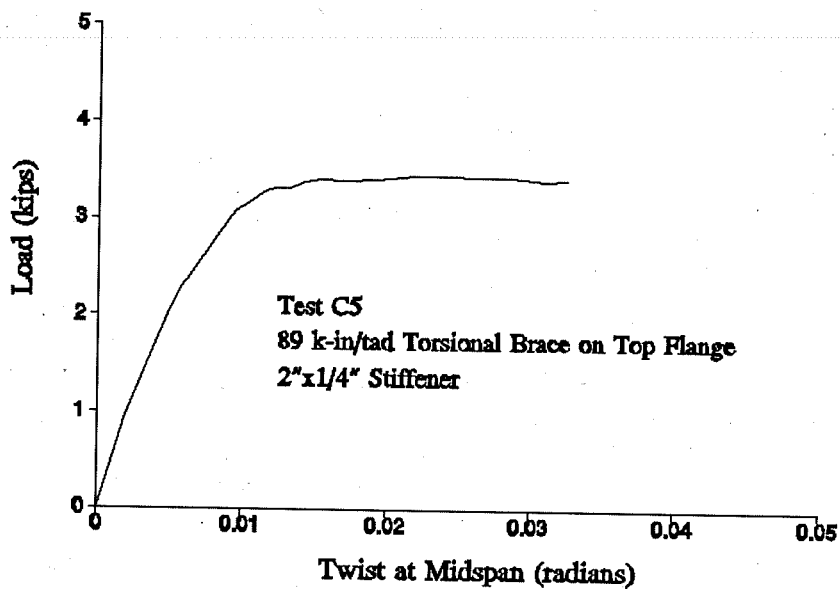


Figure 4.3 - Typical Load-Twist Curve for First Mode Test

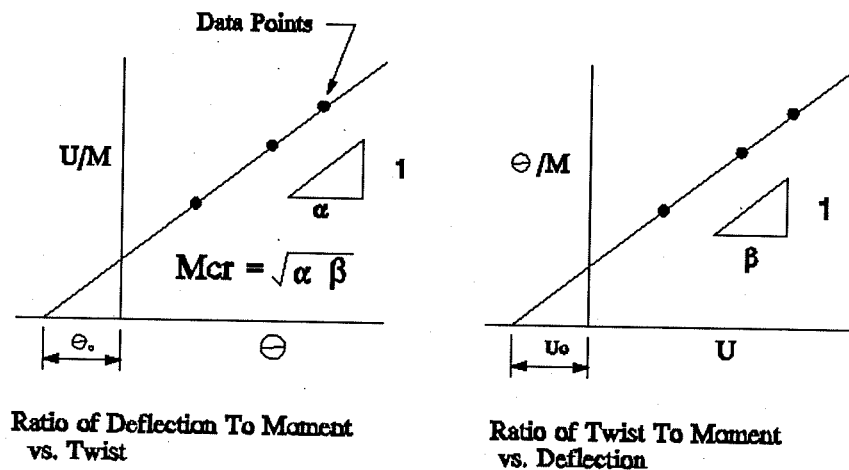


Figure 4.4 - Meck Plotting Technique

### 4.3 Determination of Initial Imperfections

Two types of initial imperfections were studied during the testing program. The first type of imperfection will be referred to as natural imperfections. All tests except Group D tests were performed with natural imperfections obtained by buckling the beams in the first mode beyond their yield point. Test A1, A5, and A6 in Table 4.1 give values of initial displacement and initial twist at mid-span for the three levels of natural imperfections used during testing. The second type of imperfection will be referred to as forced imperfections. These were applied at the quarter point of the beam by displacing the compression flange of the test beam laterally with a rigid stop and then securing the stop in the displaced position. Tests D1 through D4 give measured values of initial deflection and initial twist at the mid-span of the test beams for tests with forced imperfections. All forced imperfections listed are in addition to the 0.04 inch natural deflection of test beam A1.

Test Number	Initial Deflection (in)	Initial Twist (degrees)
A1	0.04	0.26
A5	0.16	0.01
A6	0.22	0.13
D1	0.26	0.17
D2	0.15	0.07
D3	0.12	0.05
D4	0.31	0.12

**Table 4.1 - Measured Initial Deflection and Twist**

#### 4.4 Test Series A - No bracing

The first test series consisted of six tests with different loading beams. Test A1 was loaded with knife edges between the loading member and the test beam and can be considered a basically straight beam with no bracing other than the friction in the gravity load simulator. Test A2 had the same configuration as A1 with a forced imperfection imposed at the quarter point of one beam.

The term "tipping effects" describes tests in which the loading beam was placed directly on the compression flanges of the test beams without the use of the knife edges. Tests A3 and A4 were performed to study the effects of the externally applied flange rotation which occurs when the loading member is placed directly on the compression flanges of the test beams. Tests A5 and A6 were loaded with the original knife edge loading and are similar to test A1 except for the level of initial imperfection present. Table 4.2 gives a summary of these tests and the corresponding experimental buckling loads. The reported buckling load is an average of the two test beams. Tests marked with a plus sign were reproduced to check for repeatability. With the exception of tests C4 and C29, all duplicate tests gave a critical load within 6 percent of the original test. Test C4 had a variation of 28 percent and test C29 had a variation of 51 percent.

TEST No.	DESCRIPTION	STIFFENER SIZE	INITIAL IMPERFECTION (INCHES)	CRITICAL LOAD (KIPS)	"S" SHAPE
+ A1	Knife edge loading	NONE	0.04	1.6	NO
A2	Knife edge loading	NONE	0.45	1.6	NO
+ A3	Tipping Effects	NONE	0.04	3.8	NO
A4	Tipping Effects	2"X1/4"	0.04	6.2	YES
+ A5	Knife Edge Loading	NONE	0.16	1.6	NO
+ A6	Knife Edge Loading	NONE	0.22	1.7	NO

+ Test was repeated

**Table 4.2 - Test Series A, No Bracing**

#### 4.5 Test Series B Lateral Bracing

The second series of tests as well as all subsequent tests were loaded using the steel loading beam and knife edges as shown in Figure 3.7. All boundary conditions were the same as Test Series A except that a lateral brace was added as shown in Figure 3.8 and 3.9. Six levels of lateral bracing and two levels of initial imperfections were tested. Table 4.3 shows the amount of lateral bracing attached to the test beams through the bracing device and the corresponding critical load per beam.

TEST NUMBER	BRACE STIFFNESS (KIPS/IN)	STIFFENER SIZE	INITIAL IMPERFECTION (INCHES)	CRITICAL LOAD (KIPS)	"S" SHAPE
B1	0.22	4"x1/4"	0.22	2.8	NO
B2	0.75	4"x1/4"	0.22	4.9	NO
B3	0.36	4"x1/4"	0.22	3.0	NO
B4	1.20	4"x1/4"	0.22	4.9	NO
B5	0.36	4"x1/4"	0.16	3.7	NO
B6	1.20	4"x1/4"	0.16	6.1	NO
B7	1.90	4"x1/4"	0.16	6.5	YES
B8	0.65	4"x1/4"	0.16	5.0	NO
B9	0.65	NONE	0.16	5.1	NO
B10	1.90	NONE	0.16	6.5	YES

**Table 4.3 - Test Series B, Lateral Bracing**

#### **4.6 Test Series C, Compression Flange Torsional Bracing**

Test Series C consisted of 40 tests with varying levels of torsional brace stiffness, initial imperfection, and stiffener size. A total of eight levels of brace stiffness, three levels of initial imperfection, and two stiffener sizes were tested. Tests were also performed with no stiffener and with the 4"x1/4" stiffener touching the compression flange at both brace locations. Tests performed with the stiffeners touching the compression flange are marked with an asterisk in the table.

As described in Chapter 3, the torsional bracing was attached to the compression flange of each test beam with half the indicated amount being placed six inches on either side of the mid-span. Table 4.4 contains a summary of these tests and the corresponding experimental buckling loads.

TEST NUMBER	BRACE STIFFNESS (K-IN/RAD)	STIFFENER SIZE	INITIAL IMPERFECTION (INCHES)	CRITICAL LOAD (KIPS)	"S" SHAPE
C1	55	NONE	0.22	2.9	NO
C2	55	2"X1/4"	0.22	2.9	NO
C3	55	4"X1/4"	0.22	2.9	NO
+ C4	89	NONE	0.22	2.9	NO
+ C5	89	2"X1/4"	0.22	3.5	NO
+ C6	89	4"X1/4"	0.22	3.6	NO
C7	175	NONE	0.22	4.4	NO
+ C8	175	2"X1/4"	0.22	4.4	NO
C9	175	4"X1/4"	0.22	4.5	NO
C10	462	NONE	0.22	4.8	NO
C11	462	2"X1/4"	0.22	5.2	NO
C12	462	4"X1/4"	0.22	5.2	NO
C13	666	NONE	0.22	4.9	NO
C14	666	2"X1/4"	0.22	5.4	NO
C15	666	4"X1/4"	0.22	4.3	NO
C16	855	4"X1/4"	0.22	5.7	NO
+ C17	1030	4"X1/4"	0.22	5.7	NO
C18	1190	4"X1/4"	0.22	6.0	NO
C19	1190	* 4"X1/4"	0.22	6.8	YES
C20	1030	* 4"X1/4"	0.22	6.8	YES
C21	666	* 4"X1/4"	0.22	6.8	YES
C22	462	* 4"X1/4"	0.22	6.4	NO
C23	175	* 4"X1/4"	0.22	5.1	NO
C24	89	* 4"X1/4"	0.22	3.3	NO
C25	55	NONE	0.16	2.9	NO
C26	55	2"X1/4"	0.16	2.9	NO
C27	55	4"X1/4"	0.16	3.0	NO
+ C28	89	NONE	0.04	4.5	NO



TEST NUMBER	BRACE STIFFNESS (K-IN/RAD)	STIFFENER SIZE	INITIAL IMPERFECTION (INCHES)	CRITICAL LOAD (KIPS)	"S" SHAPE
+ C29	89	2"X1/4"	0.04	4.1	NO
C30	89	4"X1/4"	0.04	5.1	NO
C31	175	NONE	0.04	5.5	NO
+ C32	175	2"X1/4"	0.04	6.3	YES
+ C33	175	4"X1/4"	0.04	6.5	YES
C34	175	* 4"X1/4"	0.16	4.1	NO
C35	462	* 4"X1/4"	0.16	6.6	YES
+ C36	462	4"X1/4"	0.16	5.6	NO
+ C37	666	4"X1/4"	0.16	5.8	NO
C38	855	4"X1/4"	0.16	6.3	NO
C39	1030	4"X1/4"	0.16	6.5	NO
C40	1190	4"X1/4"	0.16	6.4	NO

\* Stiffener Touching Compression Flange  
+ Test was repeated

**Table 4.4 - Test Series C, Compression Flange Torsional Bracing**

#### 4.7 Test Series D, E, and F

Test Series D consists of six tests where the initial imperfection was applied to the beam by a forced displacement at the quarter span of one beam. The forced displacement was transferred to the other beam through the loading tube. As mentioned in the previous sections, the initial imperfection reported for all other test series was the natural state of the test beams due to a previous yielding or manufacturing process. Test Series E consisted of ten tests similar to those in series C except the torsional bracing

was attached to the tension flange instead of the compression flange. Test Series F consisted of 6 tests similar to those in series C except half the indicated value of torsional bracing was attached to the compression flange and half was attached to the tension flange. Table 4.5 contains a summary of these tests and the corresponding experimental buckling loads.

TEST NUMBER	BRACE STIFFNESS (K-IN/RAD)	STIFFENER SIZE	INITIAL IMPERFECTION (INCHES)	CRITICAL LOAD (KIPS)	"S" SHAPE
Forced Imperfections					
D1	89	NONE	0.26	3.6	NO
D2	175	NONE	0.15	4.2	NO
D3	175	4"X1/4"	0.12	5.8	NO
D4	175	4"X1/4"	0.31	5.2	NO
Tension Flange Torsional Bracing					
E1	175	NONE	0.22	4.3	NO
E2	175	* 4"X1/4"	0.22	6.6	NO
E3	666	*4"X1/4"	0.22	6.7	YES
E4	666	4"X1/4"	0.22	6.8	YES
E5	666	NONE	0.22	4.6	NO
E6	175	NONE	0.16	3.8	NO
+ E7	175	* 4"X1/4"	0.16	4.8	NO
E8	666	* 4"X1/4"	0.16	6.7	YES
E9	666	4"X1/4"	0.16	6.7	YES
E10	666	NONE	0.16	4.8	NO
Combined Compression and Tension Flange Torsional Bracing					
F1	462	NONE	0.22	6.5	YES
F2	175	NONE	0.22	4.8	NO
F3	175	4"X1/4"	0.22	4.8	NO
F4	462	NONE	0.16	6.6	YES
F5	175	NONE	0.16	4.9	NO
F6	175	4"X1/4"	0.16	4.9	NO

\* Stiffener Touching Tension Flange

+ Test was repeated

Table 4.5 - Test Series D, E, and F

## Chapter 5 Comparison and Discussion of Test Results

### 5.1 General

Using the test results presented in Chapter 4, the effects of brace stiffness, brace location, stiffener size, and initial imperfections on the lateral buckling of beams will be evaluated. The design equations developed for straight beams in Chapter 2 will be extended to cover beams with imperfections. Both natural and forced imperfections will be evaluated. The effects of torsional brace location will also be examined.

### 5.2 Effect of Imperfections on Lateral Bracing Requirements

Since the design equations for lateral bracing presented in Chapter 2 were previously verified for straight beams, only a correction for imperfections is needed. As discussed in Chapter 1, Winter (1960) indicated that initial imperfections decrease the effectiveness of lateral bracing for columns. He concluded that the required brace stiffness increased as a linear function of the initial imperfection.

Figure 5.1 shows a plot of critical load vs. brace stiffness for all tests with lateral bracing and natural imperfections (Group B). For each level of brace stiffness, the beam with an imperfection of 0.22 inches gave a lower buckling load than the beam with an imperfection of 0.16 inches. No test data were obtained for the beam with an imperfection of 0.04 inches since the beam was accidentally yielded before any tests were performed.

Timoshenko (1960) has shown that an unbraced elastic column with an initial imperfection will ultimately reach the same critical load as the straight column. He has shown that the deflection at any load level is given by,

$$\Delta = \frac{\Delta_o}{1 - \frac{P}{P_{cr}}} \quad (5.1)$$

Since the imperfection does not affect the ultimate buckling load of an unbraced elastic beam, it can be reasoned that the imperfection reduces the effective brace stiffness. Based on the test data from Group B, it was determined that the effect of imperfections on laterally braced beams could be estimated by applying the following equations,

$$M_{cr} = \sqrt{(M_o^2 + \frac{P_y h^2 A}{4})(1 + A)} \quad (5.2)$$

$$A = \frac{L^2}{\pi} \sqrt{\frac{.67 c_L \beta_L}{EI_y}} \quad (5.3)$$

$$c_L = \frac{1}{1 + 1500 \frac{\Delta_o}{L}} \quad (5.4)$$

where  $\beta_L$  = equivalent continuous lateral brace stiffness (k/in per in. length),  $c_L$  = reduction factor for the imperfection and  $\Delta_o$  = imperfection value.

Figure 5.2 shows plots of Equation 5.2 for a beam with three different levels of initial imperfection. The beam with an imperfection of  $L/1000$  requires about 2.2 times the brace stiffness of the straight beam to reach the second mode maximum. Similarly, the beam with an imperfection of  $L/500$  requires about 3.5 times the brace stiffness to reach the second mode maximum.

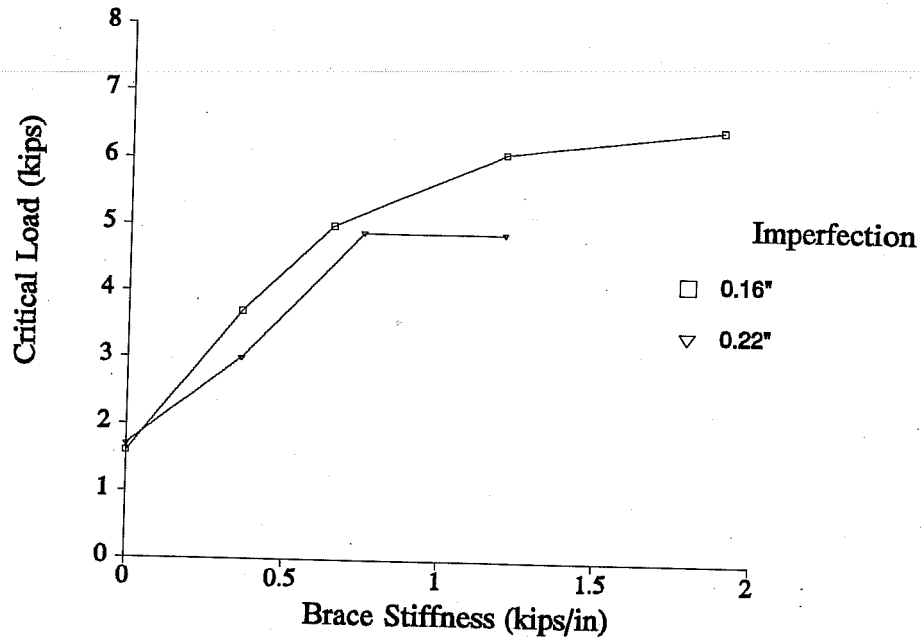


Figure 5.1 - Test Results for Beams with Lateral Bracing

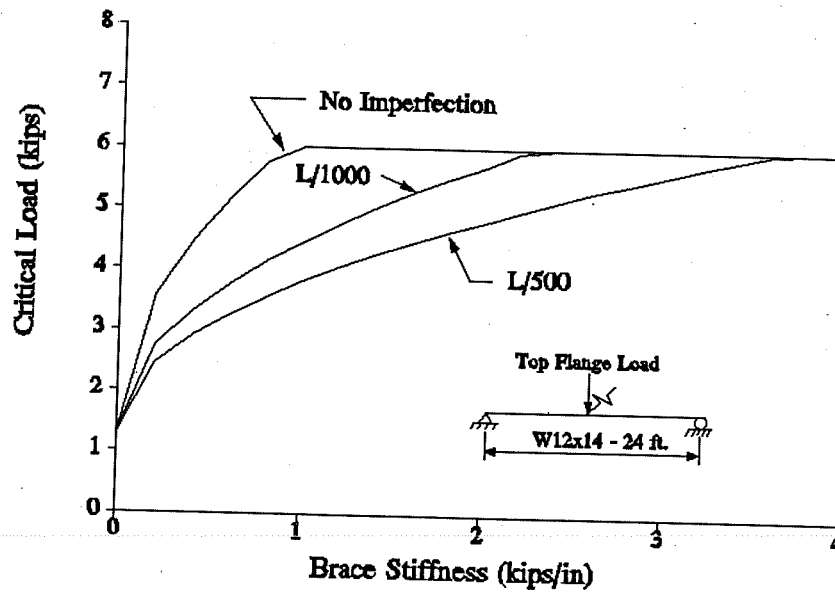


Figure 5.2 - Effect of Initial Imperfections on Lateral Bracing

### 5.3 Comparison of Test Results and Design Equations for Lateral Bracing

A total of 10 tests were performed with compression flange lateral bracing to examine the effects of brace stiffness and initial imperfections. Figures 5.3 and 5.4 compare the design equations presented in the previous section to the test data presented in Chapter 4. These figures include curves plotted from the design equations both including and excluding the restraint from the gravity load simulator. The curve labeled "GLS Included" was calculated by utilizing the gravity load simulator calibration shown in Figure 3.5.

For cases with no attached bracing, the design equations labeled "GLS Not Included," closely compare to the test data. This may indicate that the lateral restraint of the gravity load simulator is being over-estimated at low load levels. Since the gravity load simulator could only be calibrated without the vibration devices, it is possible that the actual friction may be significantly less than the values reported by the calibration.

Since only mid-span bracing was tested, the stiffness of each brace was divided by 75 percent of the beam length to determine the equivalent continuous brace. A  $C_b$  factor of 1.30 was used to account for point loading and the warping term was ignored in the determination of  $M_o$  to include the effects load height. Imperfections were considered as discussed in Section 5.2.

A 4"x1/4" stiffener was used for all tests presented in Figure 5.3 and 5.4; however, identical results were obtained in additional tests performed with no stiffener. This indicates that cross-section distortion does not significantly affect the buckling load of a beam supported solely by lateral bracing at the compression flange.

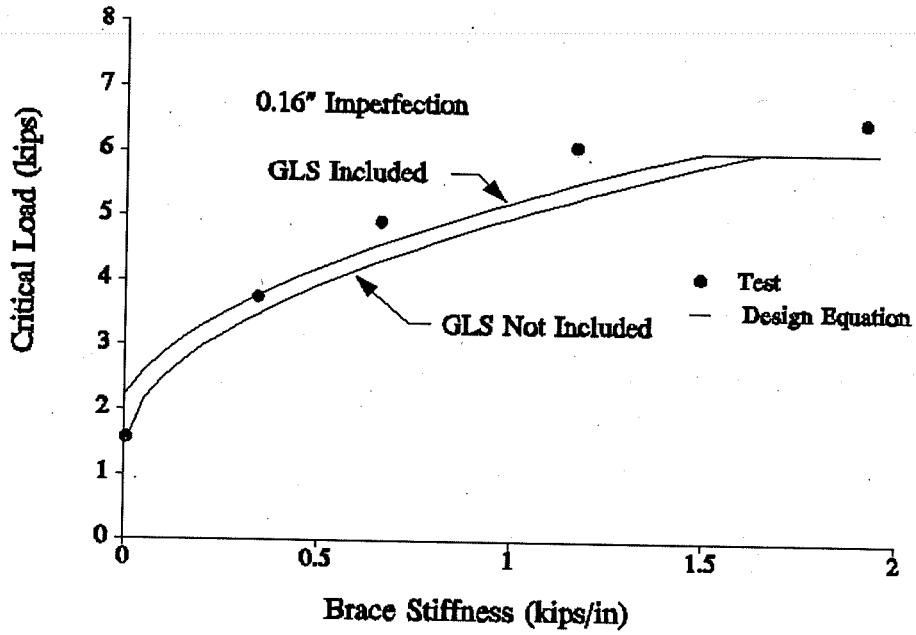


Figure 5.3 - Lateral Bracing, 0.16" Imperfection

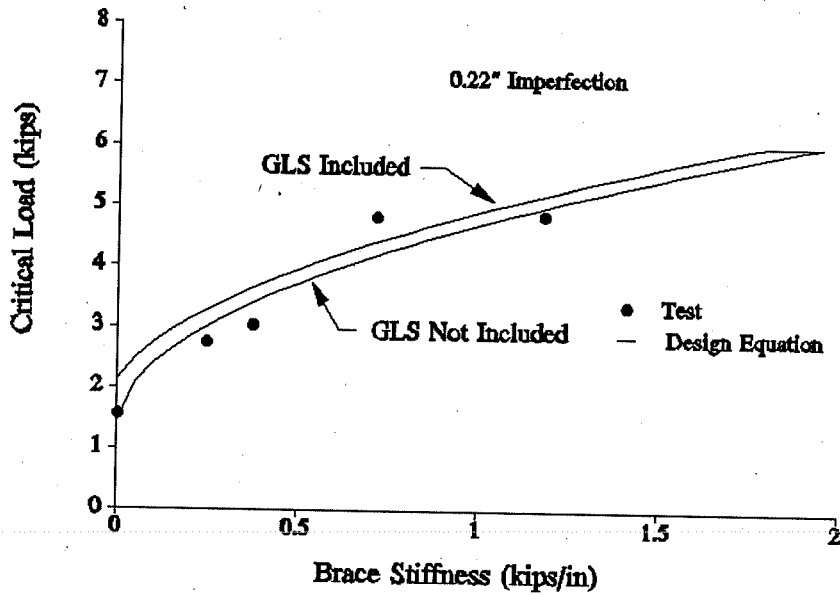


Figure 5.4 - Lateral Bracing, 0.22" Imperfection



#### 5.4 Effect of Imperfections on Torsional Bracing

As presented in Chapter 2, the critical moment of a beam braced continuously along the compression flange by a torsional brace is given by the following,

$$M_{cr} = \sqrt{M_o^2 + \beta_T EI_y} \quad (5.5)$$

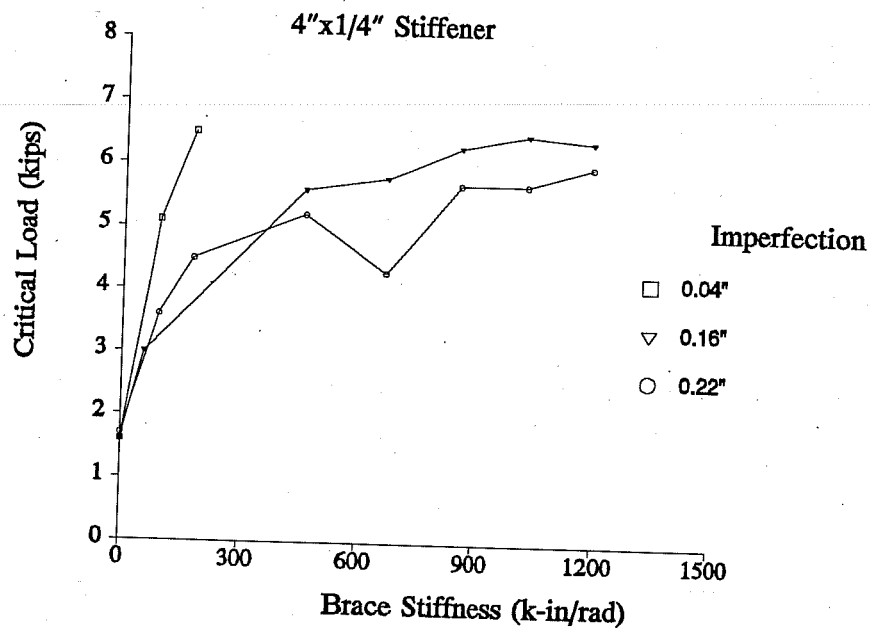
where  $\beta_T$  = equivalent continuous torsional brace.

Experimental results presented in Figure 5.5 indicate that initial imperfections have a significant effect on the effective torsional brace stiffness. In all tests with bracing, an increase in initial imperfection led to a decrease in buckling load. Based on test data presented in Figure 5.5, modifying factors for initial imperfections are applied as follows,

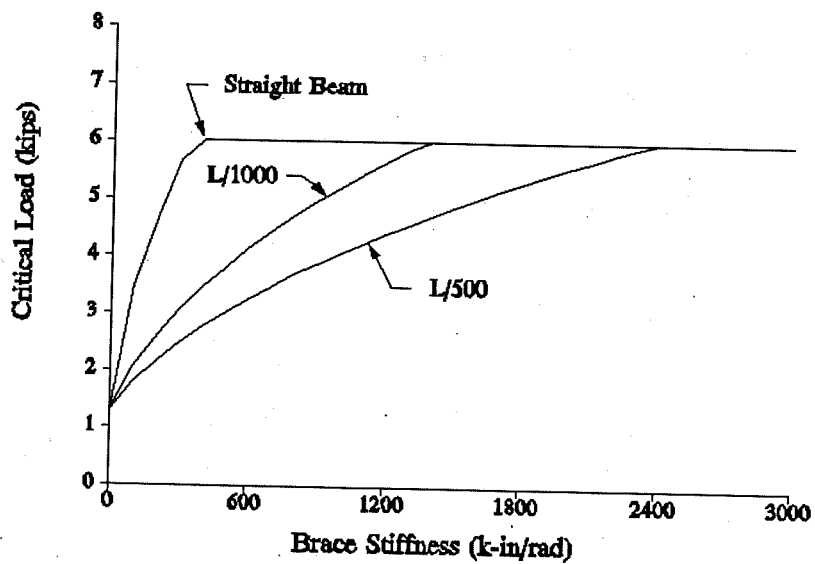
$$\frac{1}{\beta_t} = \frac{1}{c_t \beta_b} + \frac{1}{\beta_{sec}} \quad (5.6)$$

$$c_t = \frac{1}{1 + 3000 \frac{\Delta_o}{L}} \quad (5.7)$$

Figure 5.6 shows plots of Equation 5.5 for a beam with three different levels of initial imperfection. The beam with an imperfection of  $L/1000$  requires about 3 times the brace stiffness of the straight beam to reach the second mode maximum. Similarly, the beam with an imperfection of  $L/500$  requires about 5 times the brace stiffness to reach the second mode maximum.



**Figure 5.5 - Test Results for beams with Torsional Bracing**



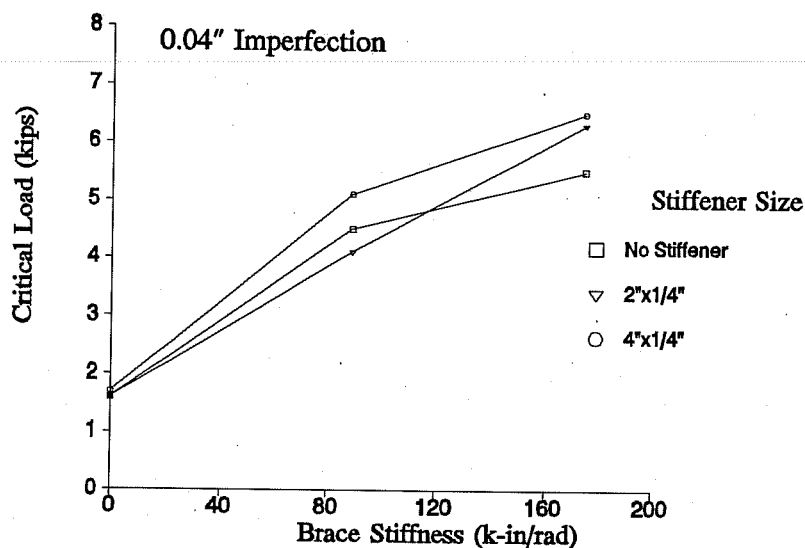
**Figure 5.6 - Effect of Imperfections on Torsional Bracing**

### 5.5 Comparison of Test Results and Design Equations for Torsional Bracing

A total of 30 tests were performed with compression flange torsional bracing to examine the effects of brace stiffness, stiffener size, and initial imperfections. The stiffeners were made of 11 inch long steel angles bolted to the web of the test beam directly below the brace attachment points. This permitted both the stiffener size and vertical location of the stiffener to be easily adjusted.

Figures 5.7 and 5.8 show test data with various stiffener sizes for tests with 0.04 inch and 0.22 inch imperfections respectively. In almost every case, an increase in stiffener size resulted in an increase in buckling load. The increase in load was most apparent when the stiffener was adjusted so that it was touching the compression flange of the test beam (Figure 5.8). Undoubtedly, this adjustment led to the highest section stiffness.

Figures 5.9 through 5.17 compare the design equations, including the modifications for imperfections, to test data presented in Chapter 4. The restraint added to the test specimen by the gravity load simulator was included in the design curves by applying a lateral brace in combination with the torsional brace. Since only mid-span bracing was tested, the stiffness of each brace was divided by 75 percent of the beam length, as discussed in Section 2.4, to determine the equivalent continuous brace. A  $C_b$  factor of 1.30 was used to account for point loading and the warping term was ignored in the determination of  $M_o$  to include the effects of load height. The effects of imperfections were included as discussed in Section 5.4.

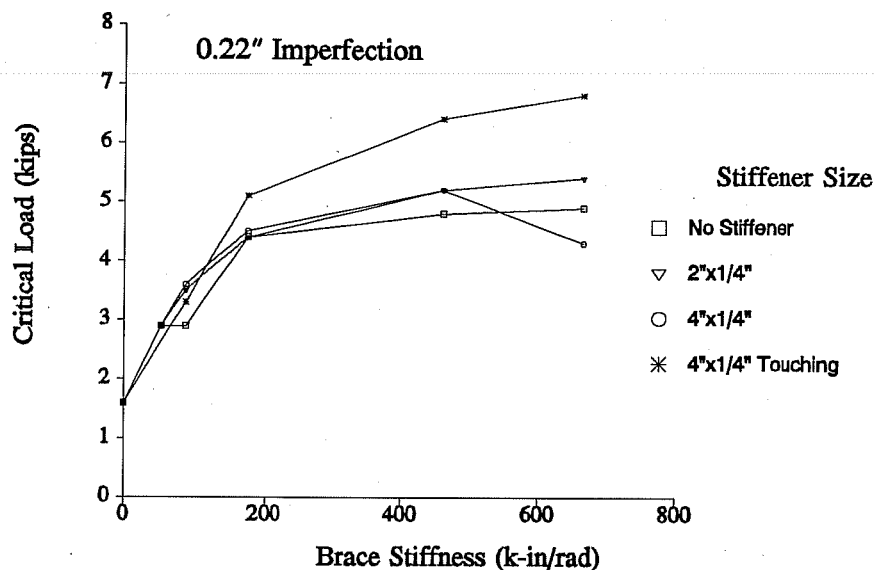


**Figure 5.7 - Test Results, Torsional Bracing with 0.04" Imperfection**

The largest difference between the estimated load using the design equations, including the gravity load simulator, and the test load (56 percent), occurred in tests with no bracing, however, the maximum error for all tests with bracing was 27 percent for a 4"x1/4" stiffener, 29 percent for a 2"x1/4" stiffener, and 34 percent for tests with no stiffener.

Figure 5.9 and 5.15 indicate that the design equation is very conservative for beams with no stiffener. The following factors could have contributed to the conservativeness of the design equations: 1) An effective width of  $1.5h$  was used to calculate  $\beta_{sec}$  in Equation 2.6, a larger value may have been appropriate. 2) Since the torsional braces in the experiment consisted of two braces  $h$  apart, the actual effective width may be closer to  $1.5h + h$ .

Figure 5.14 and 5.16 indicate that the design equations accurately



**Figure 5.8 - Test Results, Torsional Bracing with 0.22" Imperfection**

predicted the buckling load for tests with a 4"x1/4" stiffener. Since the majority of the cross-section stiffness (Equation 2.6) is coming from the stiffener, these figures indicate that the stiffness contribution from the stiffener is being estimated accurately.

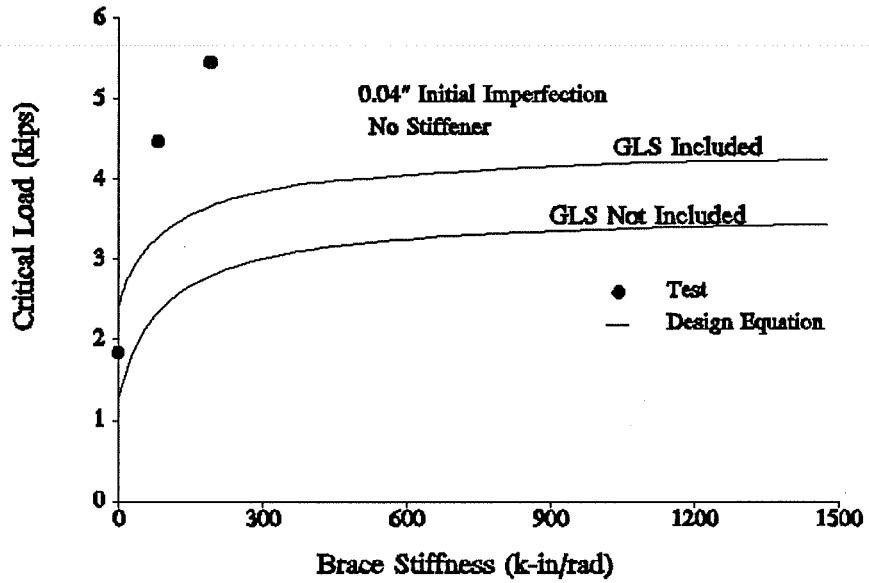


Figure 5.9 - Torsional Bracing, 0.04" Imperfection, No Stiffener

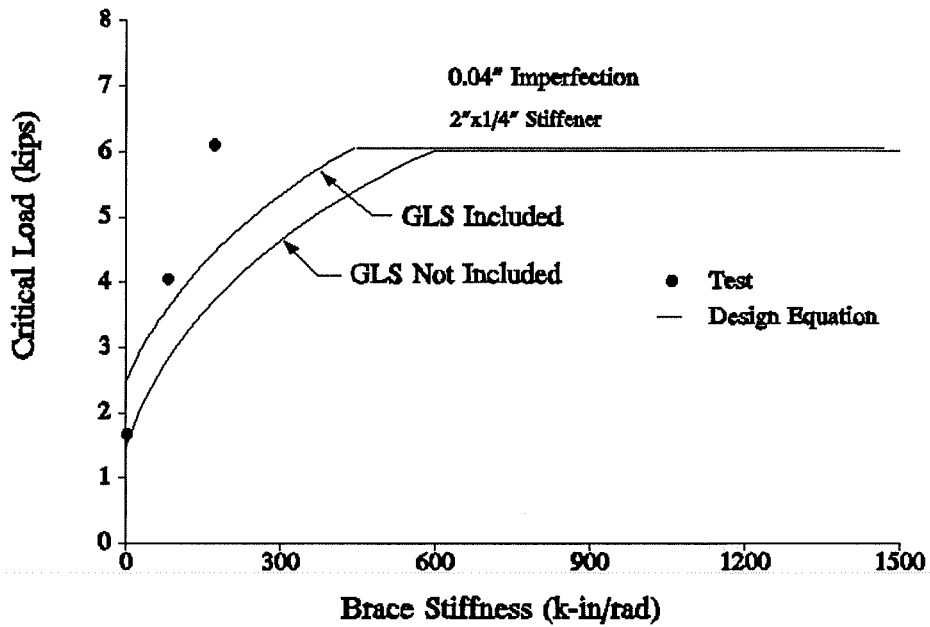


Figure 5.10 - Torsional Bracing, 0.04" Imperfection, 2"x1/4" Stiffener

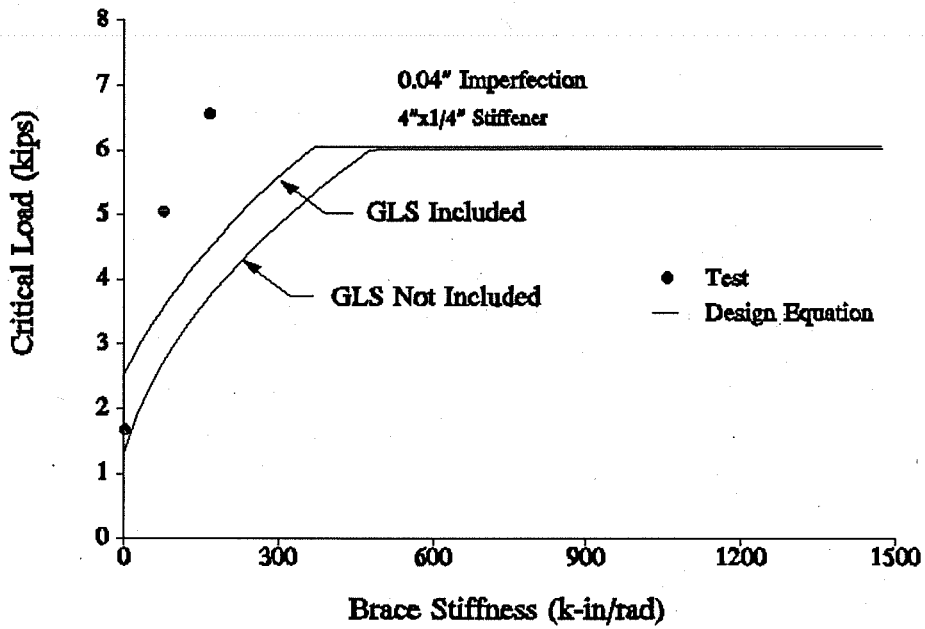


Figure 5.11 - Torsional Bracing, 0.04" Imperfection, 4"x1/4" Stiffener

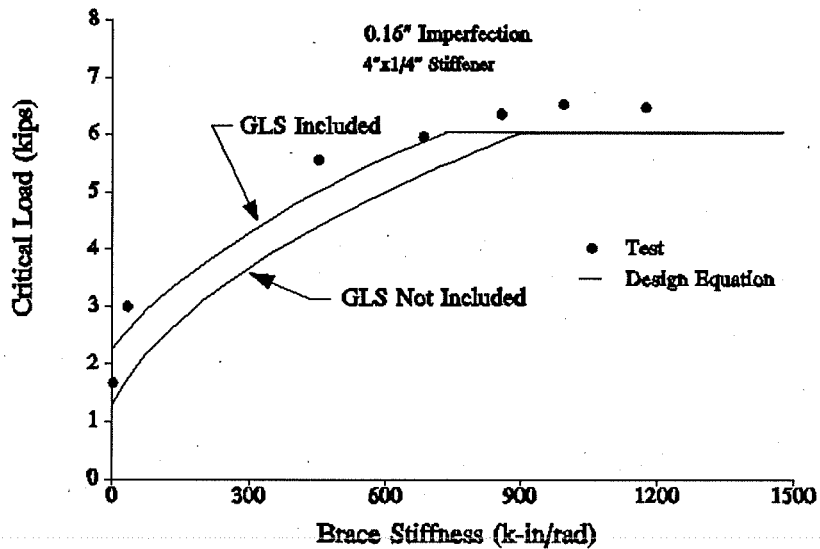


Figure 5.12 - Torsional Bracing, 0.16" Imperfection, 4"x1/4" Stiffener

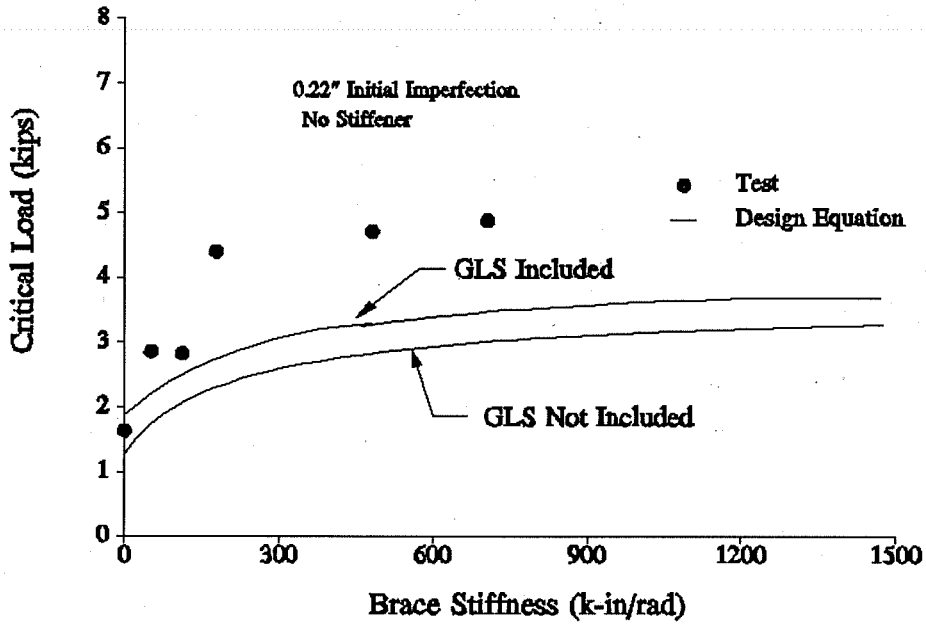


Figure 5.13 - Torsional Bracing, 0.22" Imperfection, No Stiffener

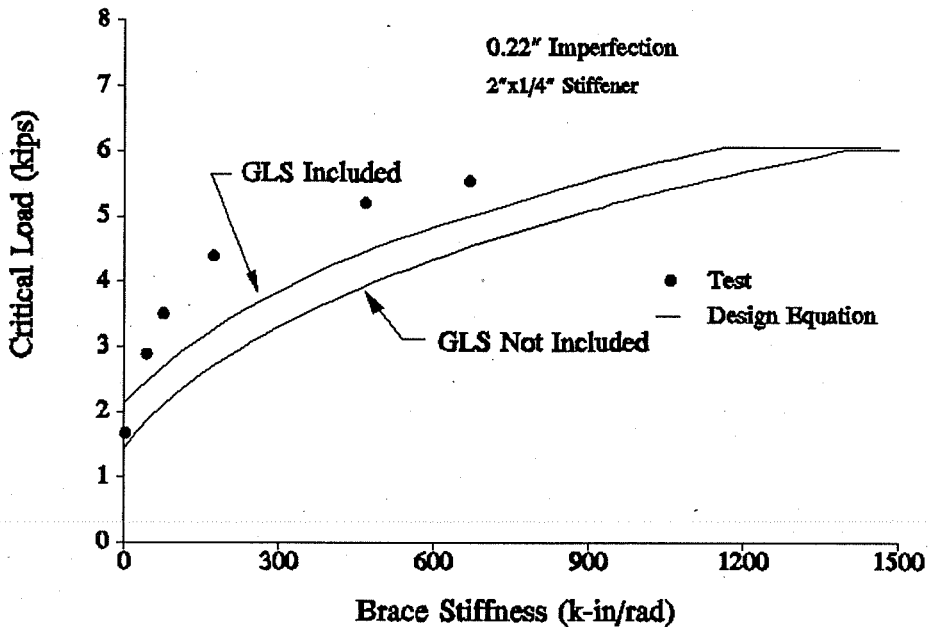


Figure 5.14 - Torsional Bracing, 0.22" Imperfection, 2"x1/4" Stiffener



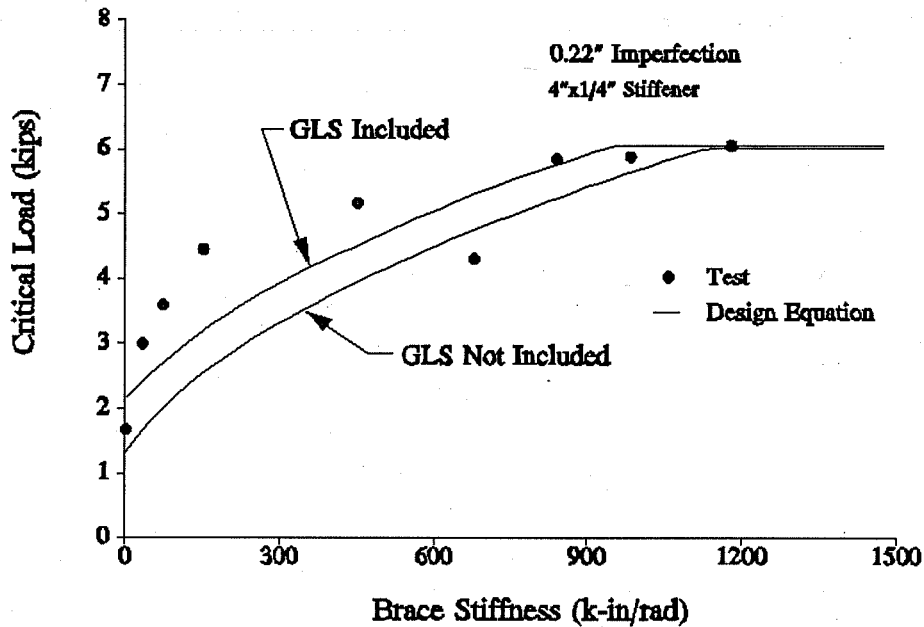


Figure 5.15 - Torsional Bracing, 0.22" Imperfection, 4"x1/4" Stiffener

### 5.6 Effect of Torsional Brace Location

Theoretically, the attachment height of a torsional brace should have no effect on the buckling load if the beam web does not distort. Figure 5.16 and 5.17 show values of critical load for tests with torsional bracing placed on the compression flange, tension flange, or split evenly between the compression and tension flanges (combined bracing). Figure 5.16 and 5.17 show that the combined bracing produced a slightly higher critical load for beams with no stiffener, however, the beam with a 4"x1/4" and a brace stiffness of 175 k-in/rad also showed an increase in critical load. Based on these tests, the brace location did not significantly affect the critical load regardless of the cross-section stiffness of the test beam.

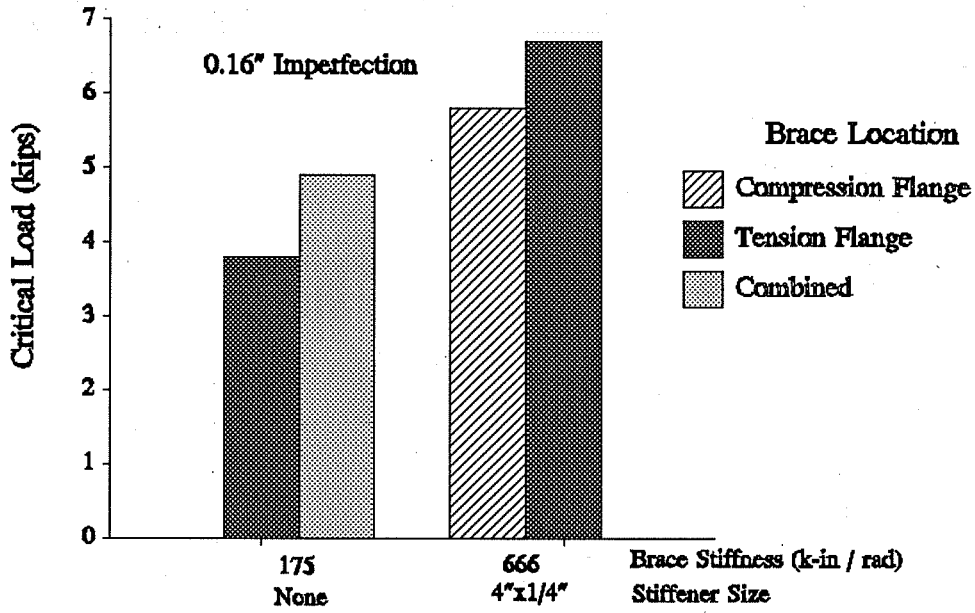


Figure 5.16 - Torsional Brace Location, 0.16" Imperfection

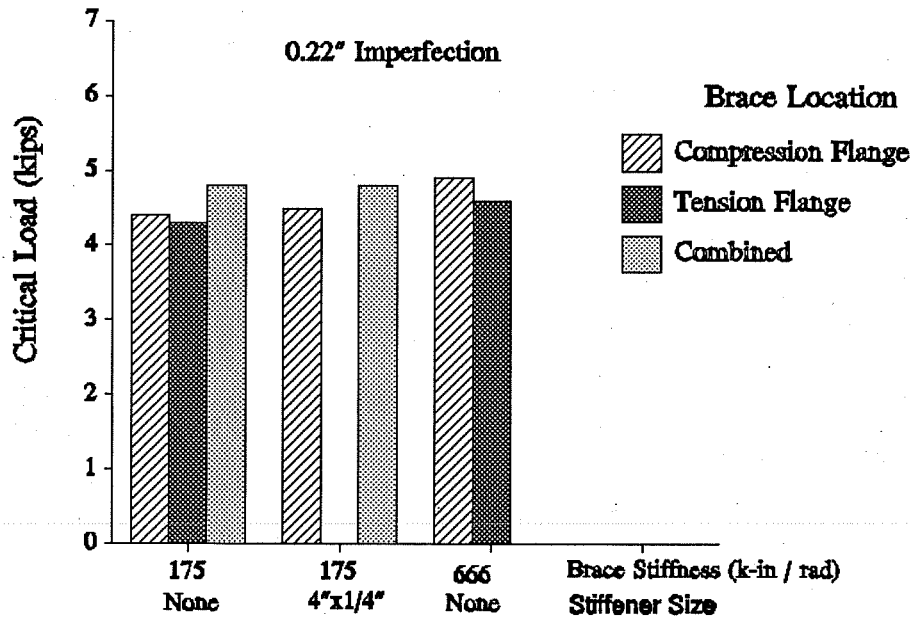


Figure 5.17 - Torsional Brace Location, 0.22" Imperfection

### 5.7 Forced Imperfections

In the experiments, two types of imperfections were tested; natural imperfections and forced imperfections. Since a natural imperfection requires equilibrium of internal stresses and a forced imperfection requires equilibrium with an applied external reaction, there is no theoretical basis for assuming that both types of imperfection would have the same impact on the effective brace stiffness.

Based on Figure 5.18, a forced imperfection has an effect similar to a natural imperfection. Since lateral-torsional buckling involves both a twist and a lateral displacement, the magnitude of initial twist may also have an effect on the brace stiffness.

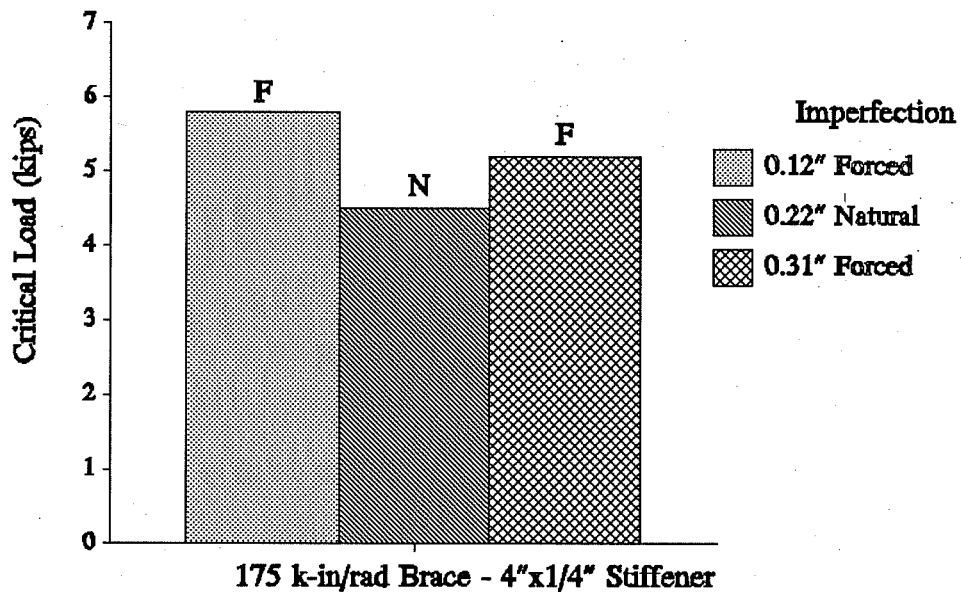


Figure 5.18 - Forced Initial Imperfections

## Chapter 6 Summary and Conclusions

### 6.1 Summary of the Investigation

The purpose of the investigation was to evaluate the effects of intermediate lateral and torsional bracing on the lateral-torsional buckling of steel beams. Design equations were developed to determine the critical load for beams braced by lateral and/or torsional bracing.

The effects of brace stiffness, brace location, and stiffener size were studied both experimentally and analytically. Since the finite element program cannot solve problems with initial imperfections, the effects of imperfections were studied only with the experimental program. The design equations are presented and compared to finite element solutions for straight beams in Chapter 2 and are compared to experimental results in Chapter 5.

### 6.2 Conclusions

For the cases examined, the design equations presented give an adequate determination of the buckling strength of the member when corrections for cross-section distortion and initial imperfections are performed. For most tested cases, the critical load given by the design equations was less than or equal to the test load.

Both the analytical and experimental studies indicate that a slender beam web can lead to a substantial decrease in buckling strength. In almost every tested case, an increase in stiffener size resulted in an increase in buckling strength. The increase in buckling strength was most apparent when the stiffener was positioned so that it was touching the compression flange of the test beam.

The experimental program indicated that initial imperfections have a significant effect on buckling strength. The design equations were first verified for straight beams using the BASP program. After these verifications were made, a modifying factor for imperfections was applied so that the design equations matched the experimental data. Many of the tests were performed with an imperfection of only 0.04 inches thus giving an indication of the validity of the design equations for nearly straight beams.

### 6.3 Recommendations

The buckling strength of beams with bracing can be accurately evaluated using the design equations summarized in Appendix B. In general, the equivalent continuous brace can be determined by summing all point-braces on the span and dividing by the span length. For beams that are braced with a single lateral or torsional brace at mid-span, the equivalent continuous stiffness can be determined by dividing the single-brace stiffness by 75 percent of the span length.

All calculations of buckling strength should include the effects of cross-section distortion and initial imperfections. When stiffeners are required at torsional brace locations they should be attached so that they are in contact with the flange being braced.

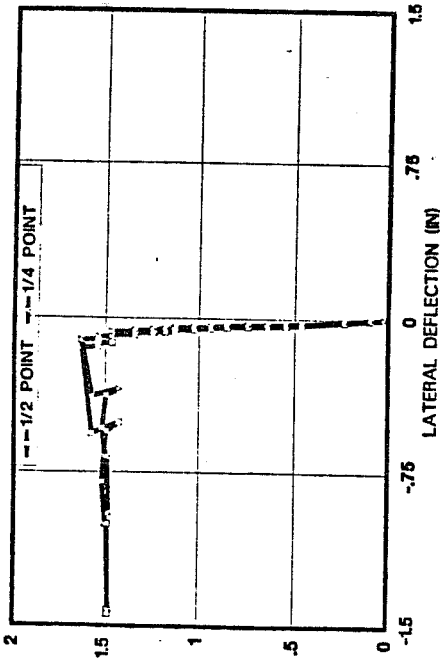
For beams within a sweep tolerance of  $L/500$ , the following reduction factors for imperfections can be used in lieu of measurements of sweep. The constant  $c_t$  should be taken as 0.15 for torsional bracing and the constant  $c_L$  should be taken as 0.25 for lateral bracing.

**Appendix A**

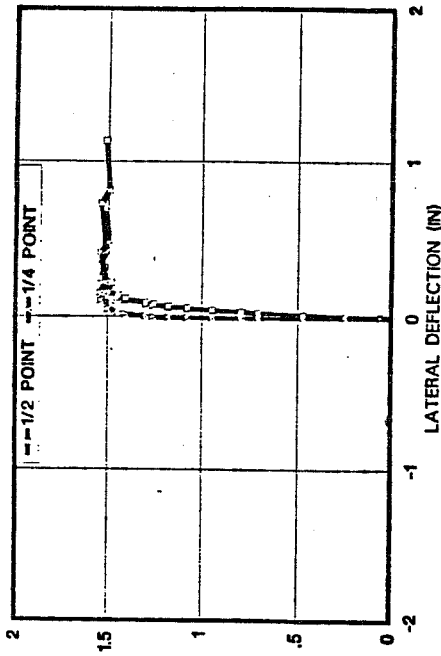
**Load-Deflection Curves**

Per = 1.58

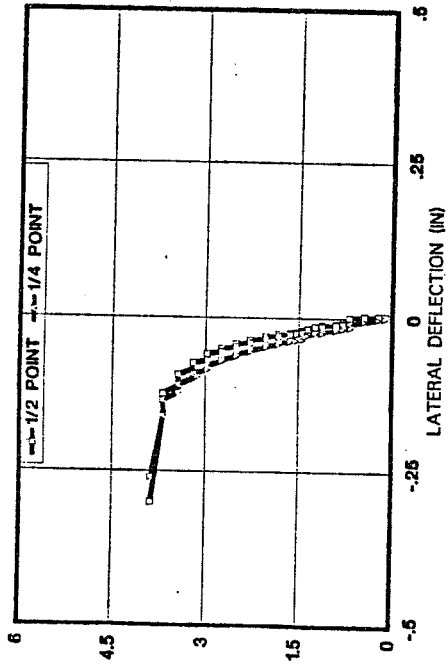
TEST A1001



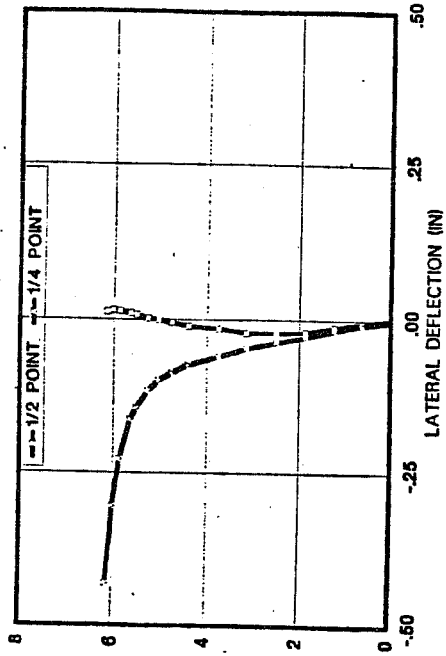
TEST A2001 Per = 1.59



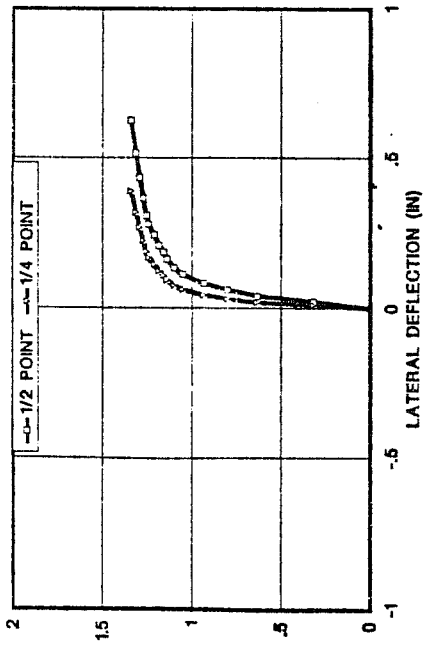
TEST A3001



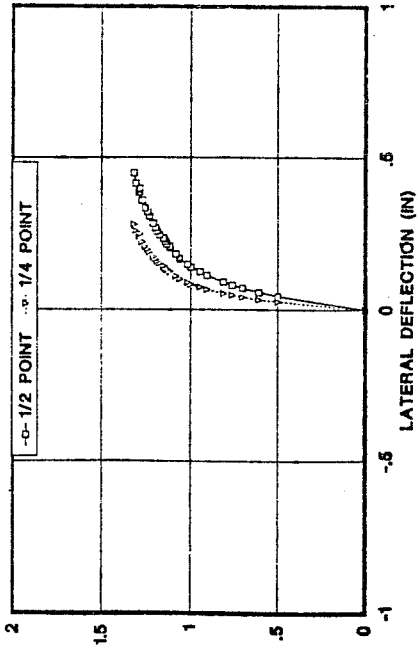
TEST A4001



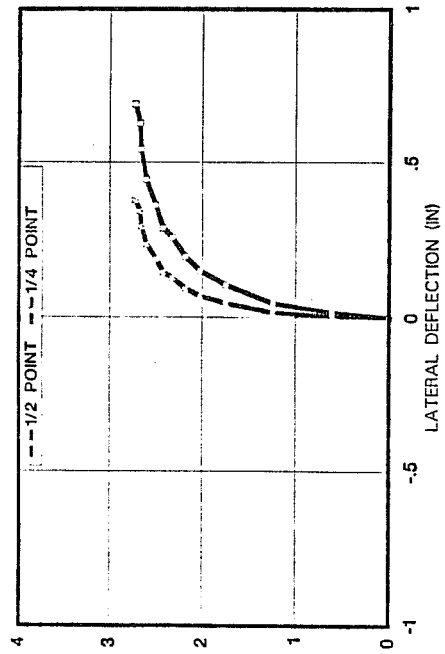
TEST A5.001



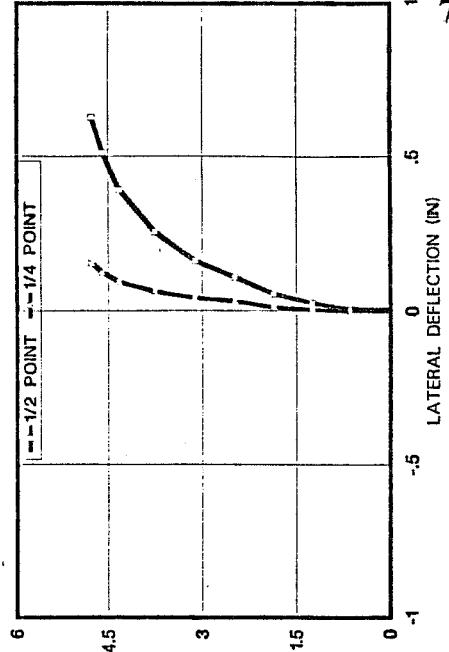
TEST A6.001



TEST B1.001

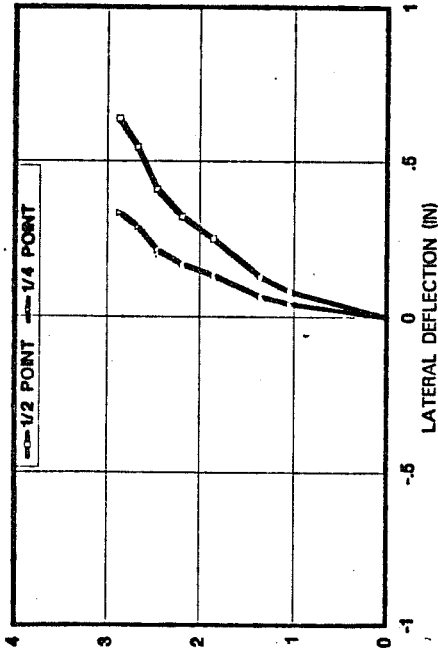


TEST B2.001





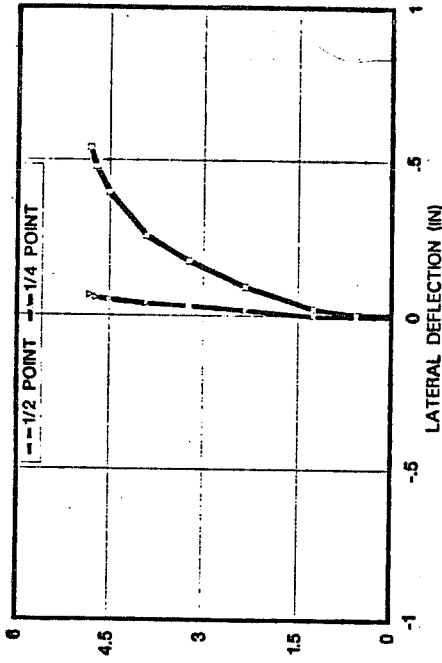
TEST B3.001



LOAD (KIPS)

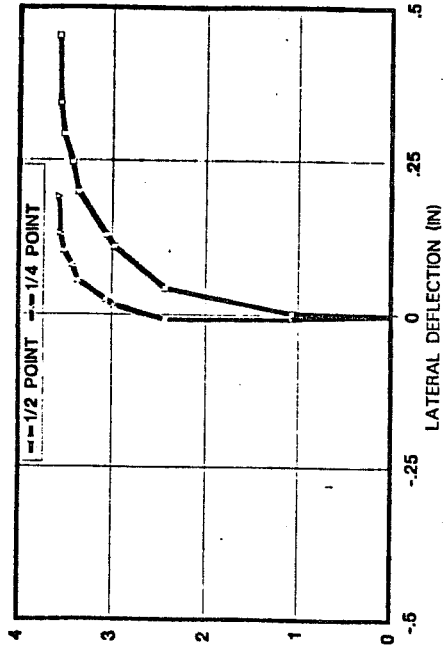
LATERAL DEFLECTION (IN)

TEST B4.001



LATERAL DEFLECTION (IN)

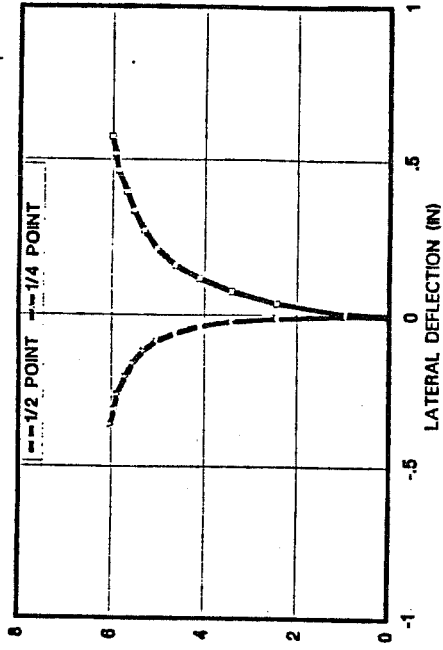
TEST B5.001



LOAD (KIPS)

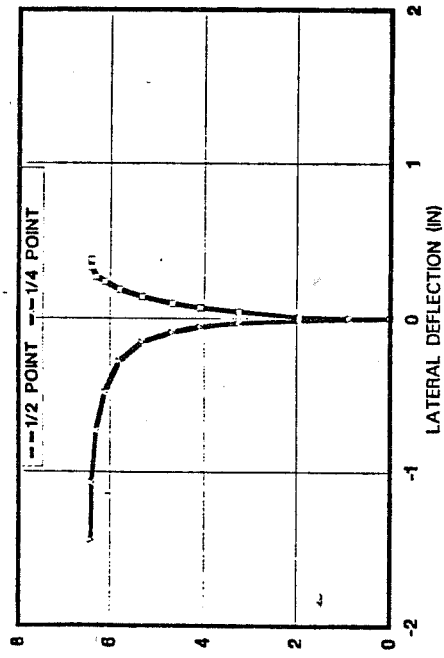
LATERAL DEFLECTION (IN)

TEST B6.001



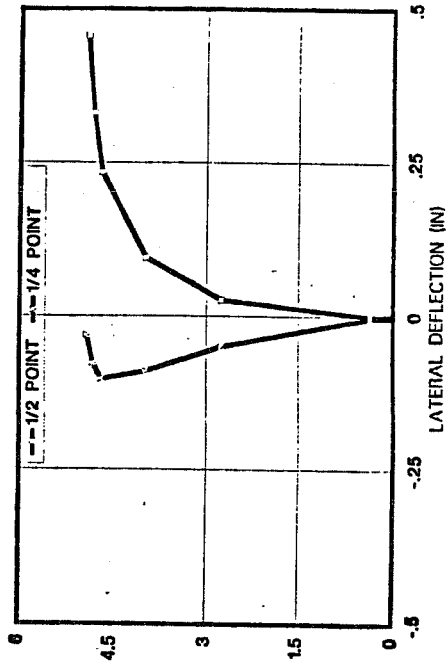
LATERAL DEFLECTION (IN)

TEST B7.001



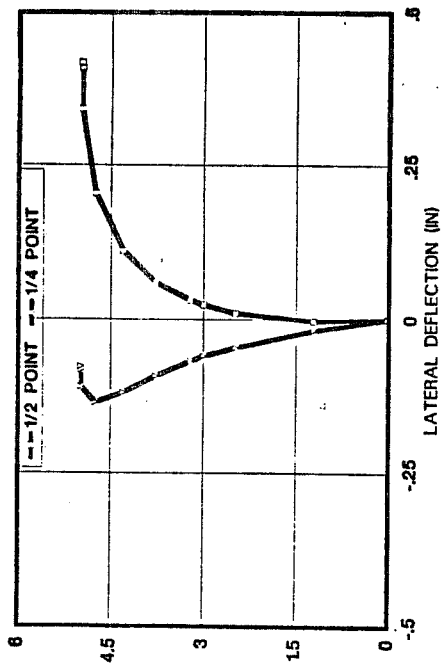
LOAD (KIPS)

TEST B8.001



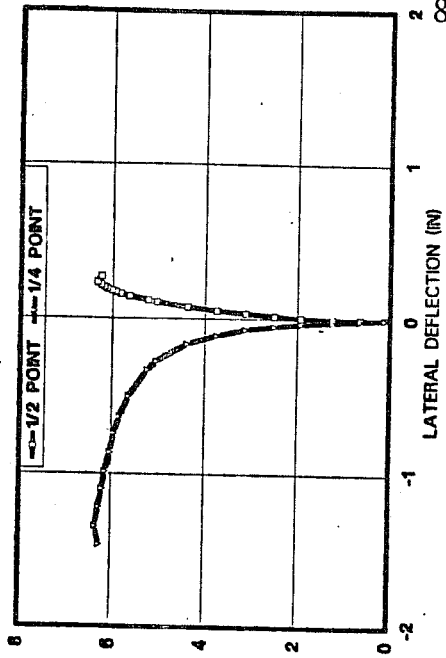
LOAD (KIPS)

TEST B9.001



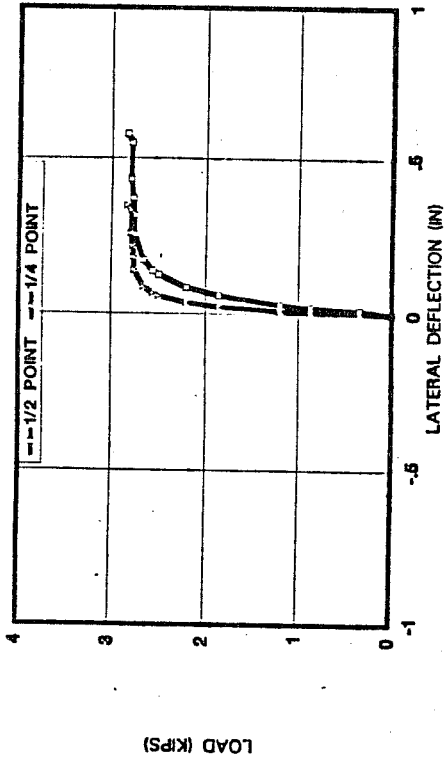
LOAD (KIPS)

TEST B10.001

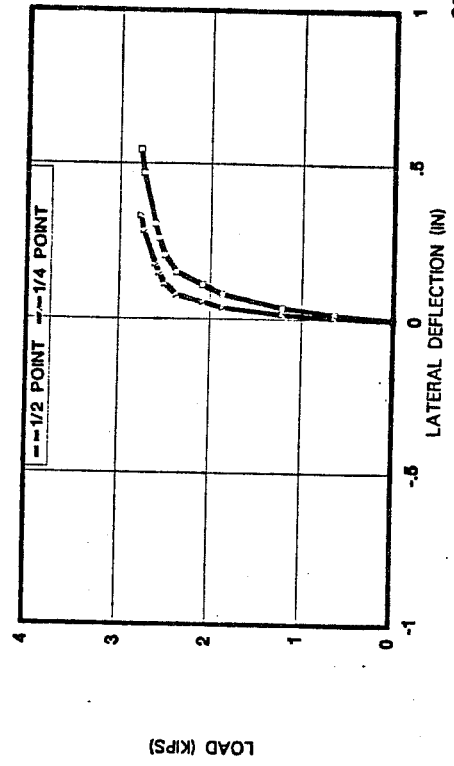


LATERAL DEFLECTION (IN)

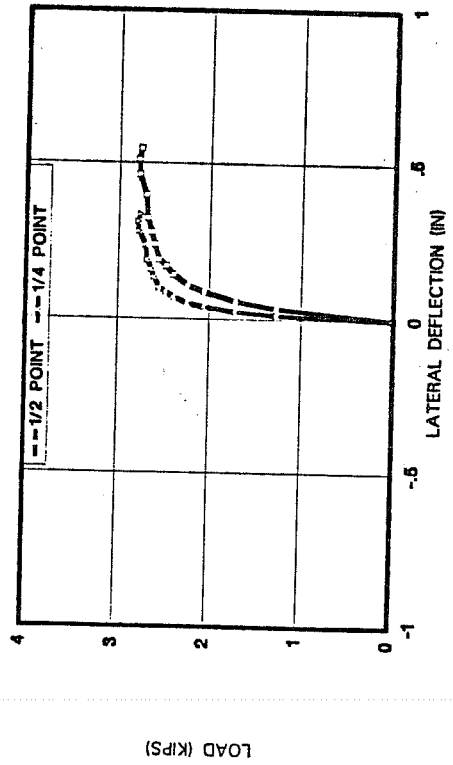
TEST C1.001



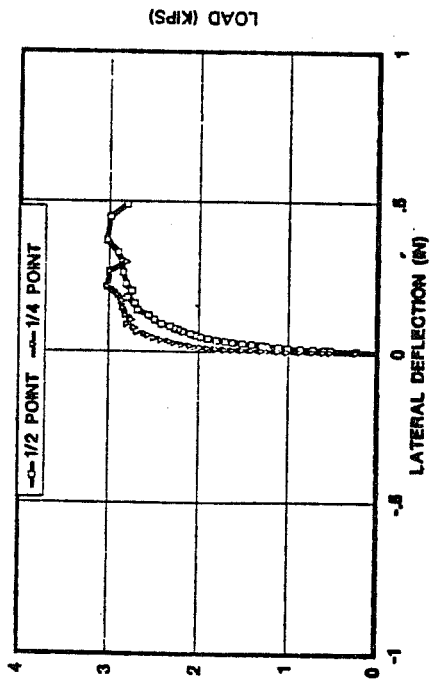
TEST C3.001



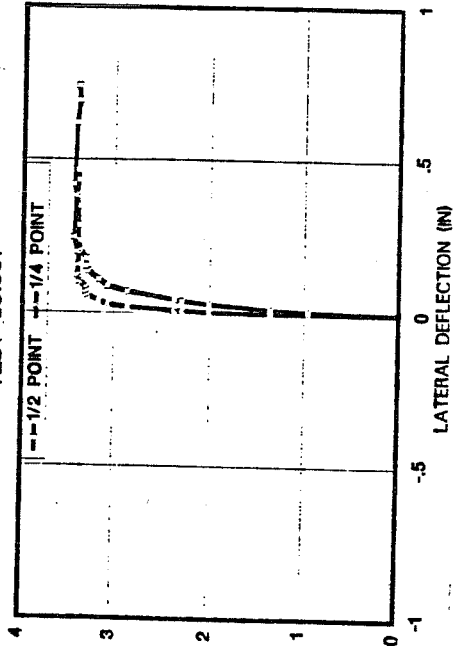
TEST C2.001



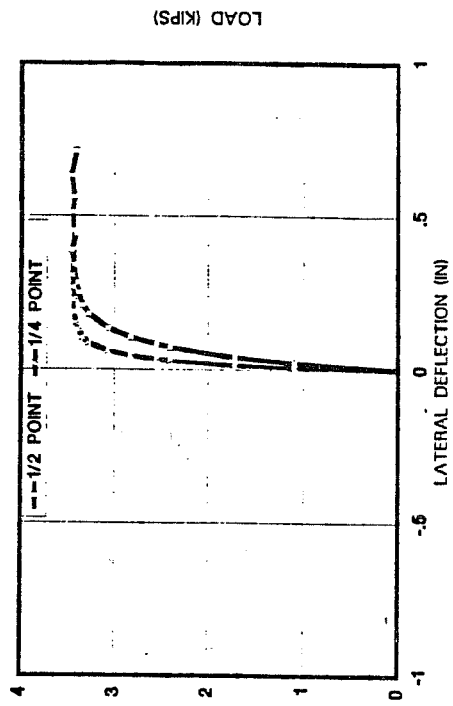
TEST C4.001



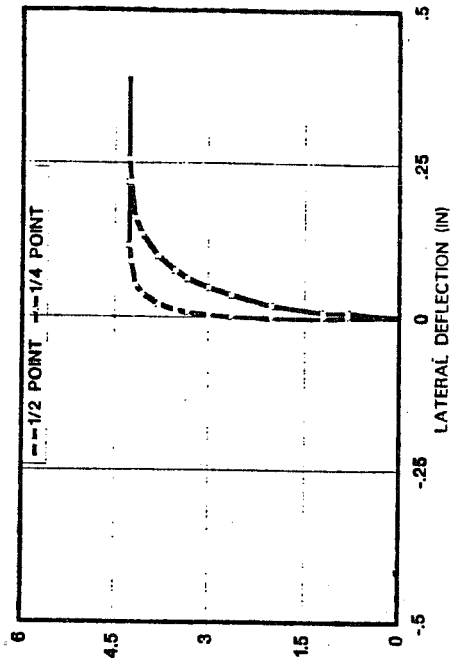
TEST C5.001



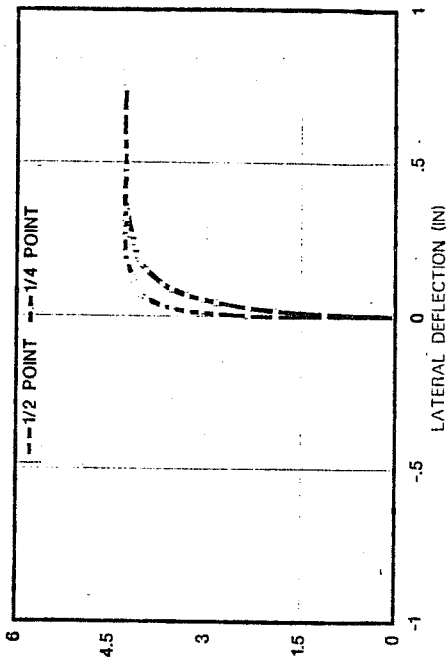
TEST C6.001



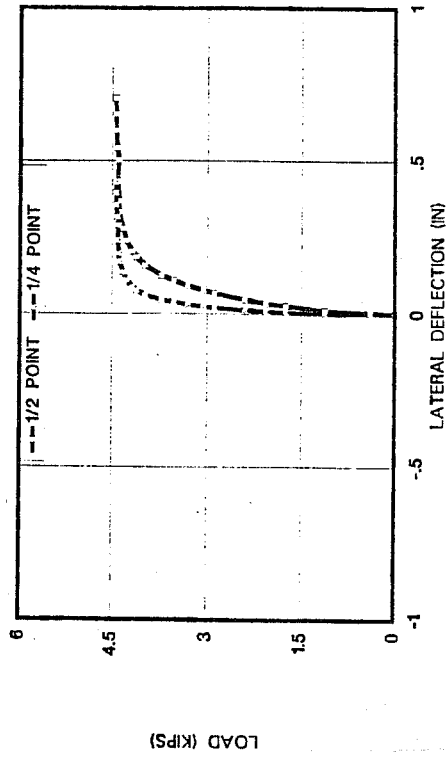
TEST C7.001



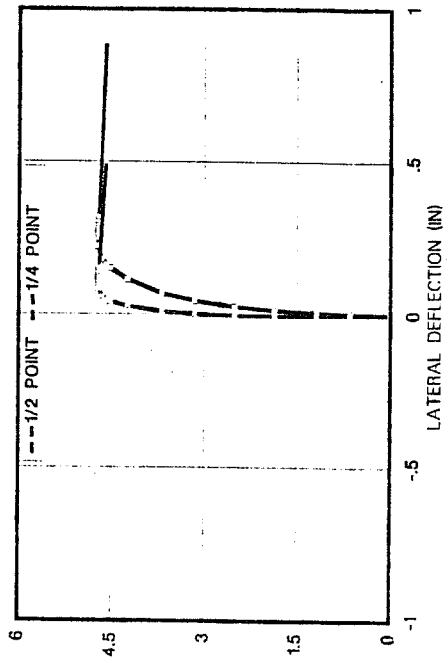
TEST C8.001



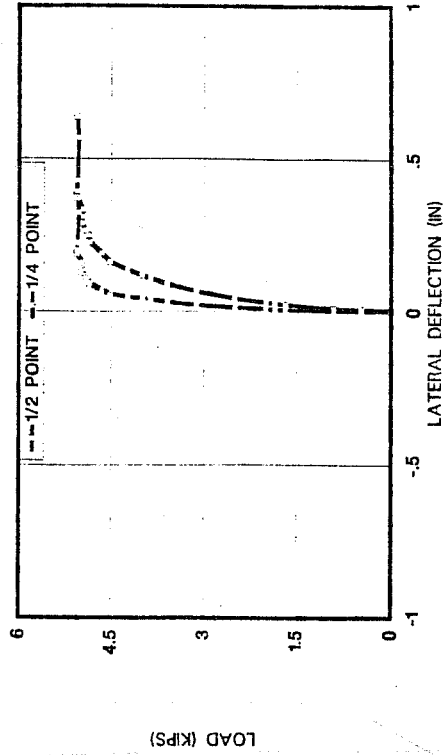
TEST C9.001



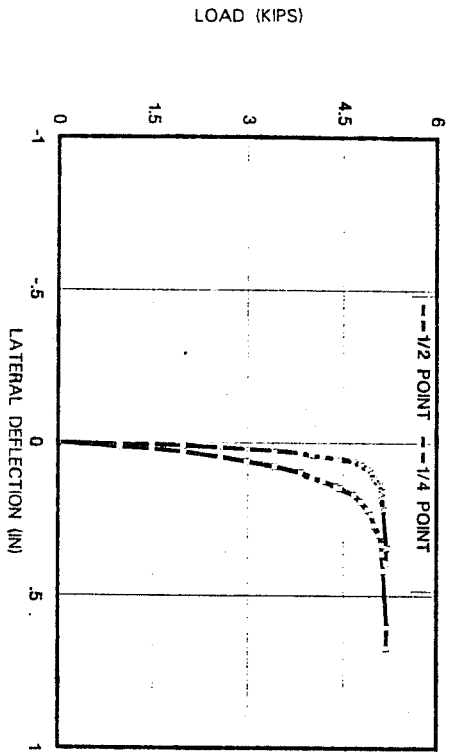
TEST C10.001



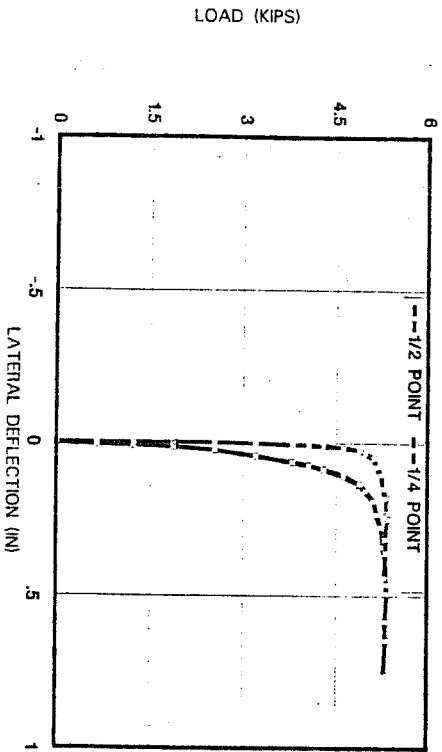
TEST C11.001



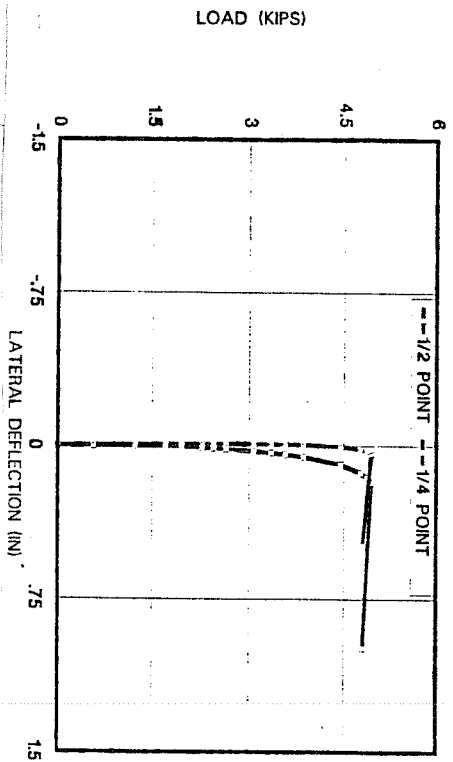
TEST C12.001



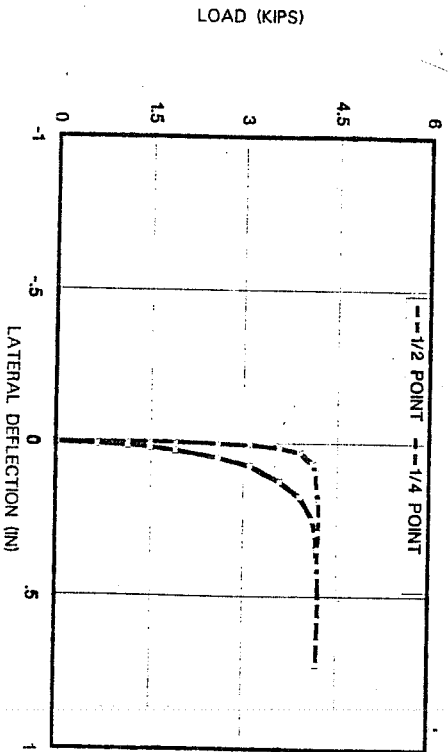
TEST C14.001

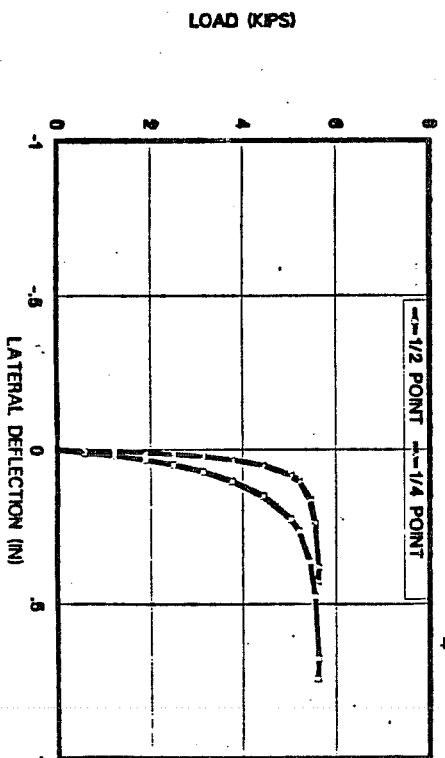
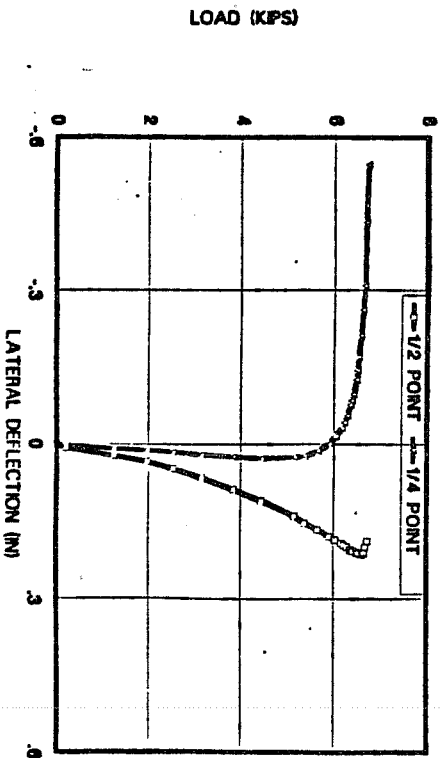
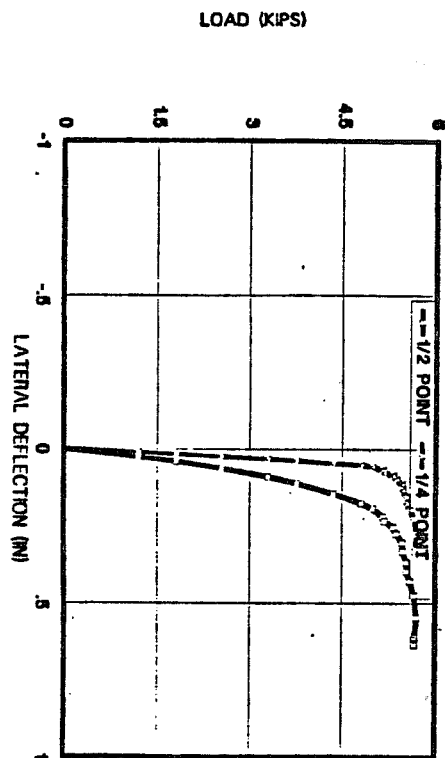
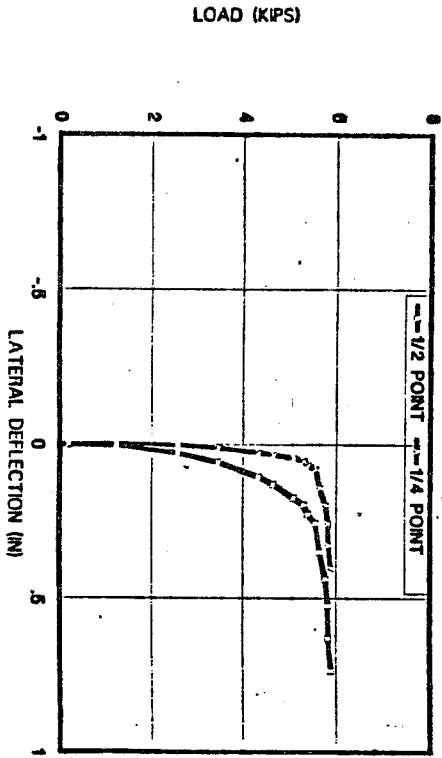


TEST C13.001

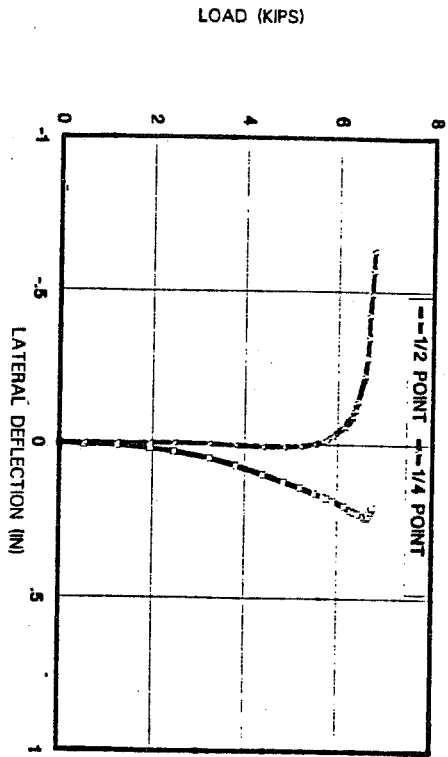


TEST C15.001

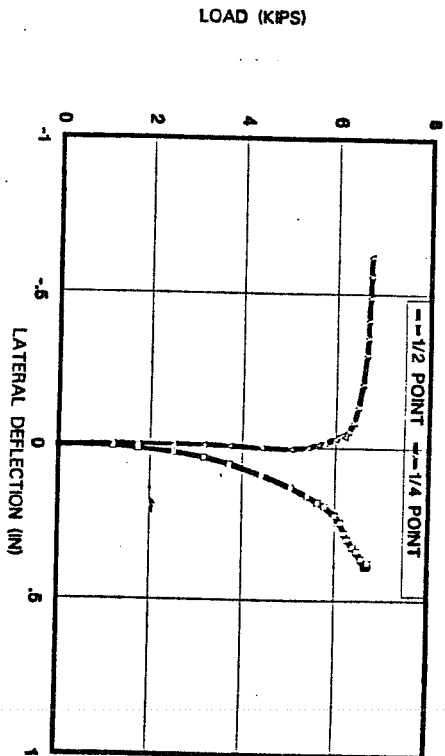




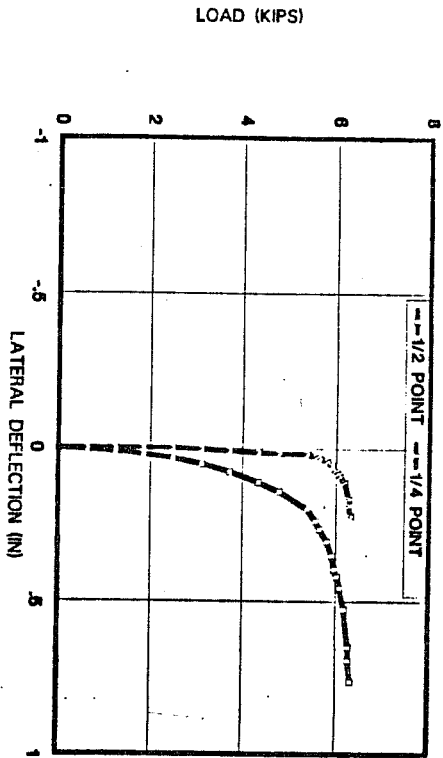
TEST C20.001



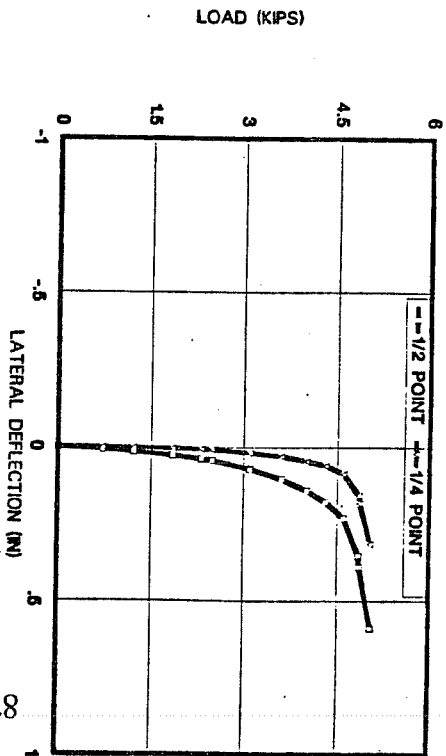
TEST C21001



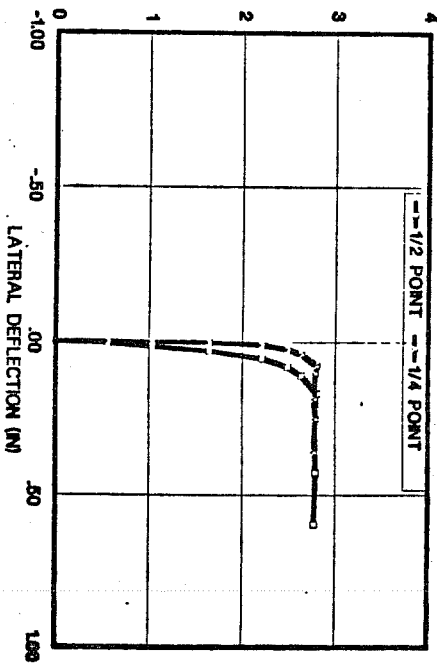
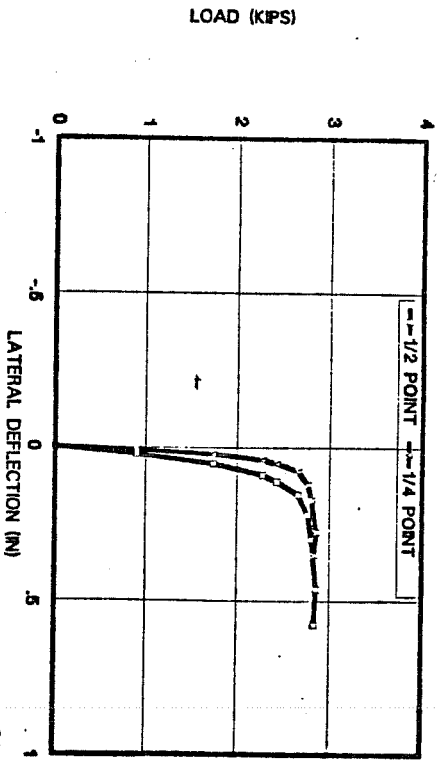
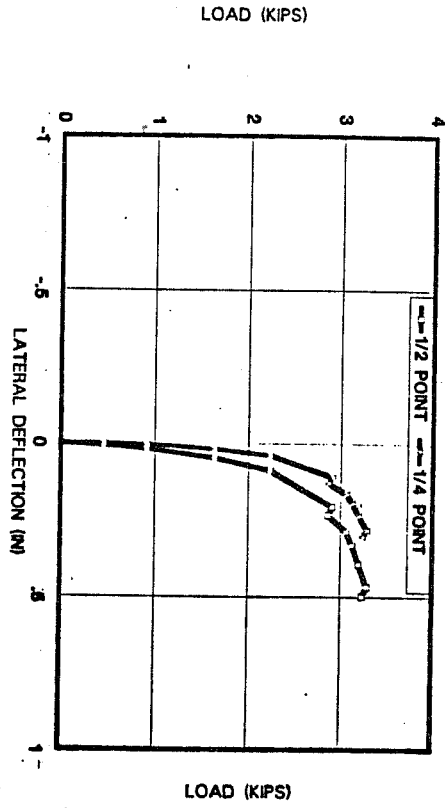
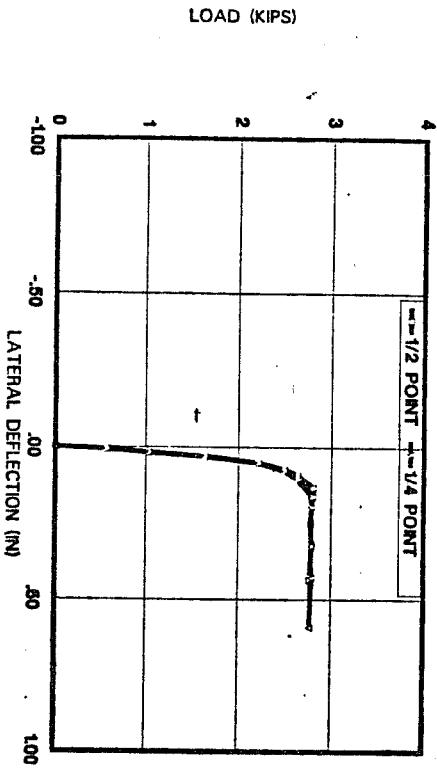
TEST C22.001



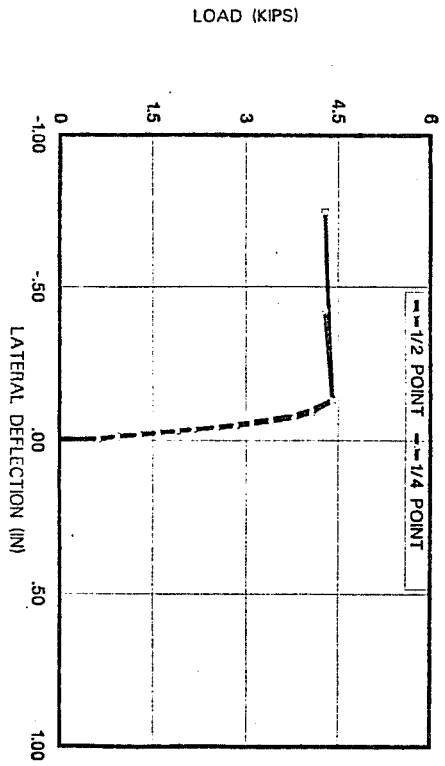
TEST C23.001



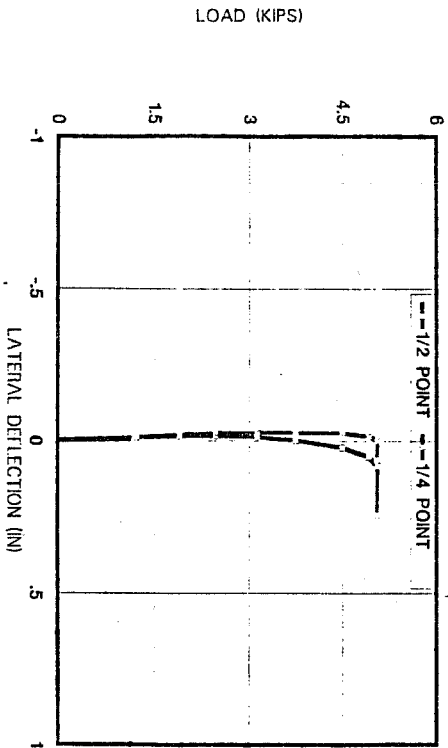




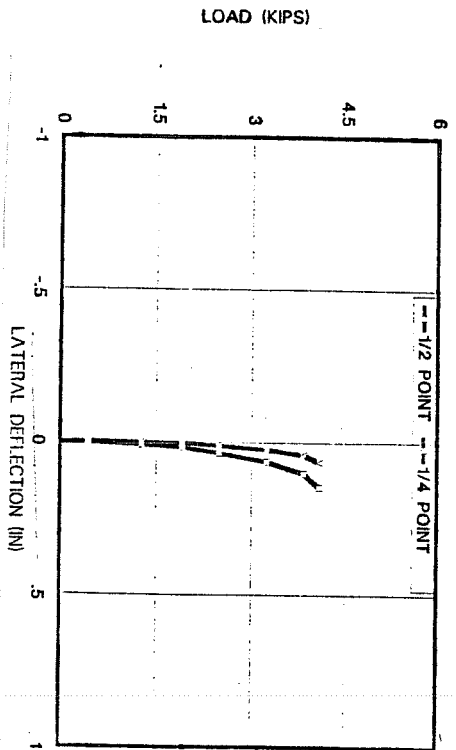
TEST C28.001



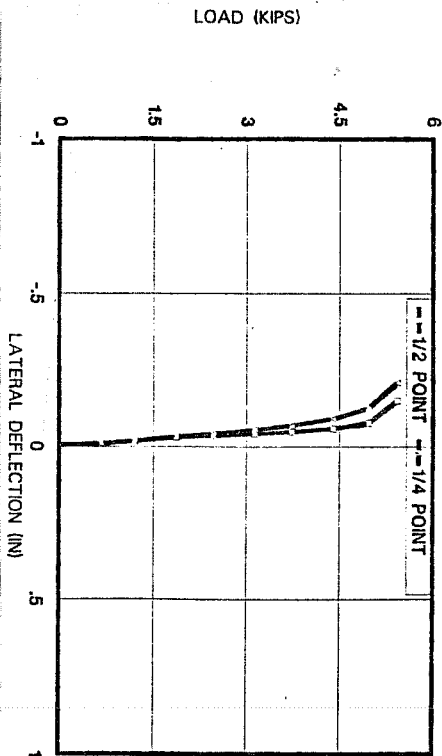
TEST C30.001



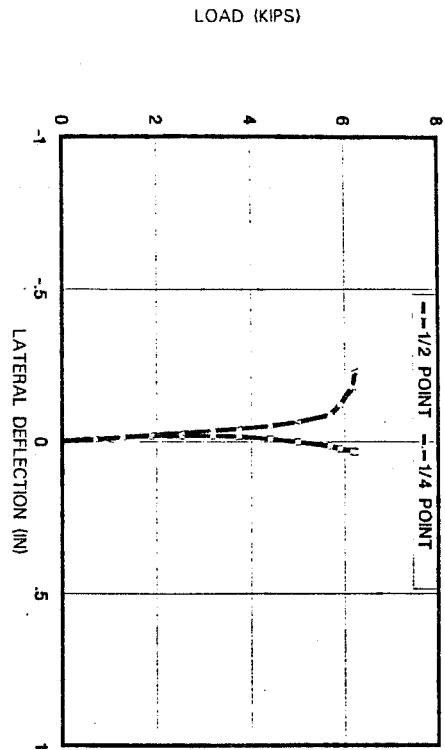
TEST C29.001



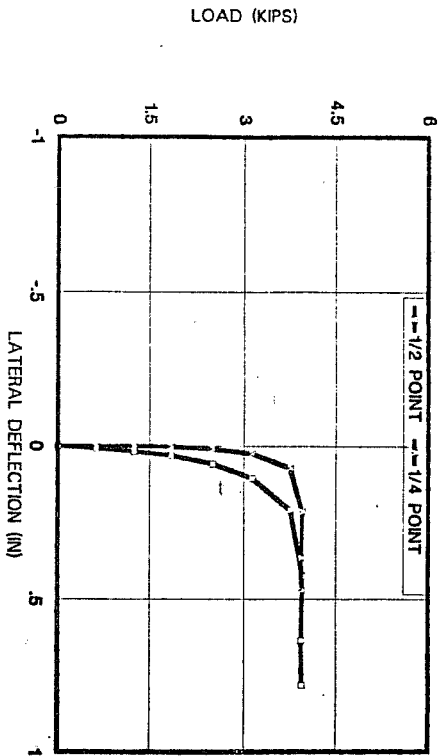
TEST C31.001



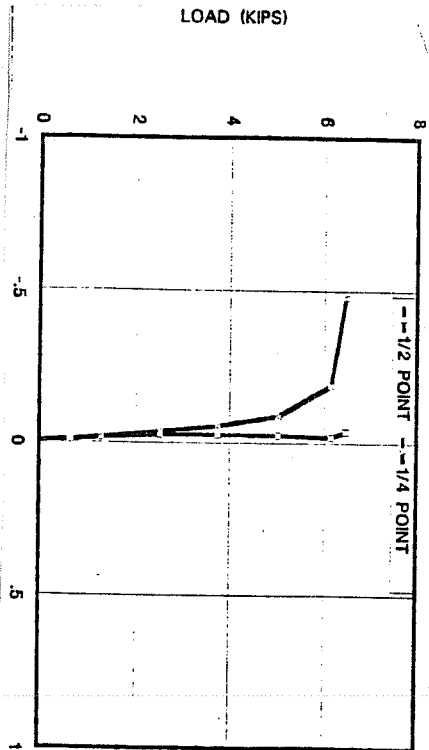
TEST C32.001



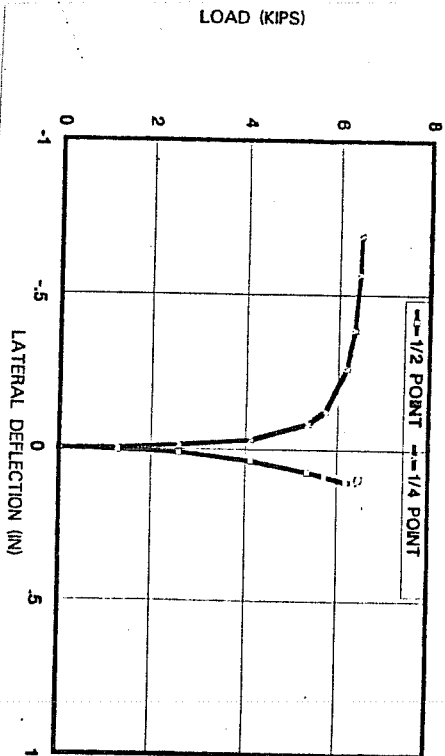
TEST C34.001

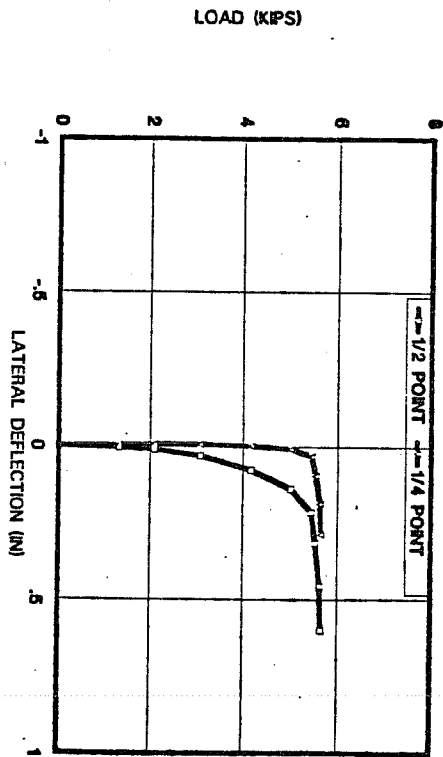
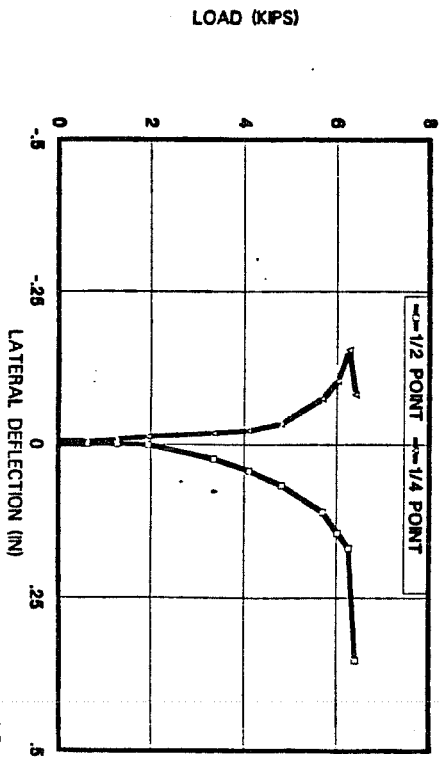
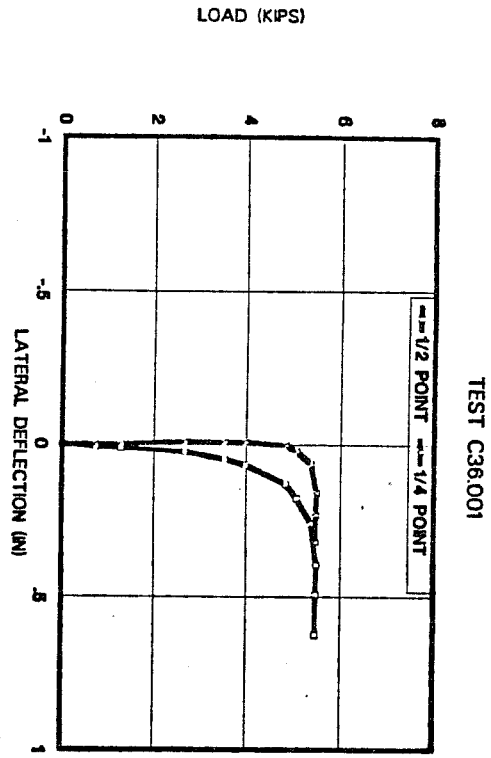
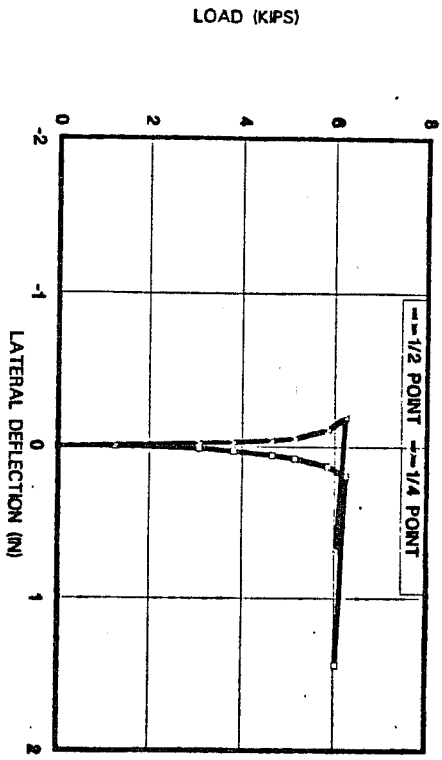


TEST C33.001

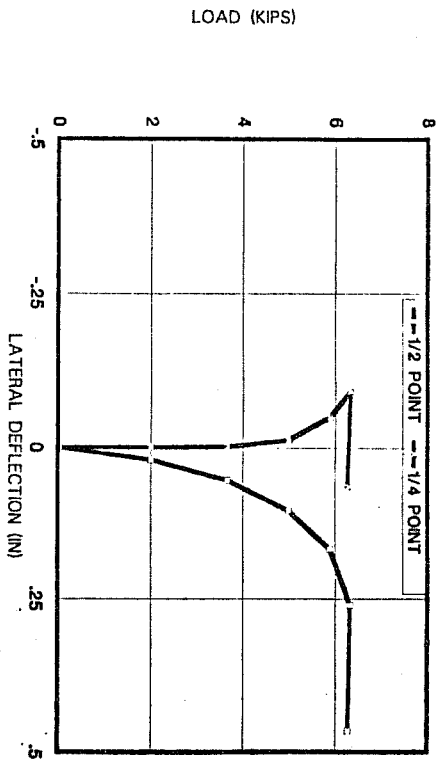


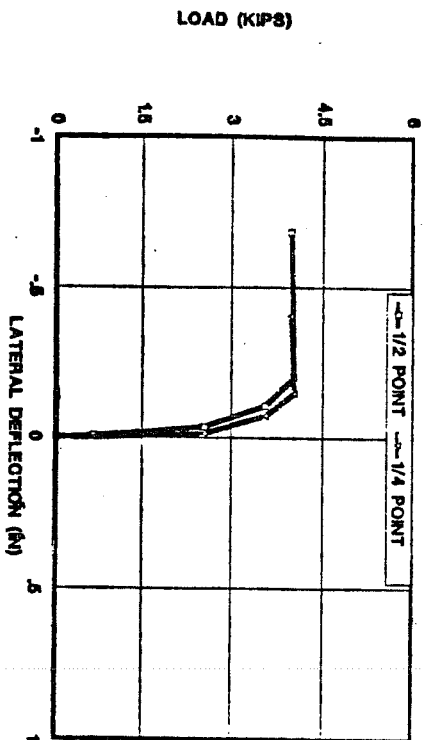
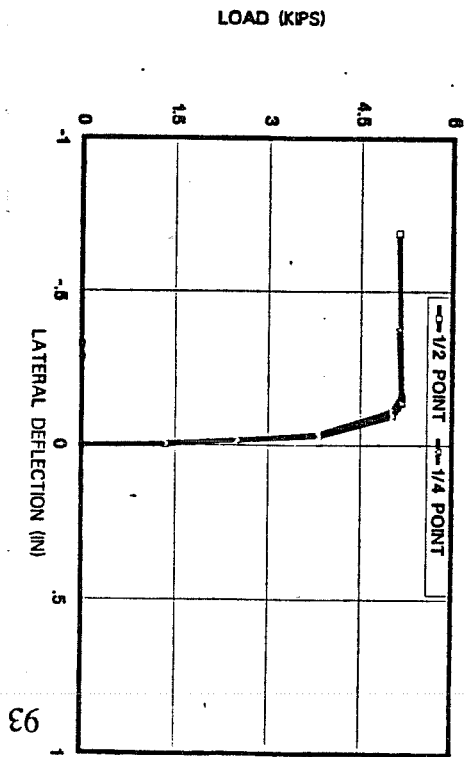
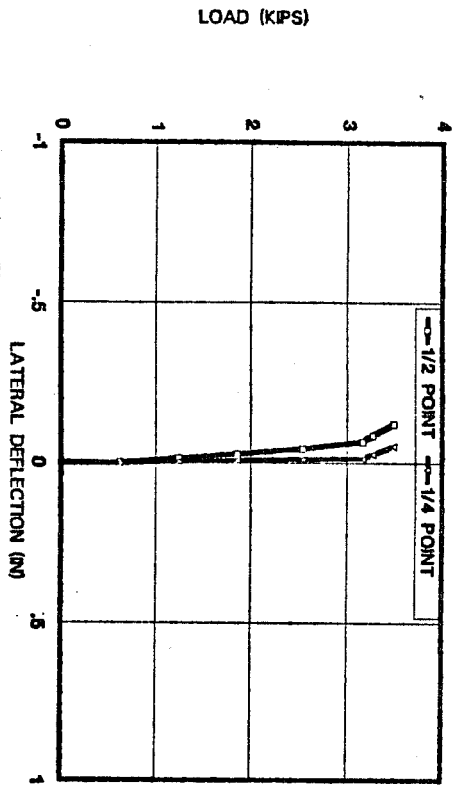
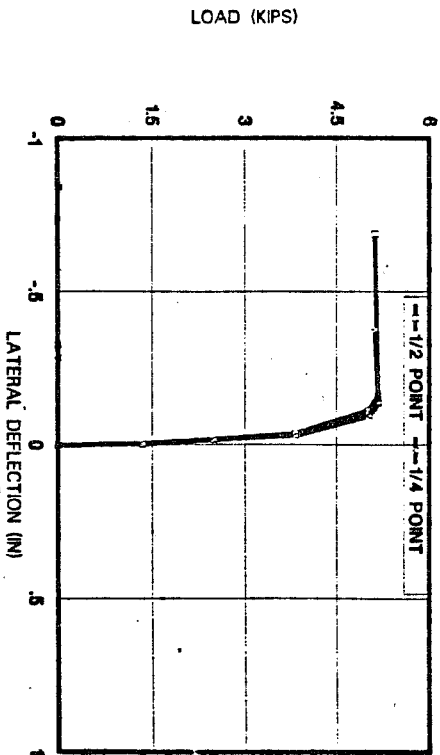
TEST C36.001

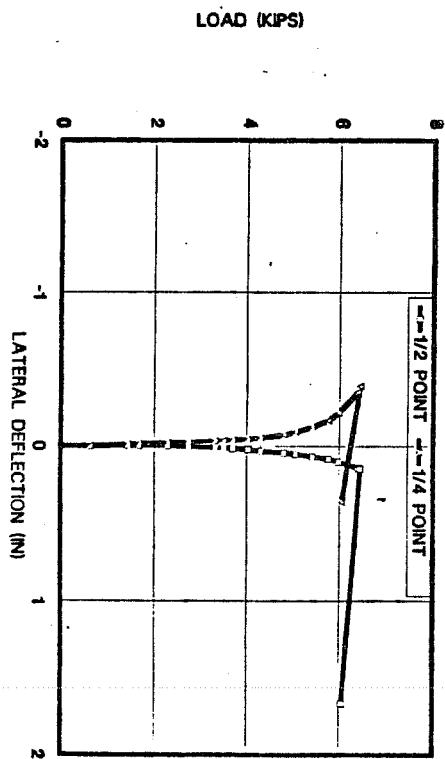
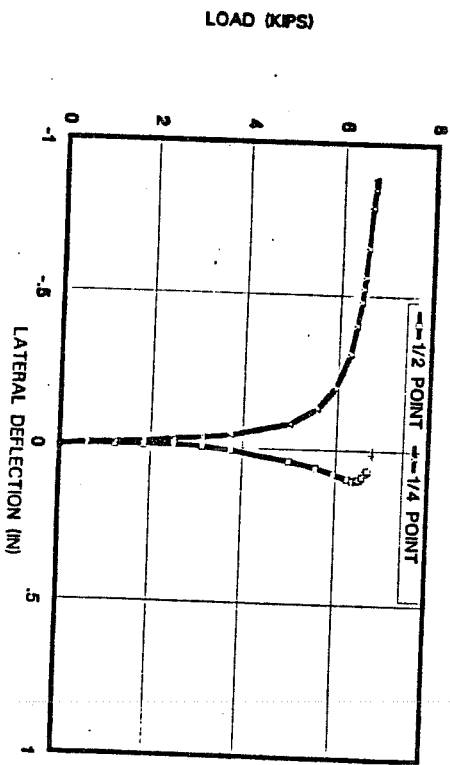
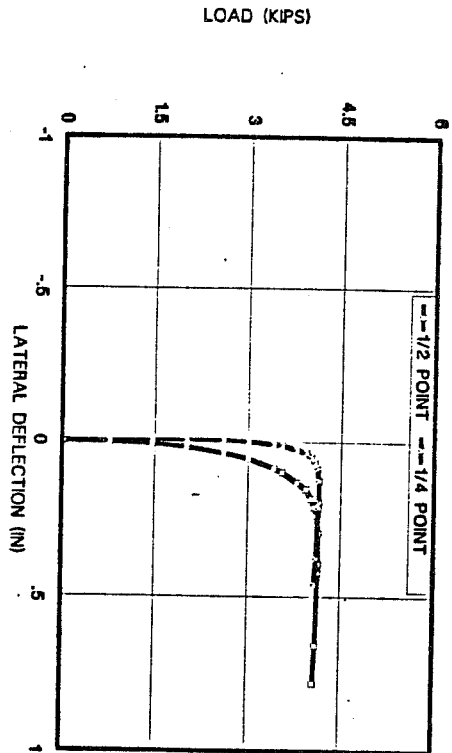
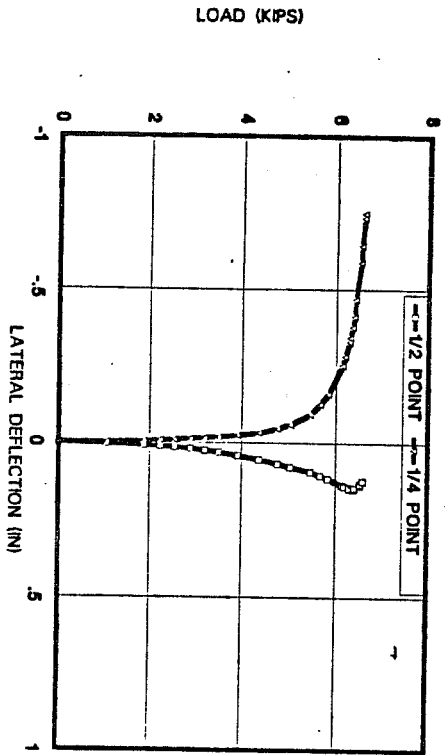


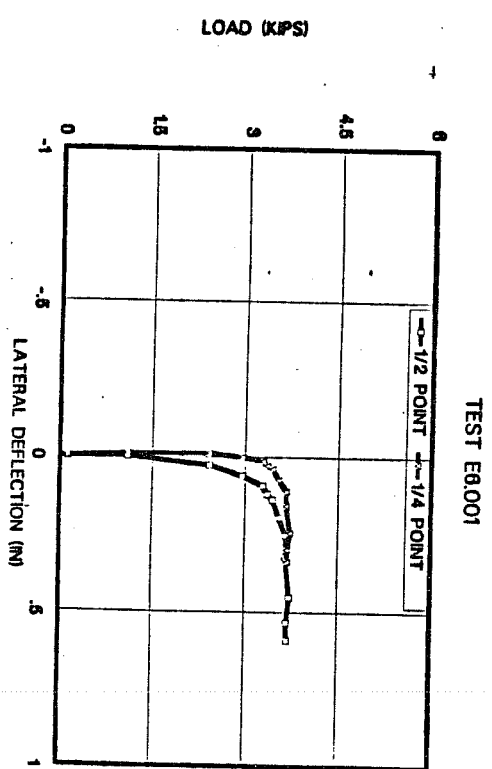
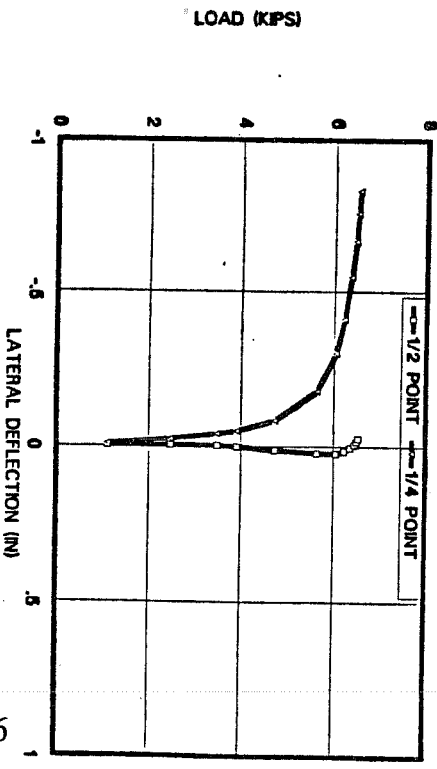
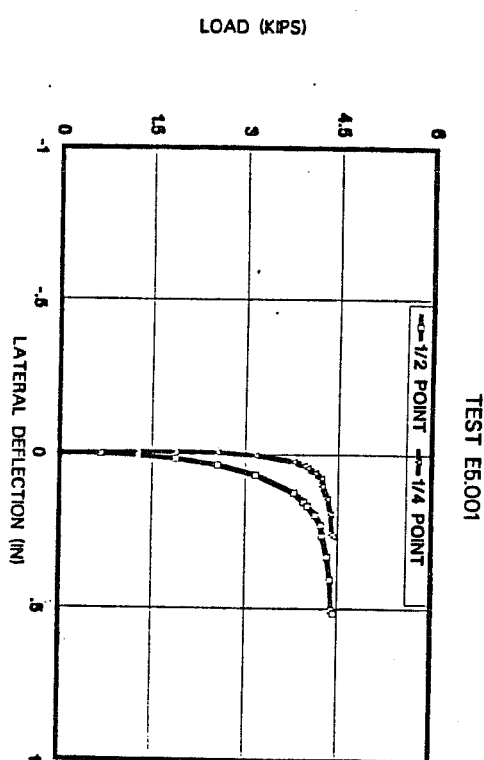
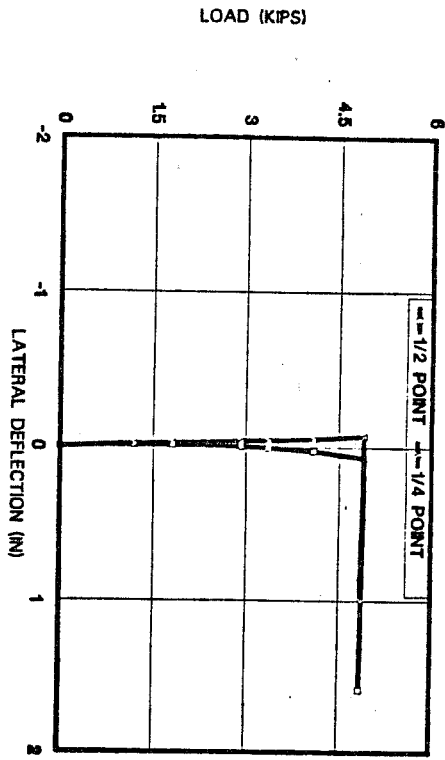


TEST C40.001

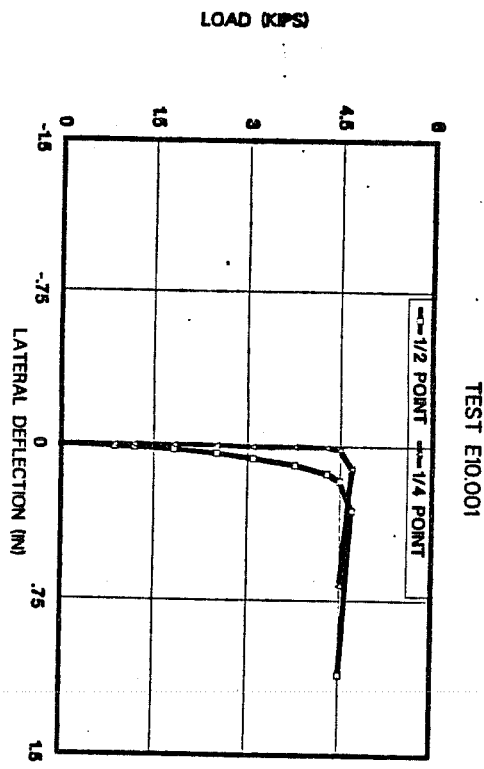
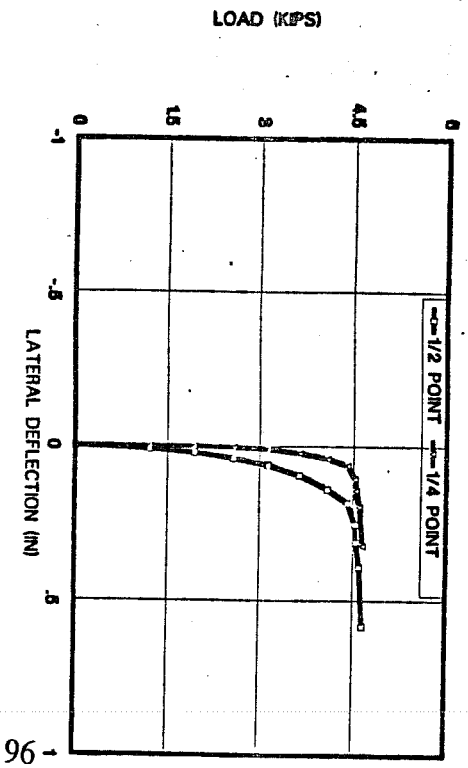
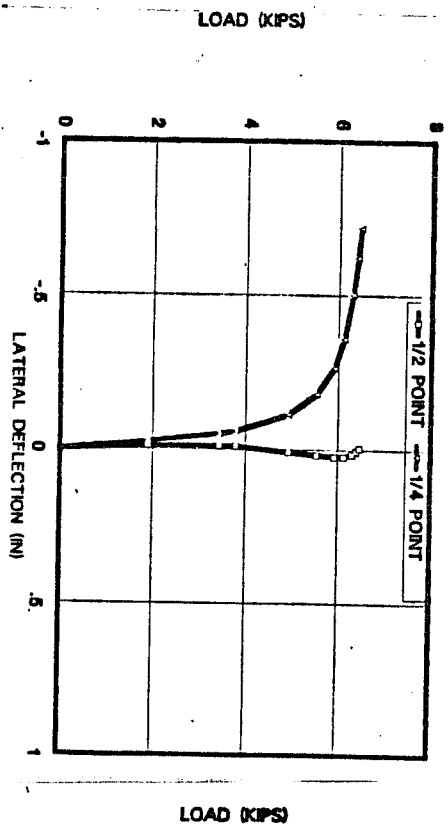
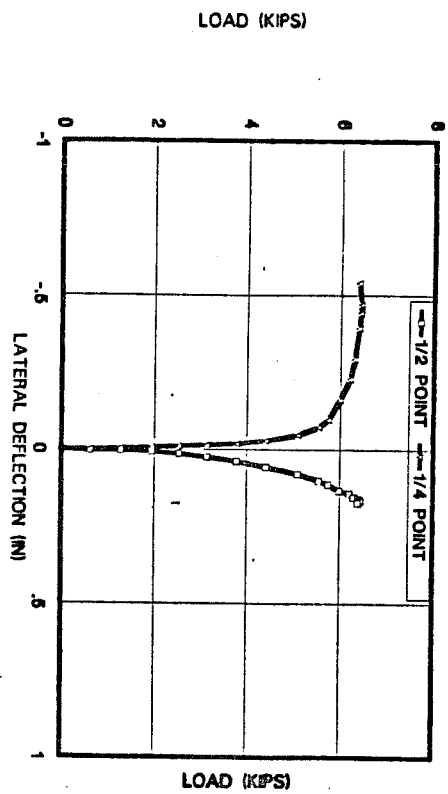




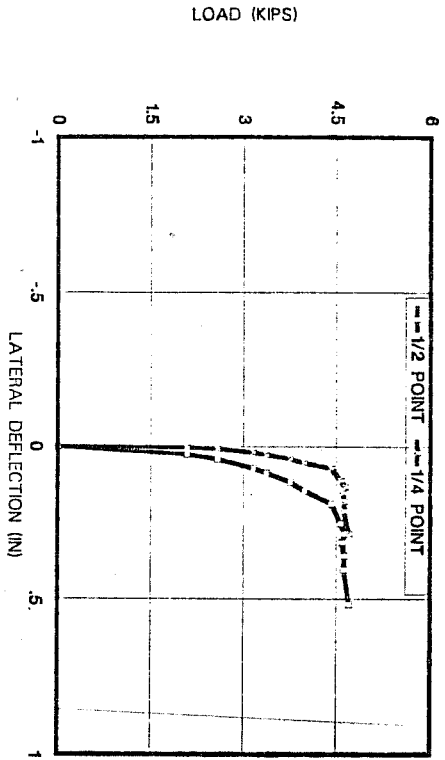




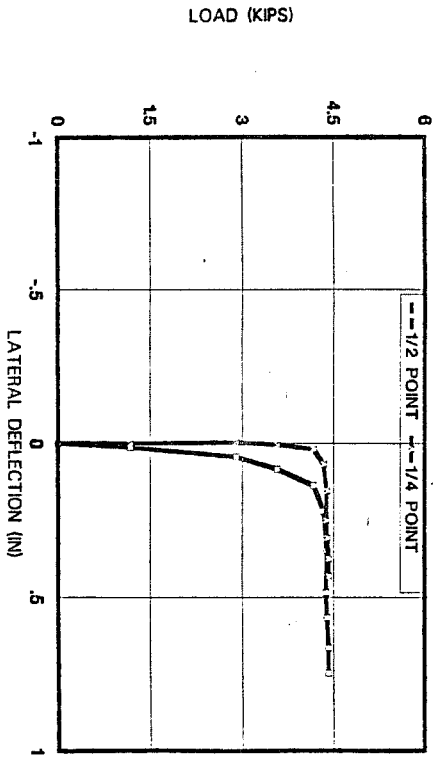




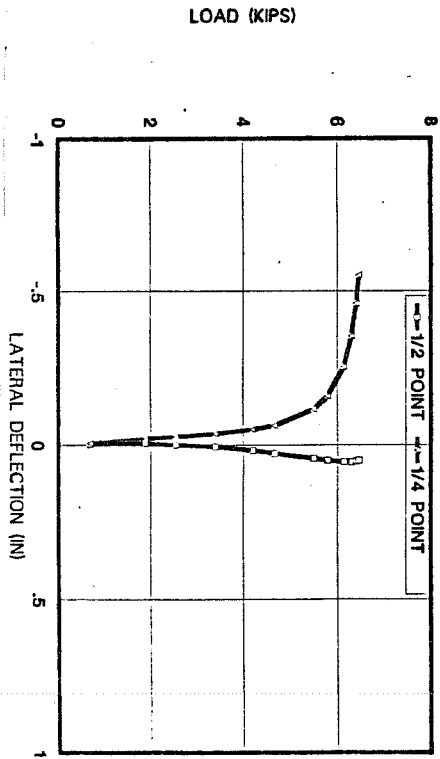
TEST F3.001



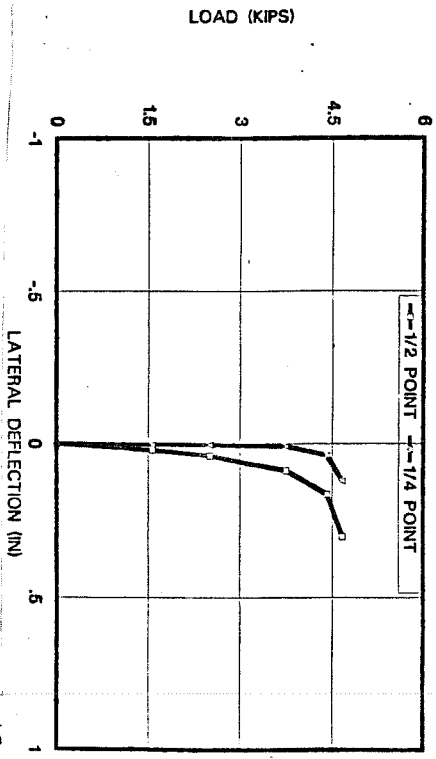
TEST F5.001



TEST F4.001



TEST F6.001



**Appendix B**  
**Summary of Design Equations**

Lateral Bracing

$$M_{cr} = \sqrt{\left(M_o^2 + \frac{P_y^2 h^2 A}{4}\right) (1 + A)} \quad (B1)$$

$$\text{where } M_{cr} = \frac{\pi}{L} \sqrt{EI_y GJ + \frac{\pi^2 E^2 I_y^2 h^2}{4L^2}} \quad (B2)$$

$$A = \frac{L^2}{\pi} \sqrt{\frac{.67 \beta_L}{EI_y}} \quad (B3)$$

$$P_y = \frac{\pi^2 EI_y}{L^2} \quad (B4)$$

$$C_L = \frac{1}{1 + 1500 \frac{\Delta_o}{L}} \quad (B5)$$

where  $E$  = modulus of elasticity,  $I_y$  = weak axis moment of inertia,  $L$  = total span length,  $h$  = distance between flange centroids,  $\beta_L$  = equivalent continuous lateral brace,  $\Delta_o$  = initial imperfection.

Torsional Bracing

$$M_{cr} = \sqrt{M_o^2 + \beta_t EI_y} \quad (B6)$$

$$\text{where } \beta_t = \frac{1}{\frac{1}{C_t \beta_b} + \frac{1}{\beta_{sec}}} \quad (B7)$$

$$C_t = \frac{1}{1 + 3000 \frac{\Delta_o}{L}} \quad (B8)$$

$$\beta_{sec} = 3.3 \frac{E}{h} \left( \frac{1.5 h t_w^3}{12} + \frac{t_s b_s^3}{12} \right) \quad (B9)$$

where  $t_s$  = stiffener thickness,  $b_s$  = stiffener width,  $\beta_t$  = equivalent continuous torsional brace.

## Bibliography

- Akay, H.U., Johnson, C.P., and Will, K.M., (1977). "Lateral and Local Buckling of Beams and Frames," Journal of the Structural Division, ASCE, ST9, September, pp. 1821-1832.
- Bleich, (1978). Buckling Strength of Metal Structures, New York.
- Choo, K.B., (1987). thesis presented to the University of Texas at Austin, May, "Buckling Program BASP For Use On A Microcomputer,"
- Flint, A.R., (1951a). "The Stability of Beams Loaded through Secondary Members," Civil Engineering and Public Works Review. vol 46 No 537-8 pp. 175-177 259-260
- Flint, A.R., (1951b). "The Influence of Restraint on the Stability of Beams," The Structural Engineer, Sept. 1951 pp. 235-246
- Galambos, T.V., (1988). ed, Structural Stability Research Council, Guide to Stability Design Criteria for Metal Structures, 4th Edition. New York: John Wiley & Sons Inc.
- Gedies, R.W., (1983). thesis presented to the University of Texas at Austin, December, "Beam Buckling Tests with Various Brace Stiffnesses,"
- Kirby, P.A. and Nethercot, D.A., (1979), Design for Structural Stability, Wiley
- Kissane, R.J., (1985). "Lateral Restraint of Non-Composite Beams.", Research Report 123, New York State Department of Transportation. August
- Kitipornchai and Richter, N.R., (1978). "Lateral Buckling of Beams with Discrete Braces," Reprint from Metal Structures Conference Nov. 30,
- Meck, H.R., (1977). "Experimental Evaluation of Lateral Buckling Loads," Journal of the Engineering Mechanics Division, ASCE, EM2, April, pp. 331-337.

- Mutton, B.R., and Trahair, N.S., (1973). "Stiffness Requirements for Lateral Bracing," Journal of the Structural Division, ASCE, ST10, October, pp. 2167-2181.
- Nethercot, D.A., and Rockey, K.C., (1972). "The lateral buckling of beams having discrete intermediate restraints," The Structural Engineer October No. 10 vol 50S.
- Nethercot, D.A., (1973). "Buckling of Laterally or Torsionally Restrained Beams," Journal of the engineering mechanics division, August pp.773-790
- Rhodes and Walker, (1982), Developments in Thin-Walled Structures-2, Elsevier Applied Science Publishers, pp. 93-129.
- Southwell, R.V., (1932). "On the Analysis of Experimental Observations in the Problems of Elastic Stability," Proceedings of the Royal Philosophical Society of London, Series A, Vol. 135, April, p. 601.
- Taylor A.C., Ojalvo, M., (1966). "Torsional Restraint of Lateral Buckling," Journal of the Structural Division, ASCE, ST2, April pp. 115-129.
- Timoshenko, S., and Gere, J., (1961). Theory of Elastic Stability, New York: McGraw-Hill Book Company
- Tong, G.S., and Chen, S.H., (1988). "Buckling of Laterally and Torsionally Braced Beams," Construction Steel Research
- Trahair, N.S., (1966). "Elastic Stability of I-Beam Elements in Rigid-Jointed Structures," The Journal of The Institution of Engineers, Australia July
- Trahair, N.S., (1969). "Deformations of Geometrically Imperfect Beams," Journal of the Structural Division, ASCE, ST7, July, p. 1475
- Winter, G., (1958). "Lateral Bracing of Columns and Beams," Journal of the Structural Division, ASCE, ST2, March, pp. 1561-1565.
- Winter, G., (1960). "Lateral Bracing," ASCE Transactions, pp. 809-825.

Wong-Chung, A.D., and Kitipornchai, S., (1986). "Partially Braced Inelastic Beam Buckling Experiments," Research Report No. CE 72 University of Queensland June,

Yarimci, E., Yura, J.A., and Lu, L.W., (1967). "Techniques for Testing Structures Permitted to Sway," Experimental Mechanics, Journal of the Society for Experimental Stress Analysis, Vol. 7, No. 8, August.

Yura, J.A., (1990), Class Notes